SYNTHESIS OF ANALOGUES OF GSK3787 AS PUTATIVE PPARδ ANTAGONISTS

Dissertation for the degree of Master of Pharmacy

Marthe Amundsen

School of Pharmacy

Faculty of Mathematics and Natural Sciences

UNIVERSITY OF OSLO

2013

SYNTHESIS OF ANALOGUES OF GSK3787 AS PUTATIVE PPARδ ANTAGONISTS

Dissertation for the degree of Master of Pharmacy

Marthe Amundsen

Department of Pharmaceutical Chemistry

UNIVERSITY OF OSLO

2013

SYNTHESIS OF ANALOGUES OF GSK3787 AS PUTATIVE PPARδ ANTAGONISTS

http://www.duo.uio.no/

Trykk: Reprosentralen, Universitetet i Oslo

Acknowledgements

First of all, I would like to thank my supervisor Professor Trond Vidar Hansen for giving me the opportunity to be a part of his group during my master thesis. Your experience, knowledge and personality have been a great motivation this year.

Assistant Professor Anders Vik, thank you for giving me chemical guidance, feedback and practical help in the laboratory, and for showing interest in my progress all the way.

Ph. D student Åsmund Kaupang, thank you for all the time you have spent, helping me with NMR-interpretation and proofreading my thesis, and for curious discussions about chemistry and other (related) topics.

My gratitude also goes to everybody at the Department of Pharmaceutical Chemistry, for their helpfulness, availability and good humor. It has been a very nice experience working with you, and I will miss it.

Espen, you deserve a gold medal for all the help and support you have given me. Thank you for being genuinely interested in my thesis.

Last, I would like to thank Frank and Nicolai, for getting me up in the morning and for taking me home in the afternoon, and for the liberating conversations we have. You two are my major inspiration.

Marthe Amundsen

Oslo, april 2013

Abstract

Efficient syntheses of the three *N*-alkylated analogues of the known PPARδ antagonist GSK3787 were investigated. In this thesis the analogues; *N*-methyl-*N*-(2-((5-(trifluoromethyl) pyridine-2-yl)sulfonyl)ethyl)-2-naphtamide (**11**), *N*-ethyl-*N*-(2-((5-(trifluoromethyl)pyridine-2-yl)sulfonyl)ethyl)-2-naphtamide (**13**) and *N*-benzyl-*N*-(2-((5-(trifluoromethyl)pyridine-2-yl)sulfonyl)ethyl)-2-naphtamide (**15**) were achieved. An additional preparation of **15** was developed and showed to be a convenient alternative to the first route.

Based on previous work performed on the PPARδ antagonist GSK3787 and analogues, we anticipate that the three compounds **11**, **13** and **15** will be potent and selective PPARδ antagonists.

Biological evaluations of all new potential PPARδ antagonists will be conducted in the near future.

Graphical abstract

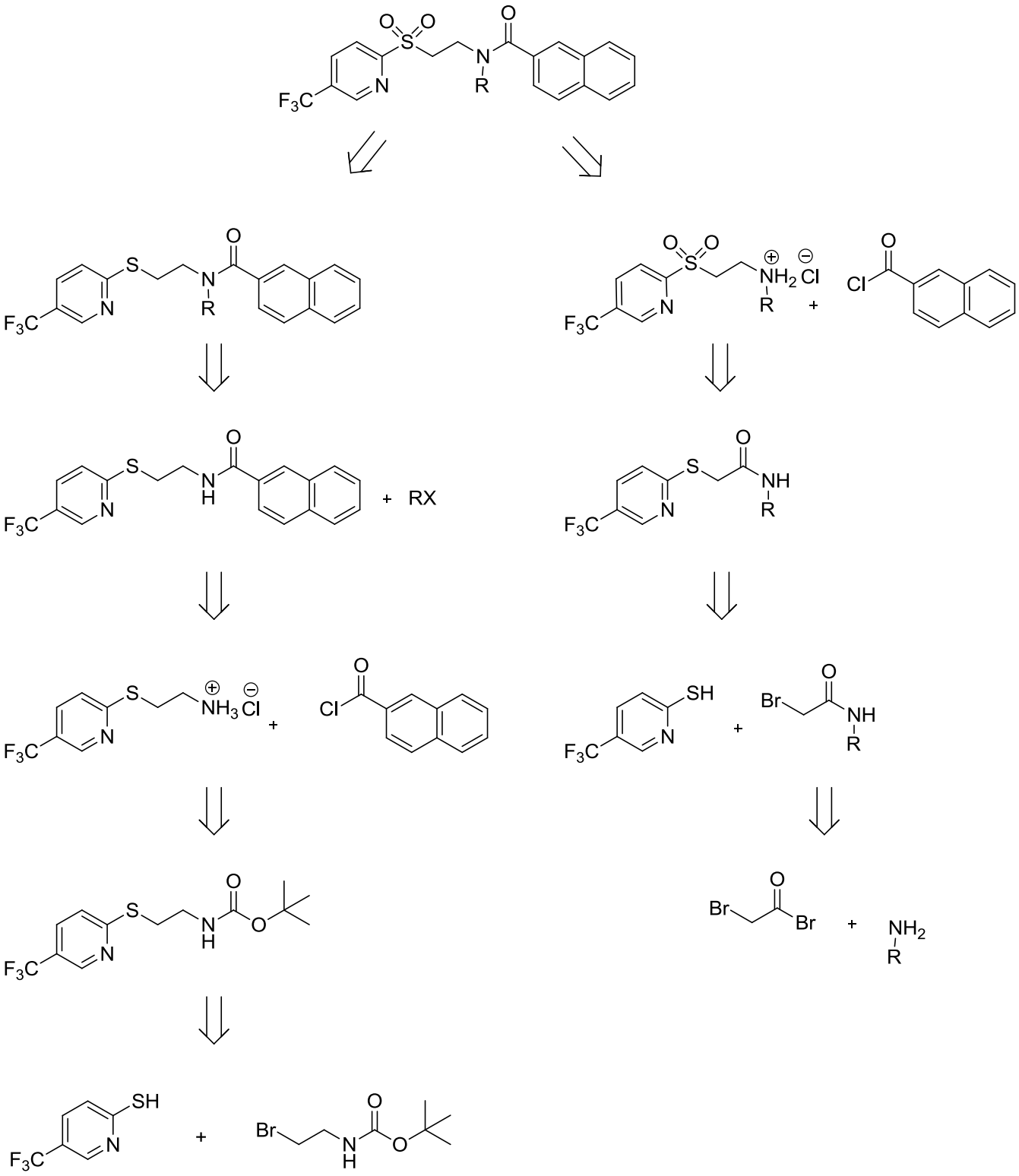

Abbreviations

AF-1	activation function 1
AF-2	activation function 2
ANGPTL4	angiopoietin-like protein 4
BMI	body mass index
BnBr	benzyl bromide
Boc	*tert*-butoxycarbonyl
CPT1a	carnitine palmitoyltransferase 1A
Cys249	cysteine numbered 249 in the LBD of PPAR
db/db	leptin-resistent
EMA	European Medicines Agency
FAT	fatty acid translocase
FATP	fatty acid transport protein
HDL	high-density lipoprotein
HODE	hydroxyoctadecadienoic acid
HPLC	high performance liquid chromatography
i-PrBr	*iso*-propyl bromide
LBD	ligand binding domain
LDL	low-density lipoprotein
NaHMDS	sodium hexamethyldisilazane
PDK4	pyruvate dehydrogenase kinase, isozyme 4
PGD_2	prostaglandin D2
PPAR	peroxisome proliferator-activated receptor
RE	response element
RXR	retinoid X receptor
SAR	structure-activity relationship
T2DM	type 2 diabetes mellitus
TBAI	*tetra*-butylammonium iodide
t-BuOK	potassium *tert*-butoxide
TLC	thin-layer chromatography
TZD	thiazolidinedione
VLDL	very low-density lipoprotein
WHO	World Health Organization

Table of contents

1 Introduction

1.1 PPAR as a therapeutic target

The ability of nuclear receptors to induce or repress the transcription of different gene programs renders them interesting pharmacological targets [1]. Contrary to this, the complexity of the transcriptional response to nuclear receptor modulation and the not yet fully understood mechanisms involved in the events that lead to the transcription of specific genes, also makes them problematic targets to work with [2]. Since the discovery of the peroxisome proliferator-activated receptors (PPARs) in the 1990s, several studies have been undertaken to elucidate their biological roles and structural features. The functions of PPARs are widespread; from cell-cycle control, to metabolism and energy homeostasis, the latter having been the main function of interest in the context of PPARs as therapeutic targets [1, 2].

1.1.1 Metabolic disorders

Overweight has in the last decade become a major health problem among people in developed countries. In 2007, the proportion of people that suffered from clinical obesity (BMI $\geq$ 30) exceeded 30% of the adult population in the USA [3]. In 2008, WHO estimated the number of overweight people to be 1.4 billion on world basis [4]. A number of severe physiological malfunctions are associated with this condition. Metabolic syndrome, with its risks of type 2 diabetes mellitus (T2DM) and cardiovascular disease, is one of the main concerns. Metabolic syndrome is a condition characterized by abdominal obesity, hyperinsulinemia, dyslipidemia and hypertension [5].

The glucose-homeostasis is held in control by insulin, a hormone secreted from the β-cells in the pancreas. Insulin increases glucose uptake by peripheral cells (mainly muscle and adipose tissue) and is secreted in response to high levels of blood glucose. In the liver insulin inhibits gluconeogenesis. In obese persons, the normal secretion of insulin may become disrupted, due to the responding cells gaining resistance against insulin, which results in continuous high levels of blood glucose. This will make the β-cells compensate by secreting more insulin,

resulting in hyperinsulinemia. If this situation persists over time, it may ultimately lead to total insulin resistance and dysfunctional β-cells [6].

Obese persons also tend to have a non-satisfactory lipid profile [7]. Lipids and cholesterol are transported in the bloodstream in complexes known as lipoproteins. There are four main classes of lipoproteins, each with a specific role in the transport of lipids. *Chylomicrons* transport intestinally absorbed triglycerides and cholesterol via the bloodstream to the tissues, where the triglycerides are split by lipoprotein lipases, releasing free fatty acids to muscle and adipose tissue. The remnants of the chylomicrons, including cholesterol, are taken up by the liver, stored here or converted into *very low-density lipoprotein* (*VLDL*). VLDL transports cholesterol and newly synthesized triglycerides from the liver to peripheral tissues, where they release the triglycerides as before and become *low-density lipoprotein* (*LDL)*, a lipoprotein with a large proportion of cholesterol. Some LDL remains in the tissues and some is taken up again by the liver. Another lipoprotein class, *high-density lipoprotein* (*HDL)*, reverses the transport, by absorbing cholesterol derived from cell breakdown in tissues and arteries, and transferring it to VLDL and LDL. It is favourable to have a high proportion of HDL compared to VLDL/LDL. However, in obese persons, the HDL level is decreased and VLDL and LDL levels are increased. This is known as dyslipidemia [8].

Both insulin resistance and dyslipidemia result in elevated blood glucose levels and hypertension, and if not controlled at an early stage, to T2DM. In fact, 80% of people with T2DM suffer from overweight [9]. These metabolic disruptions, all together as in metabolic syndrome, or individually, elevate the risk of developing potentially fatal conditions like atherosclerosis, ischemic heart disease and severe T2DM [10].

1.1.2 Current treatment of metabolic syndrome

The most effective treatment of the disorders involved in metabolic syndrome involves lifestyle modifications. Reducing weight, increasing the amount of exercise and lowering dietary fats and glucose, are all beneficial factors to prevent the development of metabolic syndrome [11]. For patients, these lifestyle changes often tend to be difficult to comply with and pharmaceutical intervention seems to be necessary in most cases. Employing the drugs

currently on the marked, the treatment of metabolic syndrome combines lipid-modifying and antihypertensive drugs, with insulin sensitizers and other blood glucose-lowering drugs. The efficacy of this therapy is varying among individuals. The side-effects of the currently available treatments are often a problem, and given the need for life-time treatment, they become important limiting factors [12, 13].

PPARs are one of the main receptor families involved in energy homeostasis and thus, targeting these receptors have, for obvious reasons, gained much interest the recent years [14]. The need for further studies on how nuclear receptors like PPARs control gene transcription is necessary, in order to develop more efficient and safe drugs than those currently on the marked. To gain the knowledge required, the development of PPAR-selective modulators is of interest [15].

1.2 PPAR biology

1.2.1 Nuclear receptors and classification of PPARs

Nuclear receptors are a family of ligand-activated transcriptions factors that regulate gene transcription by binding to specific regions in the target DNA called response elements (REs). They can be classified according to the organization of their REs and dimerization properties. The class I nuclear receptors include the steroid receptors (the estrogen receptor, androgen receptor and mineralocorticoid receptor) and are located in the cytoplasm. They bind as homodimers to the REs upon activation by hormones. The class II nuclear receptors include the endocrine receptors (such as the thyroid hormone receptor and retinoic acid receptor) and bind to the REs as heterodimers with the retinoic X receptor (RXR). In the absence of ligands, these receptors are found inside the nucleus in association with corepressor proteins that inhibit transcriptional activity. The binding of ligands results in release of the corepressors and binding of coactivators, that in turn initiates the transcription of target genes. The class III nuclear receptors comprise mostly orphan receptors, for which no respective endogenous ligands have been identified to date. [16].

The PPARs remained orphan receptors for a long time, but due to the discovery of fatty acids and eicosanoids as their endogenous ligands, in addition to current knowledge about their binding to DNA as heterodimers with the RXR (Figure 1.1), they are now included in the class II of nuclear receptors [1, 5, 12].

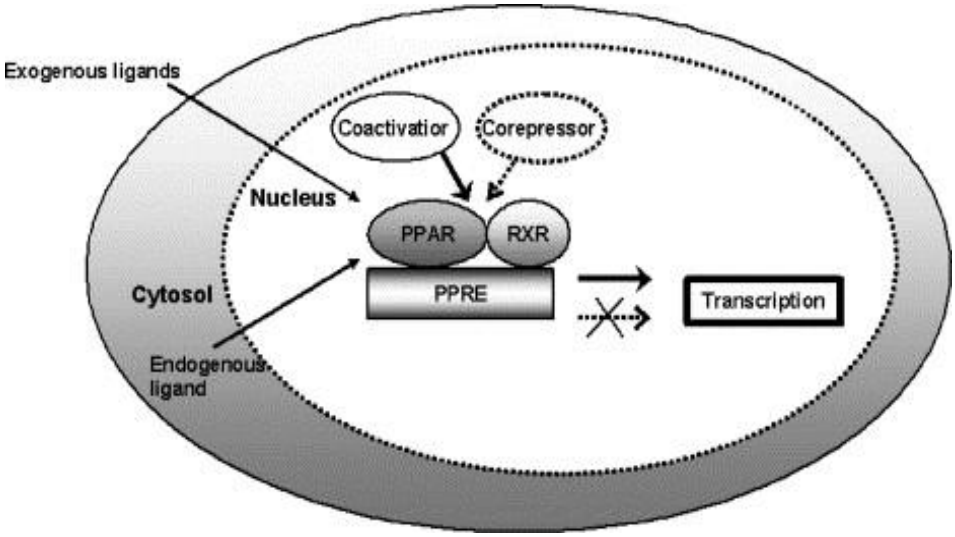

Figure 1.1: Mechanism of PPAR-induced gene transcription (copied from Kota *et al.*, 2005 [1]).

1.2.2 Structural features of the PPARs

The nuclear receptors share similar structural characteristics and contain four functional domains, named A/B, C, D and E/F, in addition to activation function 1 (AF-1) and activation function 2 (AF-2) (Figure 1.2).

Figure 1.2: Functional domains of the nuclear receptors [1].

The A/B domain hosts the ligand independent AF-1 and is an identified site of phosphorylation of the PPARs. This N-terminal domain is highly conserved among the nuclear receptors. The C domain is the region that binds to DNA and recognizes the PPAR-specific response elements (PPREs) in the promoter regions of the target genes. The D domain, together with AF-2 binds coregulator proteins. The E/F domain contains the ligand binding domain (LBD), which is specific to each receptor class and/or subtype [1, 8]. To date,

there are three identified subtypes of PPARs, named α, β/δ and γ, distinguished by differences in their LBDs [16]. The ligand binding pocket of the LBD is defined by 34 amino-acid residues, of which about 80% are homologous between the PPAR [17].

1.2.3 Endogenous ligands

PPARs are lipid-sensing receptors which mean that they are activated by fatty acids and fatty acid metabolites. Long chain fatty acids (e.g. palmitic acid, oleic acid, linoleic acid and arachidonic acid), various prostaglandins and leukotrienes, have all been shown to be endogenous activators of PPARs (Figure 1.3). The affinities of these PPAR ligands are in the μM-range. Because of uncertainty about whether the free concentrations of these fatty acids in cells become high enough to activate the receptor, it is proposed that one function of PPARs is to be a measure of the total flux of fatty-acids in metabolically active tissues, rather than being highly ligand-specific receptors [18]. On the other hand, nitrooleic acid, a nitro derivative of the unsaturated oleic acid, has been reported to activate PPAR, more specific PPARγ, with high affinity (nM-range). Nitro derivatives are endogenous products of $NO^{\bullet}$ and NO_2^- mediated redox processes in the body and levels of free nitrooleic acid have been detected in 1–3 nM in human plasma [19].

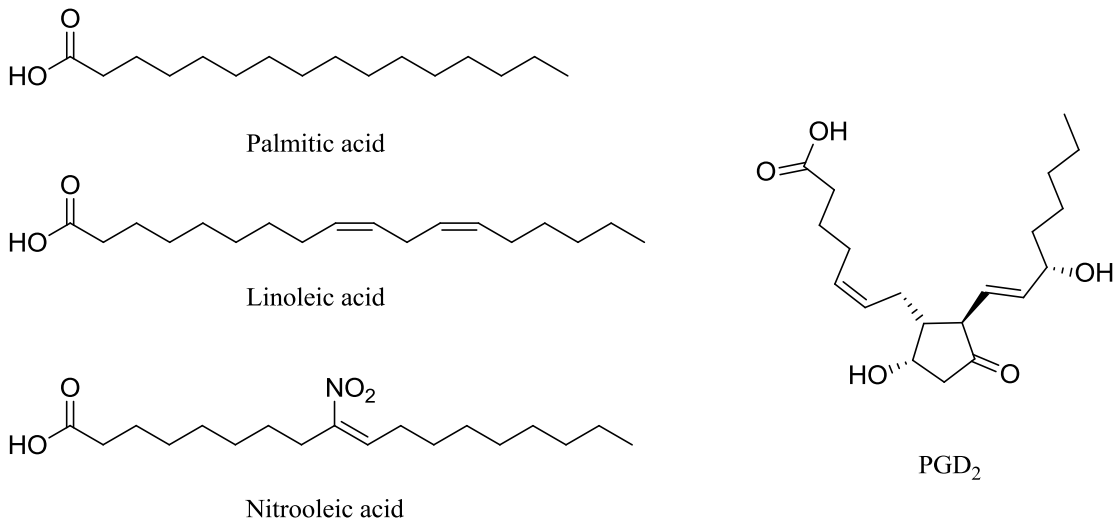

Figure 1.3: Structure of some endogenous ligands of the PPARs [19, 20].

1.2.4 Distribution and primary biological functions of PPARs

The three known PPAR subtypes have different tissue distributions in the body, overlapping each other to some extent (Table 1) [21].

Table 1: Tissue distributions of the PPAR subtypes in humans [21].

PPAR-subtype	Mainly found in	Also found in
α	Liver, brown adipose tissue	Heart, kidney, muscle
γ	Adipose tissue	Intestine, macrophages
β/δ	Heart, muscle	Skin, brain, adipose tissue

PPARα is expressed in tissues with high mitochondrial and peroxisomal activity, such as the liver and brown adipose tissue, where it is essential to maintain the lipid homeostasis. In the liver, PPARα stimulates fatty acid catabolism and gluconeogenesis. It has also been shown to increase the level of apolipoprotein A1 (a component of HDL) and decrease apolipoprotein CIII-level (a component of VLDL), thus modulating the lipid profile. The expression of fatty-acid transport proteins (FATP and FAT) is increased upon PPARα activation, resulting in improved cellular uptake of circulating fatty acids [1].

PPARγ is found as two different isoforms, γ-1 and γ-2. PPARγ-2 is expressed almost exclusively in adipose tissue, whereas PPARγ-1 is ubiquitously expressed. PPARγ is essential for adipocyte differentiation and survival, and it plays an important role in lipogenesis [22]. PPARγ improves insulin sensitivity by controlling various adipokines involved in the development of insulin resistance, but also by having beneficial effects on the glucose homeostasis [12]. Anti-inflammatory effects have also been reported [12].

PPARδ is ubiquitously expressed and its effects are similar to PPARα, in that it increases lipid metabolism and energy uncoupling. While PPARα exerts its action mainly in the liver, PPARδ is found in higher levels in heart and skeletal muscle, especially in oxidative muscle fibers. PPARδ activation has beneficial effects on the lipid profile and represses hepatic glucose output [23].

1.2.5 Synthetic ligands in clinical use

Two classes of compounds that target PPAR have reached the marked so far; the fibrates and the thiazolidinediones (TZDs).

The fibrates (e.g. gemfibrozil and fenofibrate, Figure 1.4), target the PPARα subtype and improve lipid profile and glucose-tolerance. Although they have been on the marked in European countries since 1960, the European Medicines Agency (EMA) concluded in 2005 that documentation of long-term efficacy in reducing cardiovascular disease in human was poor, compared to the alternative lipid-lowering drugs. EMA thus recommended that fibrates should not be used as first-line treatment, except in rare cases where other available drugs (such as statins) are not tolerated or in cases of severe hypertriglyceridemia. None of the fibrates are currently on the regular market in Norway [24].

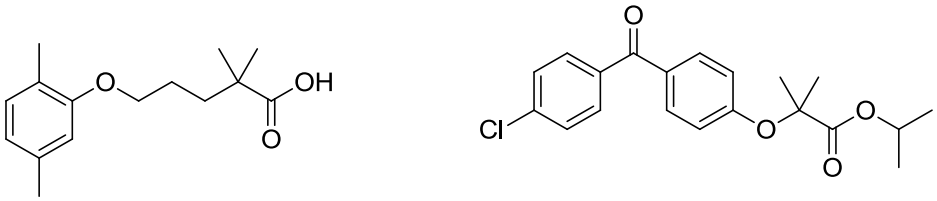

gemfibrozil (Lopid™) fenofibrate (Tricor™)

Figure 1.4: Structure of two fibrates that target PPARα [25].

The TZDs target the PPARγ subtype and are insulin sensitizing drugs that lower blood glucose, with additional positive effects on plasma triglycerides and HDL cholesterol. In Norway, the only TZD on the marked is pioglitazone (Actos™), and side effects are limiting its use. Pioglitazone may cause retention of body fluids and oedema, which can be detrimental to individuals with reduced cardiac function. Induction of lipogenesis, resulting in gain of weight, is another disadvantageous effect of TZDs [13, 26].

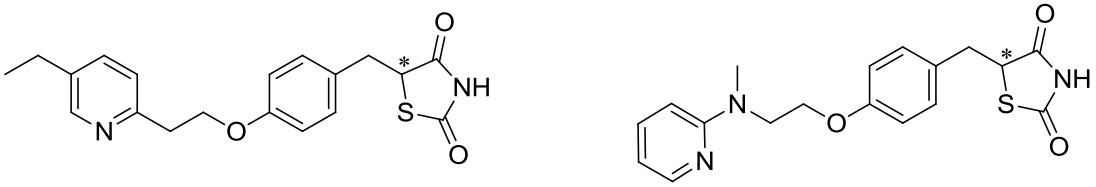

pioglitazone (Actos™) rosiglitazone (Avandia™)

Figure 1.5: Structures of two drugs in the TZDs class that target PPARγ. They are both sold as racemates. [26].

1.3 The role of PPARδ as a therapautic target

1.3.1 Discovery of PPARδ ligands

PPARδ was the last of the PPAR subtypes to be identified and for a long time, the knowledge about its biological role was limited due to its broad tissue distribution and lack of a potent and highly selective ligand. Over the past several years, this has changed dramatically. In 2003, two synthetic ligands, GW501516 and GW0742, were reported by GlaxoSmithKline. The compounds showed agonistic activities, high affinity (~ 1 nM) and more than 1000-fold selectivity for PPARδ compared to the other subtypes. This was an important contribution to the study of the biological functions of PPARδ [27].

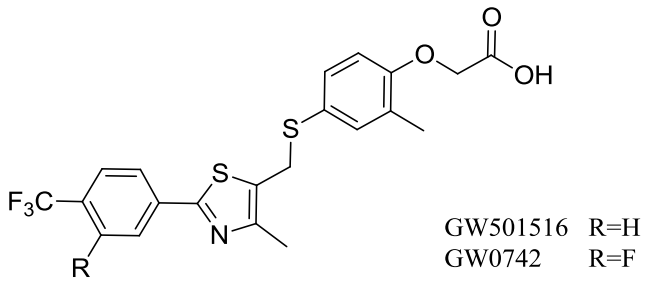

Figure 1.6: The PPARδ agonists GW501516 and GW0742 [27].

No drug targeting PPARδ is currently in clinical use, but with growing evidence for the beneficial effects the activation of this subtype has on various metabolic parameters, its potential as a therapeutic target is of great interest [28].

1.3.2 Beneficial metabolic effects of PPARδ agonism

Skeletal muscles consist of different fiber types with distinct metabolic profiles: oxidative slow-twitch (Type I), mixed oxidative/glycolytic fast-twitch (Type IIa) and glycolytic fast-twitch (Type IIb). Oxidative muscle fibers generally express enzymes that oxidize fatty acids whereas glycolytic fibers preferentially use glucose as energy source [21].

PPARδ is highly expressed in oxidative muscle fibers [23]. Animal models overexpressing PPARδ has shown a change in fiber composition in muscle, due to both increased production

of and switch to a more oxidative muscle fiber type. The animals showed a leaner phenotype, greater enzymatic activity and increased expression of genes related to oxidative metabolism [29]. Transgenic mouse overexpressing PPARδ in skeletal muscle, show a decrease in body fat content related to reduced adipocyte size and an increased proportion of oxidative slow twitch fibers [30]. Several studies in humans confirm impaired fat oxidation in obese phenotypes. Improving the fat oxidation potential, especially that of muscle and adipose tissue, may have positive effects on weight loss [12]. Slow-twitch fibers also show a greater extent of insulin stimulated glucose transport than do fast-twitch fibers, and the body's insulin sensitivity seems to be positively correlated with the proportion of slow-twitch fibers. It is proposed that PPARδ activation have a protective effect against obesity and insulin resistance [21].

Studies in insulin resistant obese monkeys show that PPARδ agonism has a beneficial effect on the lipid profile, by raising HDL cholesterol and lowering LDL cholesterol, triglycerides and fasting insulin levels [5]. *In vivo* studies in obese, diabetic db/db mice, shows that treatment with PPARδ agonists increases HDL cholesterol, with no effect on LDL cholesterol [31]. In addition, PPARδ was shown to regulate the levels of serum triglycerides in mice, by reducing VLDL production and increasing lipoprotein lipase activity on VLDL triglycerides [32].

1.3.3 PPARδ antagonism

The use of PPARδ agonists in combination with knockout models, have shown that the above mentioned effects are indeed PPARδ receptor mediated. Much effort has been put into the development of PPARδ agonists and their contribution to a better understanding of the effects of PPARδ agonism has been valuable.

Lately, the development of PPARδ antagonists has received more attention. Ligand mediated repression of the PPARδ gene program provides a valuable tool for elucidating the receptor's role in human biology. Furthermore, beneficial pharmacological effects of antagonists are observed, making them potential leads for drug development. For instance, PPARδ antagonists have been reported to inhibit cancer cell invasion by repressing ANGPTL4

induction in a study on human breast cancer cells [33]. In another study PPARδ antagonism inhibits tumor proliferation and survival of liver, breast and lung cancer cells, linked to G_1/S cell cycle block and increased apoptosis [34]. Despite of these findings, there are controversial results from other studies related to PPARδ and cancer, confirming the need for further identification of the cellular mechanisms involved. Increased knowledge about PPARδ antagonism may also contribute to a better mechanistic understanding of the transcriptional control of nuclear receptors in general, given the similarities between receptors in this family [16]. Development of new PPARδ antagonists is thus warranted.

1.4 Previously reported PPARδ antagonists

1.4.1 The GSK0660-series

The first PPARδ antagonist, GSK0660, was reported by researchers at GlaxoSmithKline in 2007 (Figure 1.7, R = Ph). It is highly selective towards PPARδ and displays an IC_{50} ~160 nM. At higher concentrations, GSK0660 can completely inhibit both the agonist-induced expression as well as the basal expression of PPARδ target genes, such as ANGPTL4 and CPT1a [35]. Unfortunately, lack of oral bioavailability of GSK0660 limits its usage in studies *in vivo* [36]. Recently, Müller *et al*., developed a series of compounds analogues to GSK0660, of which the compound with R = *n*-Bu displayed a 10-fold higher binding affinity than GSK0660 (Figure 1.7) [37, 38].

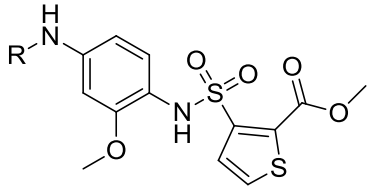

R-group	$IC_{50\ (nM)}$	$K_{i\ (nM)}$	Name
n-Bu	-	8.59	-
t-Bu	98	-	PT-S58
n-Hex	93	-	ST247
i-Pent	-	12.10	-
Ph	160	98.15	GSK0660
Bn	-	12.34	-

Figure 1.7: Structure of GSK0660 (R = Ph) and analogues, developed by Müller *et al*. [35, 37, 38].

1.4.2 DG172

The same research group, Müller *et al*., recently reported a structurally distinct PPARδ antagonist, named DG172 (IC_{50} = 26.9 nM). It has an electrophile acrylonitrile moiety, which was found to be crucial for its activity (Figure 1.8) [39].

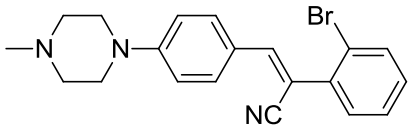

DG172

Figure 1.8: Structure of the PPARδ antagonist DG172 [39].

1.4.3 Carboxylic acid containing PPARδ antagonists

SR13904 is an antagonist reported by Zaveri *et al*. in 2009 (Figure 1.9). Surprisingly, this compound features a carboxylic acid head group, in analogy to prototypical PPAR agonists. The compound was reported to have anti-tumor activity, by inhibition of cancer cell proliferation and increased apoptosis [34]. A series of related compounds were reported by Kasuga *et al*. the same year. These compounds also contain carboxylic acid head groups and are analogues to TIPP-204, a highly potent, PPARδ selective *agonist*, also developed by Kasuga *et al*.[40] (Figure 1.9). For the latter series, the authors hypothesize that the length and rigidity of the head group induces a misfolding of helix 12 located in the AF-2, the correct folding of which is aided by the carboxylic acid head groups of prototypical PPAR-agonists [40].

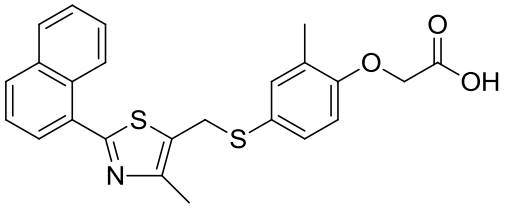

SR13904 (PPARδ antagonist)

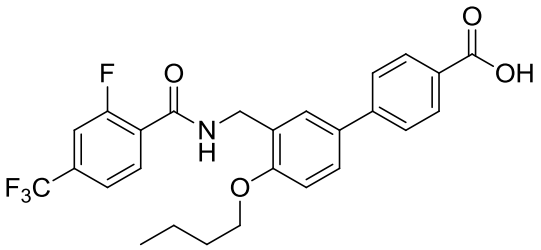

PPARδ antagonist analogue to TIPP-204

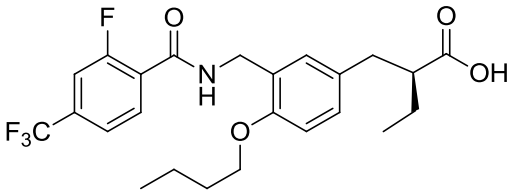

TIPP-204 (PPARδ agonist)

Figure 1.9: Structures of two PPARδ antagonists containing carboxylic acid head groups, and the agonist TIPP-204, for comparison [34, 40].

1.4.4 The GSK3787-series

Another structurally distinct PPARδ antagonist, identified during high-throughput screening at GlaxoSmithKline, is GSK3787 (Figure 1.10). This compound is selective for the δ-subtype and antagonizes 100% of the agonist-induced expression of two PPARδ target genes, CPT1a and PDK4, when coadministered with the full PPARδ agonist GW0742. When tested alone, it acted as an inverse agonist, repressing the basal level of CPT1a expression, but not that of PDK4 [36].

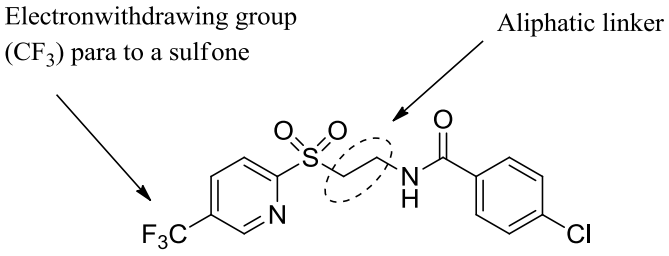

GSK3787

Figure 1.10: Structure of the PPARδ antagonist, GSK3787, and selected structural features [36].

A structure-activity relationship (SAR) study was performed by Shearer *et al.* on a series of analogues of GSK3787 to identify the pharmacophore. This established some structural features important for the activity: [36].

- The length of the aliphatic linker; both a 1- and a 3-carbon lenghts showed reduced activity, indicating that a 2-carbon chain was the most suited linker length.
- The substituent on the pyridine ring; a trifluoromethyl group gave an active compound, whereas a hydrogen or a methyl group afforded inactive compounds.
- A sulfide in the place of the sulfone resulted in an inactive compound.
- Substitution of the arylamide ring with a trifluoromethoxy group, bulky lipophilic groups or disubtitution, gave minor changes in activity.

Taken together, these results indicate that a strong electron withdrawing group para to the sulfone and a 2-carbon chain separating the aromatic rings is important (Figure 1.10) [36].

Shearer *et al*. performed mass spectrometrical analysis of the binding of GSK3787 and an analogue of different molecular weight, featuring the same pyridylsulfone moiety, to PPARδ. They found that both compounds covalently modified Cysteine (Cys249) with the same 5-trifluoromethylpyridyl fragment. Shearer *et al.* proposed a mechanism that possibly involves the nucleophilic attack of the thiol in Cys249 with the carbon in 2-position on the pyridine ring, displacing the sulfone group as a sulphinate (Figure 1.11) [36].

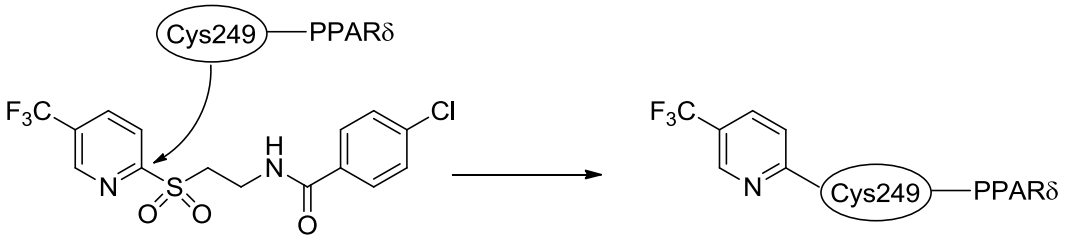

Figure 1.11: Proposed mechanism for covalent binding of GSK3787 analogues by Shearer *et al.* [36].

1.4.5 Previous work on PPARδ antagonists at The Department of Pharmaceutical Chemistry, School of Pharmacy, Oslo

Our research group has lately focused on the molecular modeling and synthesis of analogues of GSK3787 [20, 41, 42]. A compound named CC618 (Figure 1.12) was prepared by Dr. Calin C. Steindal (né Ciocoiu), which inhibited agonist-induced oleic acid oxidation in a cell-based assay, suggesting its antagonistic activity. Moreover, an IC_{50} = 0.9 µM was observed, thus making it slightly more potent than GSK3787 (IC_{50} = 3 µM in the same assay). Docking of the compound into the LBD of PPARδ indicated high affinity for the receptor [20, 42].

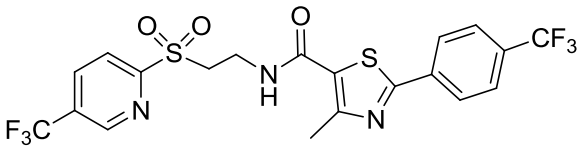

CC-618

Figure 1.12: Structure of the prepared PPARδ antagonist CC618 [20, 42].

In 2012, a series of analogues of GSK3787 were synthesized by a master student, Cecilie Xuan Trang Vo [41], in which she introduced variations in the arylamide moiety, but also made one analogue containing an *N*-methyl substituent (Figure 1.13).

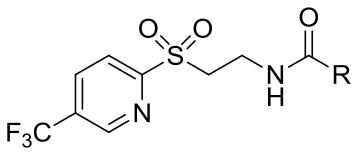

R = phenyl	R = 1-adamantyl
R = 4-fluorophenyl	R = 2-furyl
R = *i*-propyl	R = 4-methoxyphenyl
R = *t*-butyl	R = 3-pyridyl
R = 2-naphthyl	R = phenoxymethyl

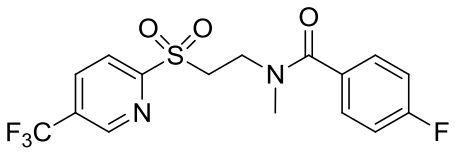

Figure 1.13: GSK3787 analogues previously synthesized by Cecilie Xuan Trang Vo [41].

Later the same year, Ph. D. student Åsmund Kaupang, performed molecular modeling studies on GSK3787 analogues. A series of analogues of GSK3787 with variations in the arylamide moiety and the *N*-alkyl substituents, were docked into the LDB of PPARδ. A 2-naphthyl-analogue with *N*-methyl substitution showed the highest docking scores of the compounds

submitted. Its poses in the ligand binding pocket, suggest that the sulfone group has a hydrogen bond to a water molecule and the electron-poor 2-carbon in the pyridine ring is located at a distance of 4.127 Å from the reactive cysteine residue (purple line, Figure 1.14).

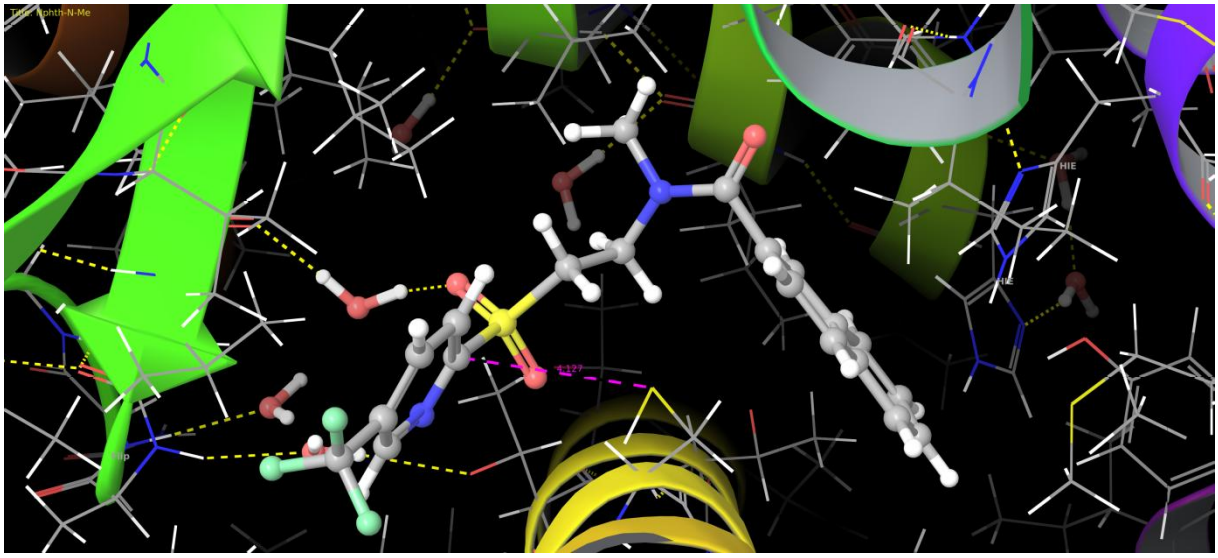

Figure 1.14: The lowest energy pose of the *N*-methyl analogue 11 docked into the LBD of PPARδ (RCSB PDB CODE: 3TKM)

1.5 Aim of the thesis

With a background in the results from the reported SAR study on GSK3787, previous syntheses of PPARδ antagonists and the results from the docking studies of a various analogues, into the LBD of PPARδ, the aim of this thesis was to develop an efficient route for making several new PPARδ- antagonists, analogues to GSK3787, with 2-naphtyl as the arylamide moiety and with variations in the *N*-alkyl substituent (Figure 1.15).

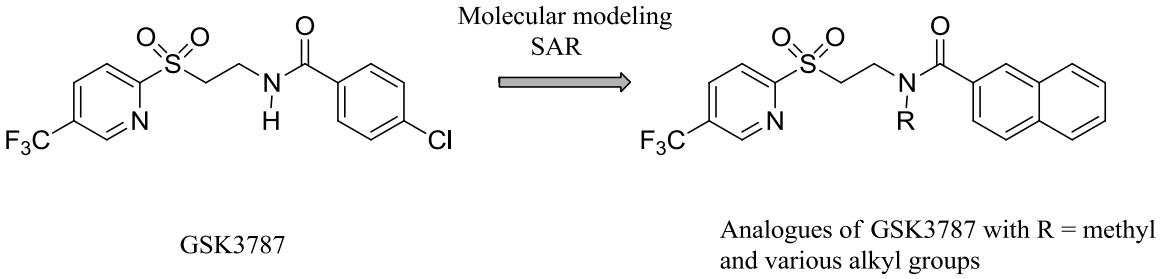

Figure 1.15: Outline of the synthesis of the target molecules.

2 Results and discussion

2.1 Synthesis of the *N*-alkylated analogues

Since the *N*-methyl analogue **11** (Figure 2.1) displayed the highest score in the docking studies, it was decided to start with the preparation of this compound.

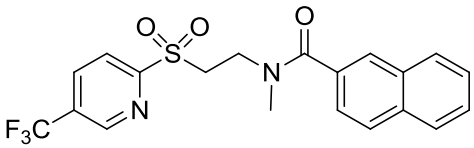

Figure 2.1 Structure of the *N*-methyl analogue 11.

We wanted to develop an efficient route for introducing different alkyl groups on the amide nitrogen. Five different approaches were explored.

2.2 The first approach; direct amide *N*-alkylation of the sulfone 7

A previous attempt to directly *N*- alkylate an analogous secondary amide, using NaHMDS for the deprotonation of the amide, was not successful [41]. An explanation for this could be the acidic protons alpha to the sulfone. With only slightly higher pK_a-values than the amide proton, they are also prone to deprotonation, that would lead to alpha-alkylation instead of *N*-alkylation.

With this in mind, we wanted to attempt deprotonation with *t*-BuOK instead, as it is a weaker base and hopefully a better choice to remove only the amide proton. By managing to directly *N*-alkylate the amide of sulfone **7**, we would gain easy access to the target molecules from a common precursor (Scheme 2.1).

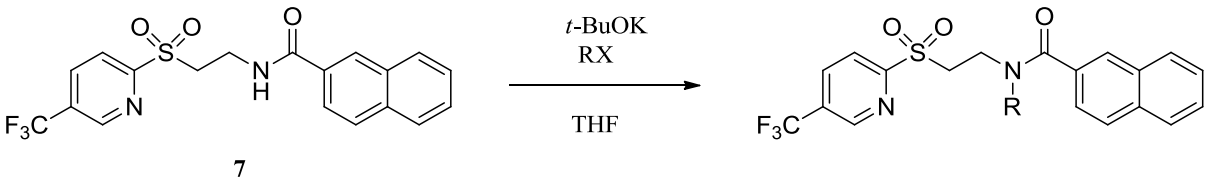

7

Scheme 2.1: Outline of direct N-alkylation of the sulfone 7.

To investigate this possibility, we needed to make the sulfone **7** for use in the alkylation (Scheme 2.2).

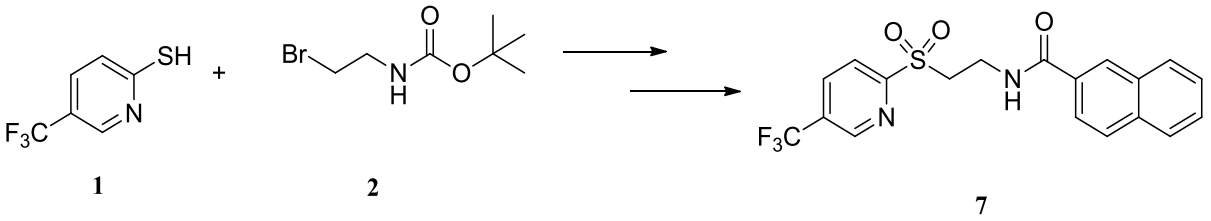

1 **2** **7**

Scheme 2.2: Outline of the synthesis of the sulfone 7 needed for the first approach.

The first step in the synthesis towards **7** was to prepare the intermediate **5** (Scheme 2.3), which in the next step could be acylated with the desired acid chlorides, according to the procedure previously reported by Shearer *et al.* [36].

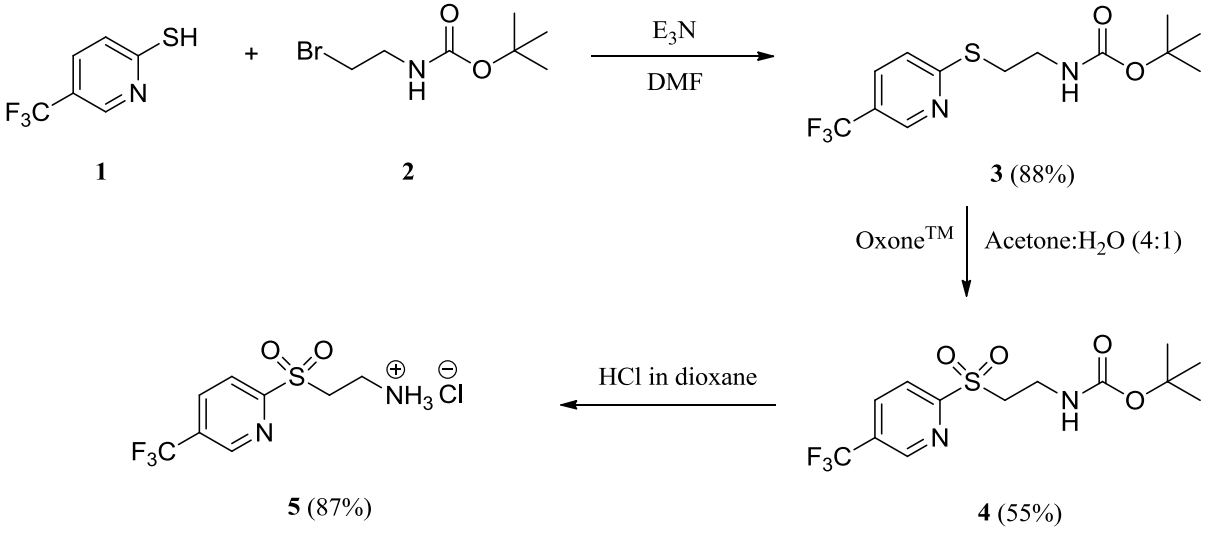

1 **2** **3** (88%) **4** (55%) **5** (87%)

Scheme 2.3: Synthesis of intermediate 5.

Reacting the thiol **1** with the bromide **2** in a nucleophilic substitution reaction afforded the thioether **3**. Oxidation of **3** to sulfone **4**, in the next step, was performed using potassium

peroxymonosulfate triple salt (Oxone^{TM}). Removal of the Boc-protection group from sulfone **4**, with HCl in dioxane, yielded the hydrochloride salt **5**.

The final step involved acylation of intermediate **5** with 2-naphthoyl chloride **6**, to afford **7 in** 63% yield (Scheme 2.4).

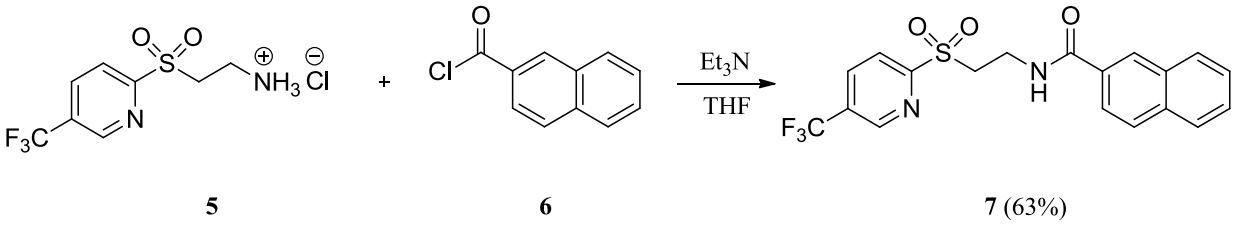

5 **6** **7** (63%)

Scheme 2.4: The final step in the synthesis towards sulfone 7.

Thus, in an attempt to prepare **11**, sulfone **7** was treated with *t*-BuOK, followed by the addition of MeI in large excess (Scheme 2.5).

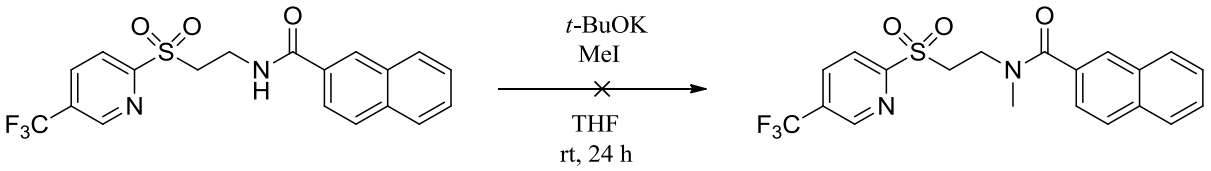

7 **11**

Scheme 2.5: Attempted direct *N*-alkylation of compound 7.

Unfortunately, the desired product could not be isolated from the complex mixture obtained and this route was thus abandoned.

2.3 The second approach; direct amide *N*-alkylation of the sulfide 9

Next, we wanted to investigate the possibility to perform *N*-alkylation of the sulfide **9**, rather than on the sulfone **7**, hoping that the lack of acidic alpha-protons, would facilitate the alkylation of the amide nitrogen.

We proceeded with the preparation of the sulphide **9**. Removal of the Boc-group from the previosly prepared thioether **3**, afforded the corresponding hydrochloride salt **8**, which in turn, was acylated with 2-naphthoyl chloride (**6)** to afford **9** in moderate yields (Scheme 2.6).

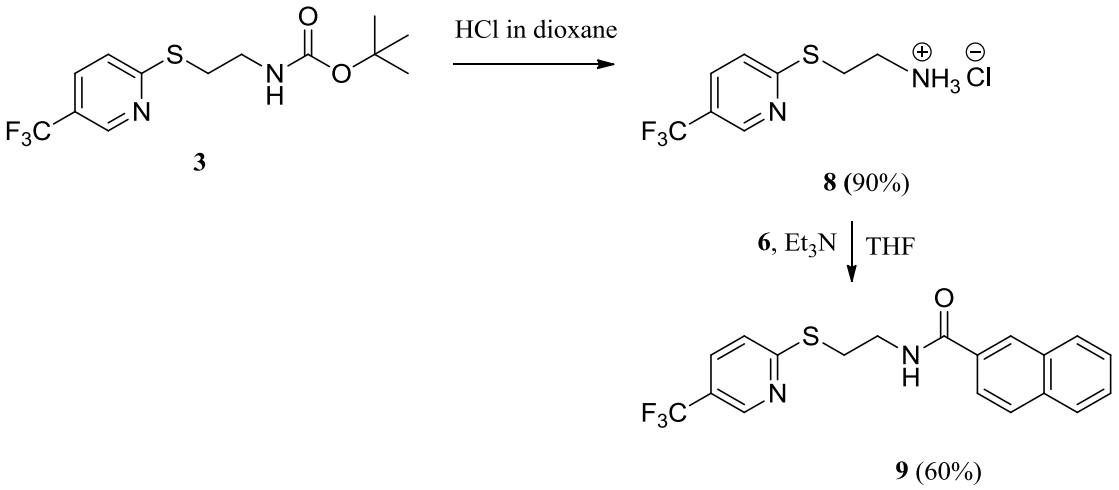

Scheme 2.6: Synthesis of the intermediate 9.

With sulfide **9**, we could successfully carry out the alkylation of the amide nitrogen with different alkyl halides, to afford the *N*-alkylated sulfides **10** (yield not determined), **12** and **14** in moderate to good yields. In the preparation of **14**, a combination of BnBr and TBAI was used successfully as a surrogate for the alkyl iodide. We then proceeded with oxidation of the sulfides with potassium peroxymonosulfate triple salt (Oxone^{TM}), to the target sulfones **11**, **13** and **15** (Scheme 2.7).

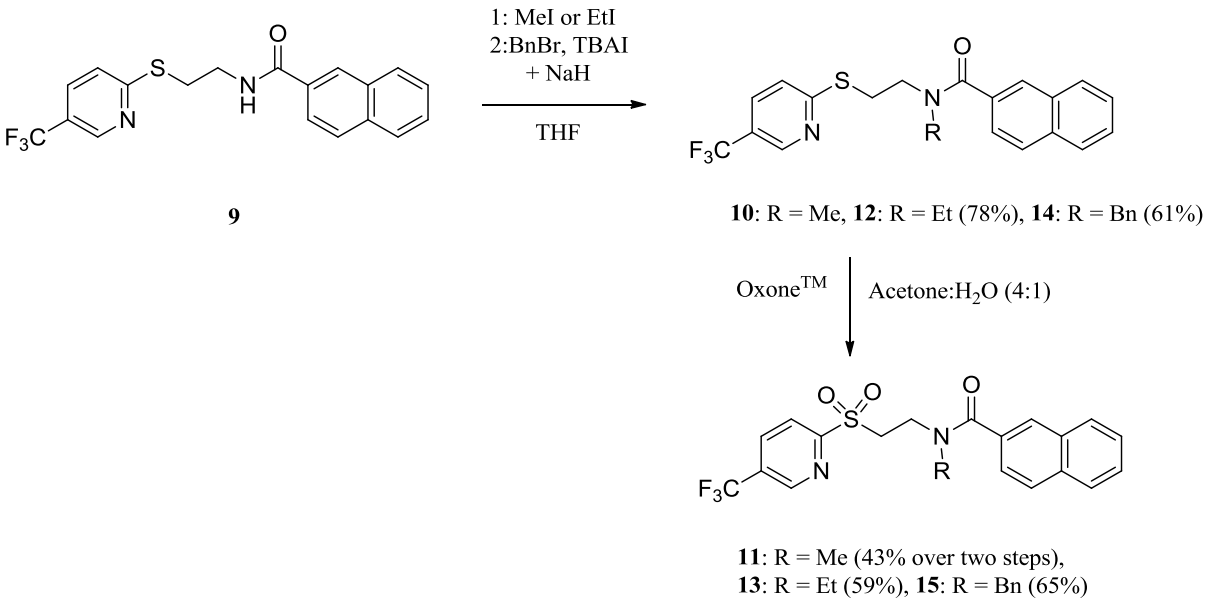

Scheme 2.7: *N*-alkylation and oxidation of the sulfide 9, affording the analogues 11, 13 and 15.

These procedures were carried out in accordance with those for the previously synthesized *N*-methyl analogue of GSK3787, containing 4-fluorobenzyl in the place of 2-naphthyl (Figure 1.13) [41].

To see if we could develop a more efficient synthesis route towards the target molecules, we continued to explore alternative routes.

2.4 The third approach; direct amide *N*-alkylation of the carbamate 3

We wanted to see if it was possible to alkylate the carbamate **3** directly. We carried out two attempts to alkylate **3** with *i*-PrBr in order to afford **16** (Scheme 2.8).

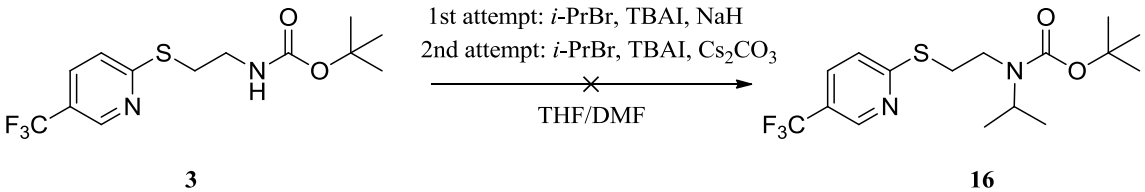

Scheme 2.8: Outline of the third approach; alkylation of the carbamate 3.

The first attempt was performed in accordance with the *N*-alkylation step described in the second approach (Scheme 2.7) in which **3** reacts with excess amounts of *i*-PrBr, in the presence of NaH and TBAI.

In the second attempt we based the procedure on a carbamate alkylation protocol reported by Salvatore *et al*. which employs Cs_2CO_3 as the base [43].

Characterization of the crude material from the first attempt showed a mixture of starting material and possibly small amounts of the desired *N*-propylated sulfide **16**. The yields were not improved compared to the second approach (direct amide *N*-alkylation of the sulfide **9**). In the second attempt, a TLC of the reaction after 5 days, showed very low conversion of the starting material, and the approach was thus abandoned.

2.5 The fourth approach; the reductive amination route

An alternative way of introducing an *N*-alkyl substituent in the target molecules was explored (Scheme 2.9). By performing a reductive amination we could maintain control of the *N*-alkyl group, and avoid the problems with the alkylation of an amide, a reaction that can be difficult due to the unreactivity of the amide nitrogen in general [44]. This reductive amination route would afford the desired *N*-alkylated compounds, but would also serve as a convergent route for making analogues with different arylamide moieties.

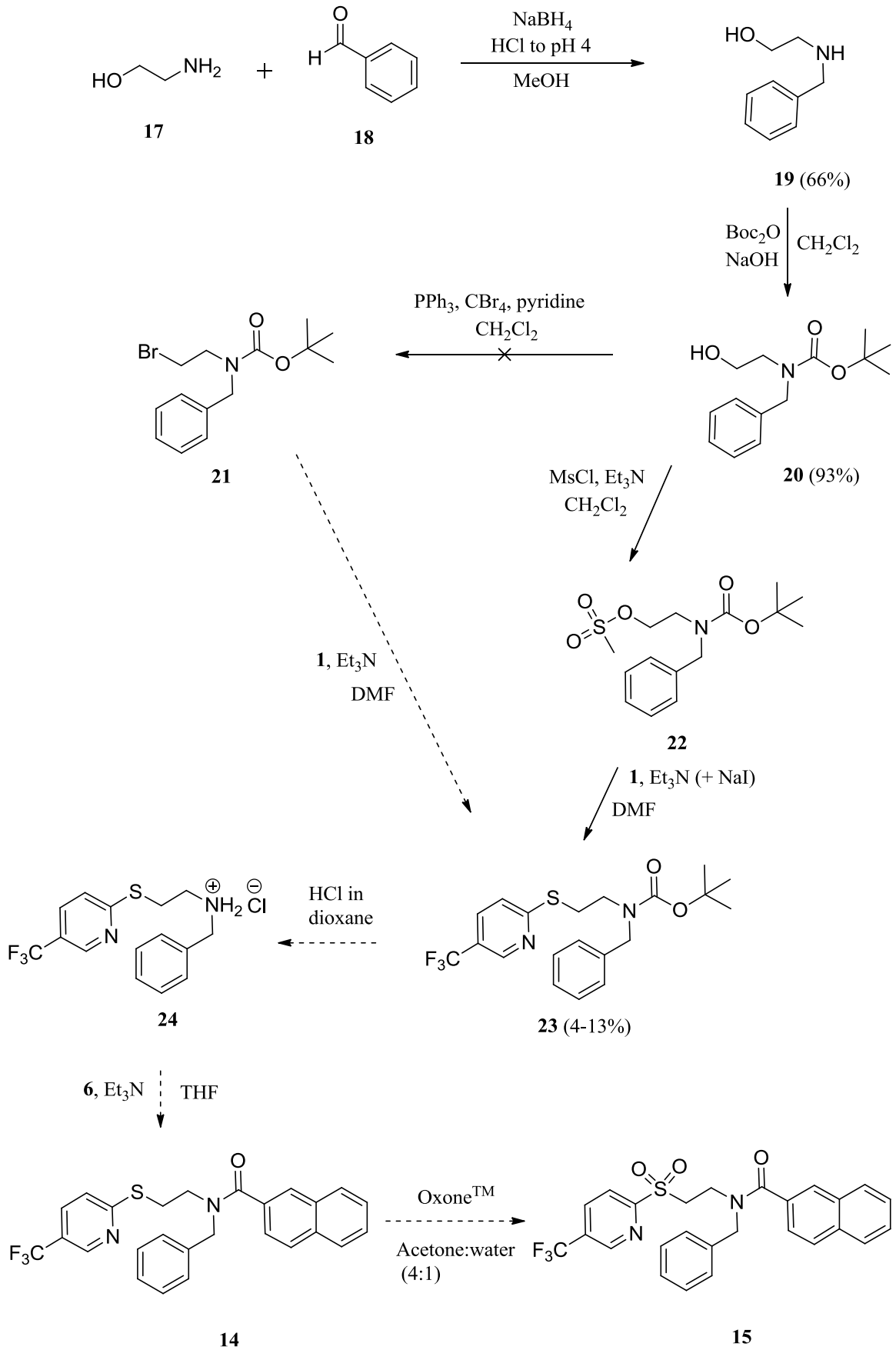

Scheme 2.9: Outline of the reactions in the fourth approach; an alternative route involving reductive amination.

By reacting etanolamine (**17**) with benzaldehyde (**18**) in methanol, followed by addition of $NaBH_4$, we were able to obtain 2-(benzylamino)ethanol (**19**) in 66% yields, according to a procedure reported by Jiang *et al*. [45]. The addition of different aldehydes in place of benzaldehyde, different *N*-alkyl subtituents could have been achieved.

Boc-proctection of 2-(benzylamino)ethanol (**19**) to **20** with Boc_2O proceeded in excellent yields (93%).

Next, we wanted to substitute the OH-group in **20**. Our first attempt employed an Appel reaction, according to a reported procedure by Baughmann *et al*. [46]. By reacting **20** with PPh_3 and CBr_4 in CH_2Cl_2, in the presence of pyridine, we could obtain the bromide **21** that could react with the thiol **1**, in the next step, in analogy to the preparation of sulfide **3**. This would afford sulfide **23**. First, we did an attempt to purify and isolate the bromide **21**, which turned out to be difficult due to the compound's invisibility upon TLC analysis. Second, we did an attempt on bromination without purification of the bromide **21**, and with addition of the thiol **1** to the crude product from the bromination. ^{1}H NMR analysis of the product showed significant amounts of PPh_3O, and made it less convenient to proceed to the next step.

Instead we decided to make a mesylate of the OH-group of **20**, by adding MsCl and Et_3N in CH_2Cl_2, followed by the addition of thiol **1**, in order to afford **23**. Unfortunately, we obtained low yields (4%). One possible explanation of this may be the instability of the mesylate **22**, which likely should be used immediately after preparation. In this case, **22** was used the day after preparation. A TLC analysis of the mesylate **22** after employing it in the reaction, showed an additional spot, probably due to decomposition of the mesylate back to the alcohol **20**. We therefore decided to attempt a second mesylation, directly followed by addition of the thiol **1**. This afforded slightly higher yields (13%) of **22**. In a last attempt to improve the yields, we added NaI together with the other reagents to improve the reactivity in the S_N2-reaction. Unfortunately, this did not improve the yields and the route was thus abandoned.

2.6 The fifth approach; acylation of the *N*-benzyl HCl-salt (29)

By this time, a Ph. D. student in the group, Åsmund Kaupang, also working on PPARδ-antagonists, had outlined a synthesis of an *N*-benzyl HCl-salt **29**, that could be acylated with 2-naphthoyl chloride **6** to yield **15** directly (Scheme 2.10).

The acylation reaction afforded **15** in good yields (84%).

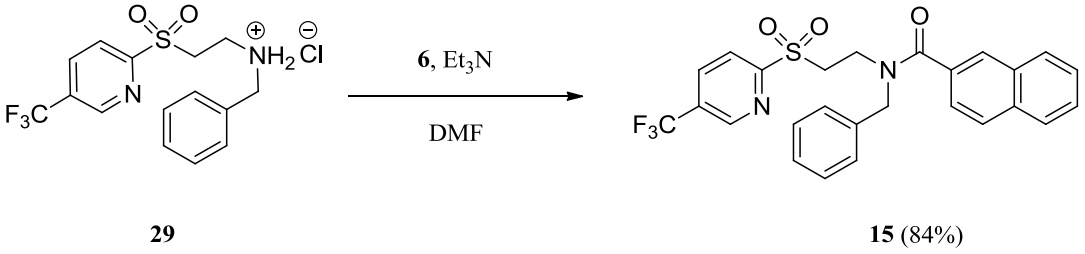

29 **15** (84%)

Scheme 2.10: Outline of the fifth approach, with acylation of the HCl-salt 29 as the final step towards 15.

The synthesis of **29** was performed as outlined in Scheme 2.11 and started with the acylation of benzylamine ($BnNH_2$) with bromoacetyl bromide **25,** to afford the amide **26** in good yields (87 %). The thiol **1**, was then reacted with **26** in an S_N2 reaction, to afford **27** (87%). The amide **27** was reduced with *in situ* generated BH_3 ($LiBH_4$ + $BF_3{\cdot}O(CH_3)_2$) to the amine **28**. Oxidation of the sulfide in **28** with aqueous H_2O_2 and $B(OH)_3$ afforded the sulfone, which was precipitated as its hydrochloride salt **29** (30% over two steps).

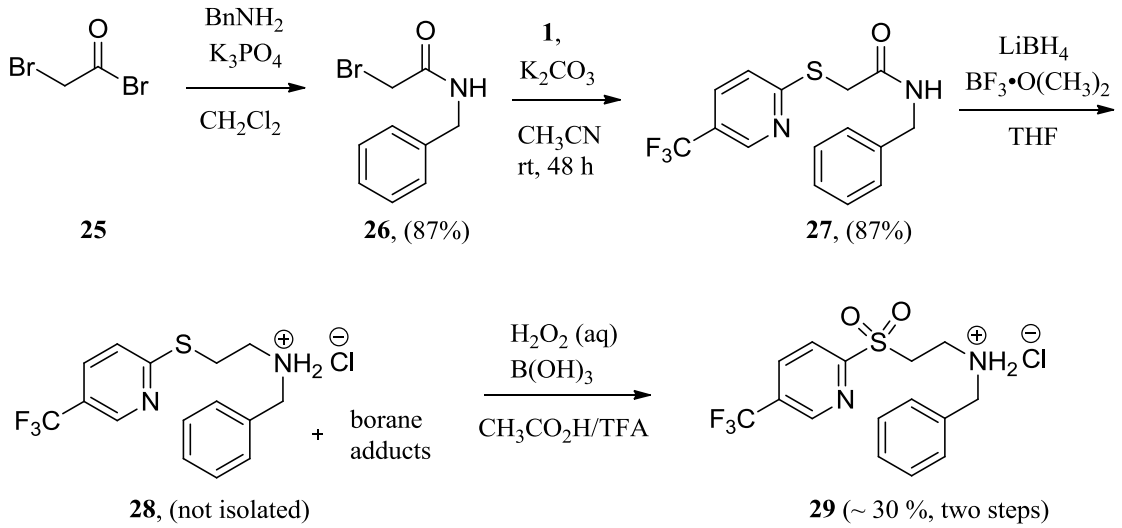

25 **26**, (87%) **27**, (87%)

28, (not isolated) **29** (~ 30 %, two steps)

Scheme 2.11: Outline of the synthesis of the intermediate 29.

3 Conclusions and future work

Five different routes towards the target molecules were explored. The synthesis of a series of three *N*-alkylated analogues **11**, **13** and **15** , by two different routes. The first one was based on a previously reported synthesis of GSK3787 and involved the *N*-alkylation of sulfide **9**, with an oxidation as the last step. This yielded all three analogues **11**, **13** and **15**. The analogue **15** was also synthesized by an alternative route, in which acylation of the *N*-benzyl HCl-salt **29** was the final step.

The aim of this thesis was to develop an efficient route for making *N*-alkylated, 2-naphthyl-analogues of GSK3787. The number of reaction steps, the yields and the overall ease of the synthesis will all be aspects to consider when comparing the two different routes.

Both routes towards the prepared *N*-alkylated analogues included five steps, with the overall yield from the first route being slightly higher than that of the second - 31% vs. 19% for the preparation of **15**. In the second route the key intermediate **29** were precipitated as its hydrochloride salt, thus reducing the number of steps requiring time-consuming preparative chromatography to two, compared to four in the first route. The reaction times were on the other hand longer in the second route.

Despite of the convenience of the second route, the first one was found to be the most suitable for introducing diverse *N*-alkyl substituents. This is because the *N*-alkylation in the first route occurs in the second last step, and thus only two steps were needed for each different *N*-alkylated analogue. In the second route the *N*-alkyl substituent was decided in the first step of the synthesis, making five steps necessary for each different *N*-alkylated analogue. Though, in the second route, the acylation with an acid chloride occurs in the last step, making this route more convergent for making analogues in which diversity in the arylamide moiety is desired.

The three prepared analogues **11**, **13** and **15** will be submitted to biological testing in the near future. Depending on the results from these tests, future work on the development of new PPARδ antagonists will be evaluated. A suggestion for further modification of the GSK3787 analogues, could be the substitution of the arylamide moiety (R_1) (2-naphthyl in the herein prepared analogues **11**, **13** and **15**) with other groups (e.g. 6-quinolyl, 6-*iso*-quinolyl or 6-fluoro-2-naphthyl, Figure 3.1).

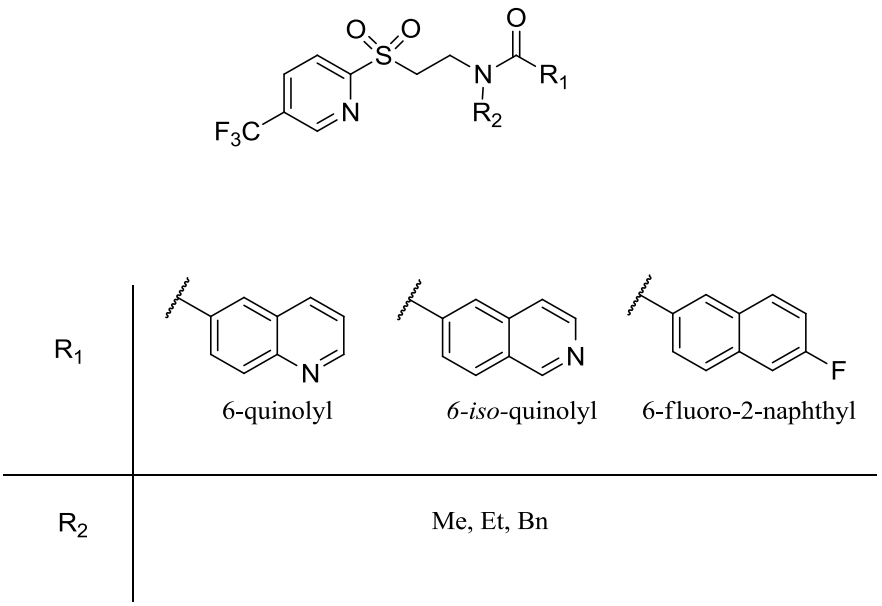

Figure 3.1: Suggested arylamide subtituents for future development of new PPARδ antagonists analogue to the GSK3787.

4 Spectroscopic elucidation and characterization of the compounds

4.1 General remarks on the characterization of intermediates and analogues

The prepared compounds consist, almost exclusively, of a common moiety (Figure 4.1), and some general characteristics in the recorded spectra of the compounds are noted here. Assigned spectra for each compound are found in the Appendix.

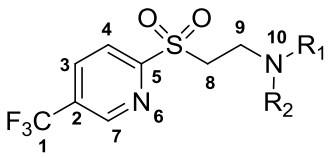

Figure 4.1: Common moiety in the prepared compounds.

The recorded ^{1}H NMR spectra show signals as expected from the available literature for the aliphatic and aromatic protons [44]. The signal from H-7, next to the nitrogen atom in the pyridine ring, appears downfield from the aromatic region, because of the deshielding from both the nitrogen atom and the CF_3-group. The signals from protons attached to N-10 in compounds where R_1/R_2 = H, vary from appearing as a triplet to a broad/narrow singlet around 6-8 ppm depending on solvents and concentration.

In the ^{13}C NMR, characteristic ^{13}C - ^{19}F splittings from the three fluorine atoms in the CF_3-group occur, and the C-1, C-2, C-3 and C-7 appear as quartets in the spectra. The C-1, closest to the fluorines, appears as a broad quartet (J = ~ 270 Hz) around 122.5 ppm, followed by C-2, as a smaller quartet (J = ~ 35 Hz) around 130 ppm (Figure 4.2). C-3 and C-7 appear as narrow quartets (J = ~ 3.5 Hz) around 136 ppm and 147 ppm, respectively (Figure 4.3).

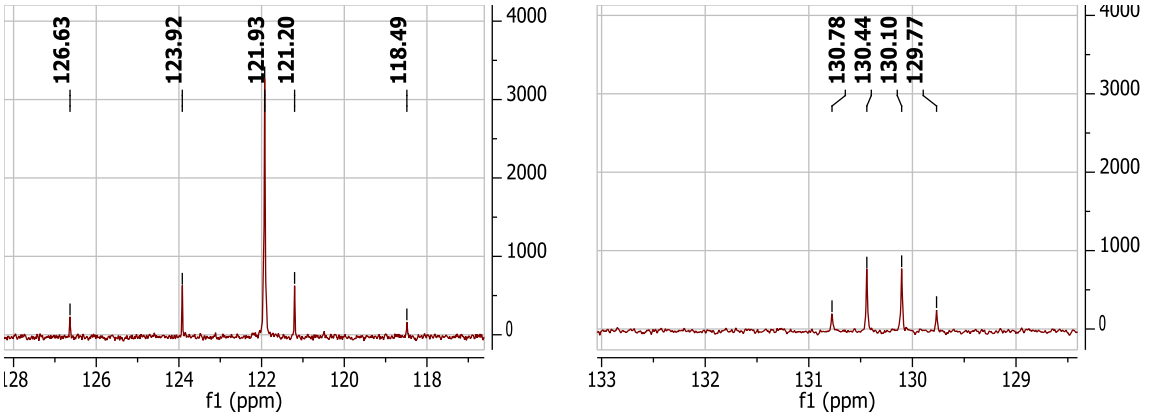

Figure 4.2: The splitting into quartets by fluorine in ^{13}C NMR spectra. The quartet (*J* = ~ 270 Hz) around 130 ppm belongs to C-1 and the quartet (*J* = ~ 35 Hz) around 122.5 ppm belongs to C-2.

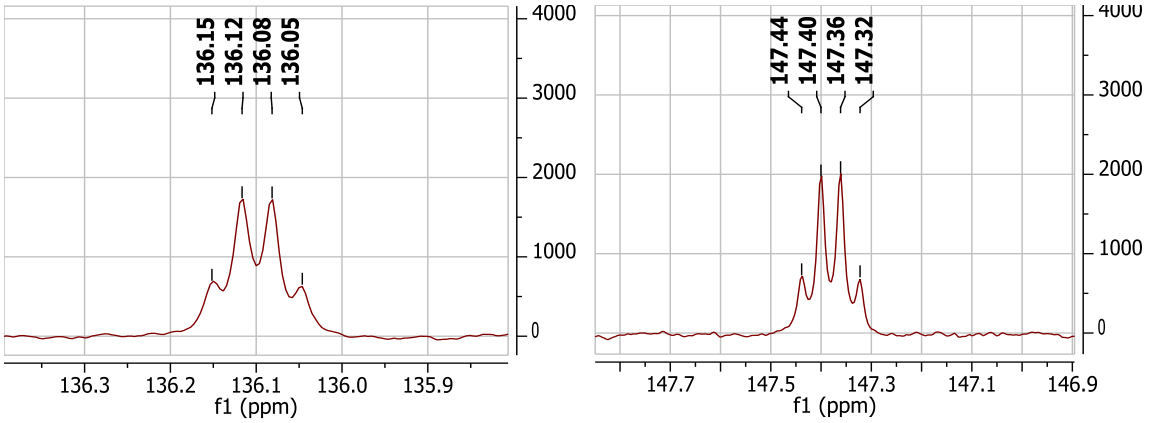

Figure 4.3: The splitting into quartets by fluorine in ^{13}C NMR spectra. These two quartets (*J* = ~ 3.5) belong to C-3 and C-7 and appear around 136 ppm and 147 ppm, respectively.

Due to this characteristic splitting of the carbon signals into quartets by fluorine, the intensity of the split signals becomes reduced, and in some spectra, the two outermost peaks in the quartets are not observable. Given the knowledge of the equidistance between the peaks of quartets in general [44], the coupling constants (*J*) of the quartets in the spectra in question, are calculated from the two observable peak values.

4.2 Observations of rotamers in the spectra of compounds 11, 13 and 15

In the ^{1}H NMR-spectra of compounds **11**, **13** and **15**, the signals from the aliphatic protons were broader than normal (Figure 4.4, Figure 4.5 and Figure 4.6).

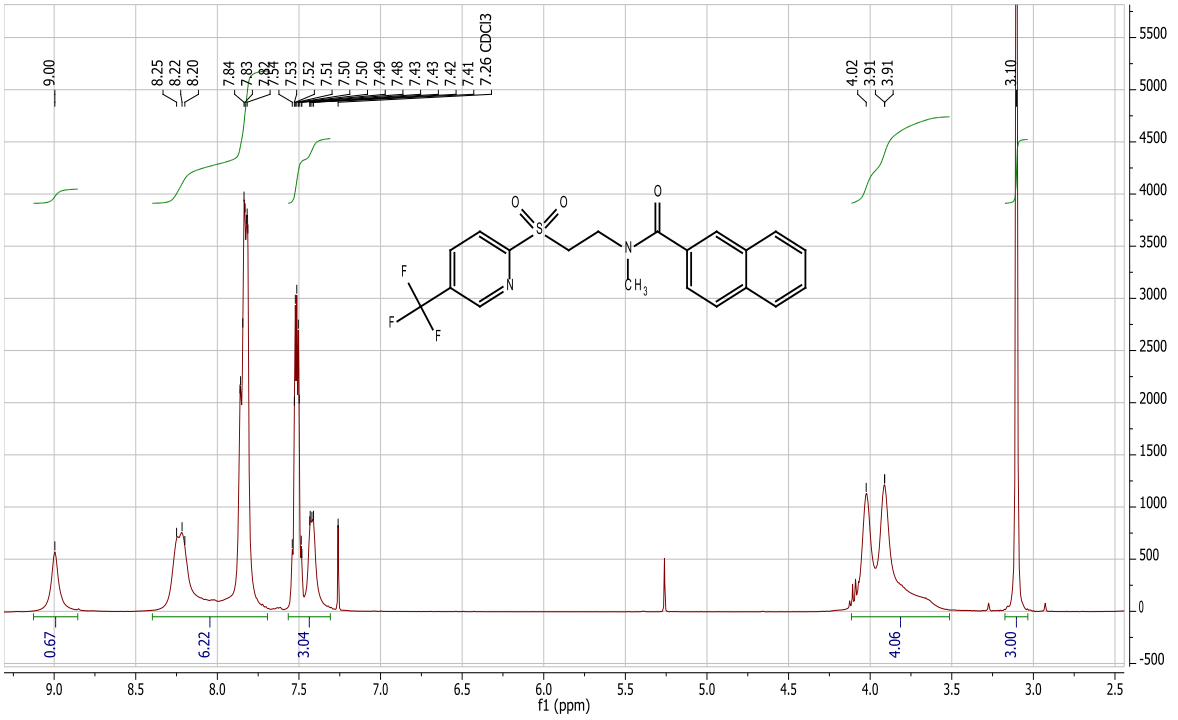

Figure 4.4: ^{1}H NMR of the *N*-methyl analogue 11, showing broad signals (3.5 - 4.0 ppm) from the aliphatic protons in the molecule.

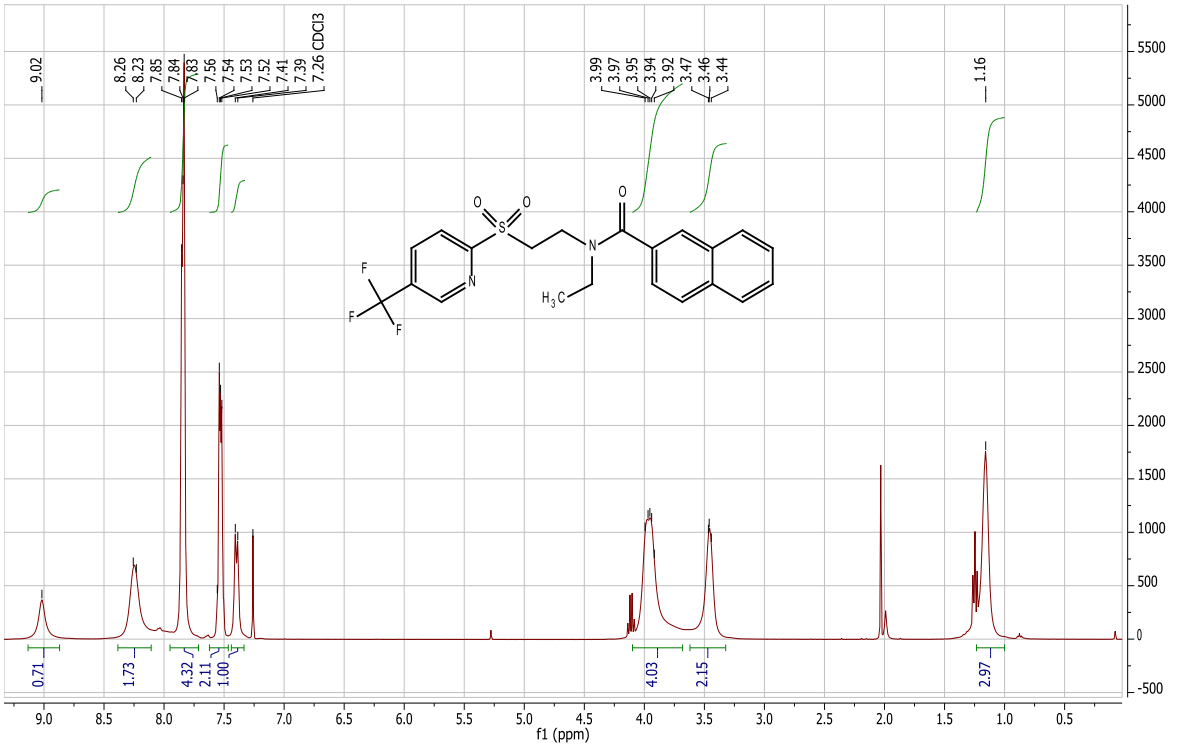

Figure 4.5: ^{1}H NMR of the *N*-ethyl analogue 13, showing broad signals (3.5 - 4.0 ppm) from the aliphatic protons in the molecule.

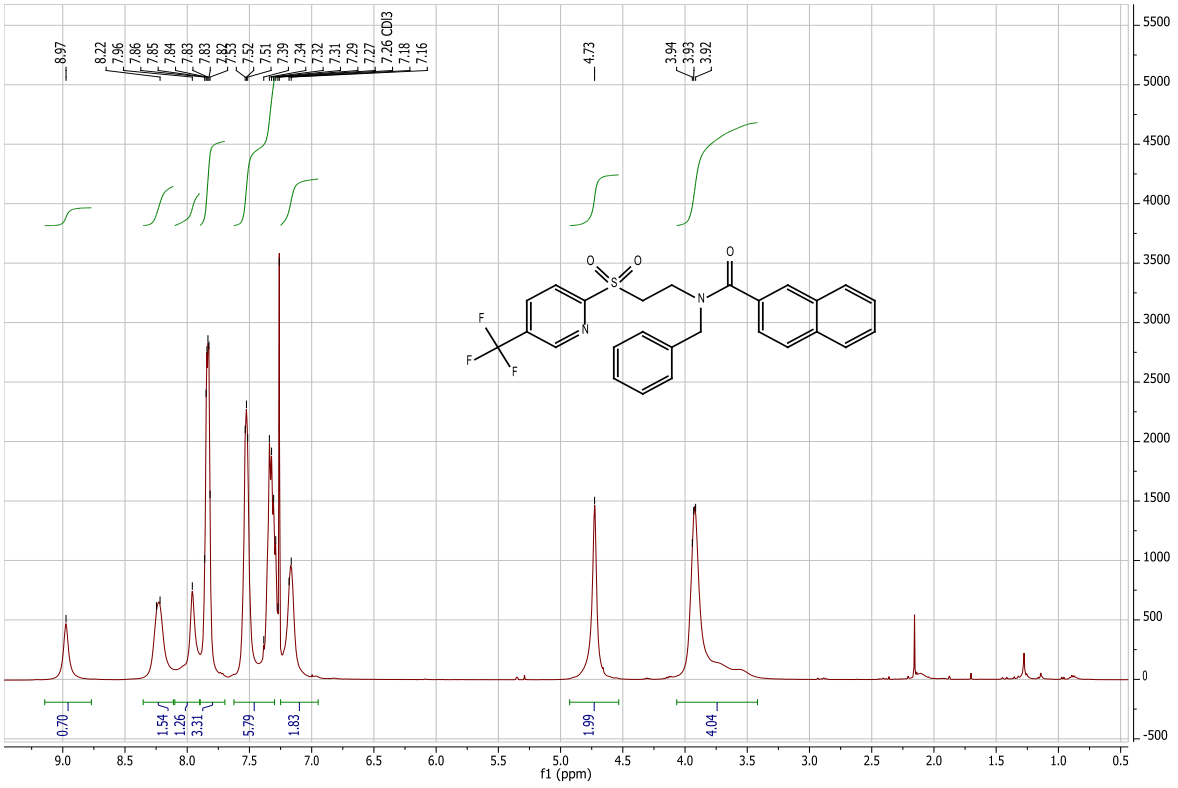

Figure 4.6: ^{1}H NMR of the *N*-benzyl analogue 15, showing broad signals (3.5 - 4.0 ppm) from the aliphatic protons in the molecule.

The compounds **11**, **13** and **15** carry alkyl substituents on their amide-nitrogens of the molecules. The structure of amides can be described with two resonance structures, of which the dominant one has a double bond between the carbonyl carbon and the amide nitrogen (Figure 4.7) [44].

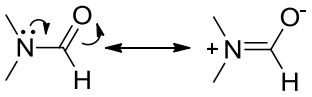

Figure 4.7: The structure of amides described with two resonance structures [44].

Rotation about the C=N double bond is very slow and more energy demanding, thus hindering the free rotation of the amide substituents [44]. The exchange of the s-*cis* and s-*trans* rotamers is sometimes observed in NMR spectroscopy when the barrier for rotation is sufficiently high, making the rotamers observable on NMR time scales [44].

In the NMR characterization of the final *N*-alkylated compounds **11**, **13** and **15**, we observed broader signals than normal for the aliphatic protons. This can be explained by the existence of rotamers. The *N*-H analogues did not show the same tendencies and rotamers were not observed until the insertion of the *N*-alkyl substituents. Interestingly, an *N*-methyl analogue with 4-fluorobenzyl as the arylamide moiety did not show rotamers in the spectra [41], as did the *N*-alkylated analogues with 2-naphthyl as the arylamide moiety. One explanation for this is probably the greater size and conformational behaviour of the 2-naphthyl group compared to the 4-fluorobenzyl group. This may cause a steric interaction with the *N*-alkyl group, that increases the energy barrier for exchange between the s-*cis*/s-*trans* rotamers, making them observable in the spectra.

To test this hypothesis, we recorded ^{1}H NMR-spectra of the *N*-benzyl analogue (**15**) at different temperatures, to see if the changes in the temperature would affect the speed of bond rotation in the molecule. The result show that as temperature increases, rotation speeds up and averages out the different rotameric conformations [44]. As we expected, coalescence of the aliphatic signals from the CH_2-groups was observed with increasing temperature.

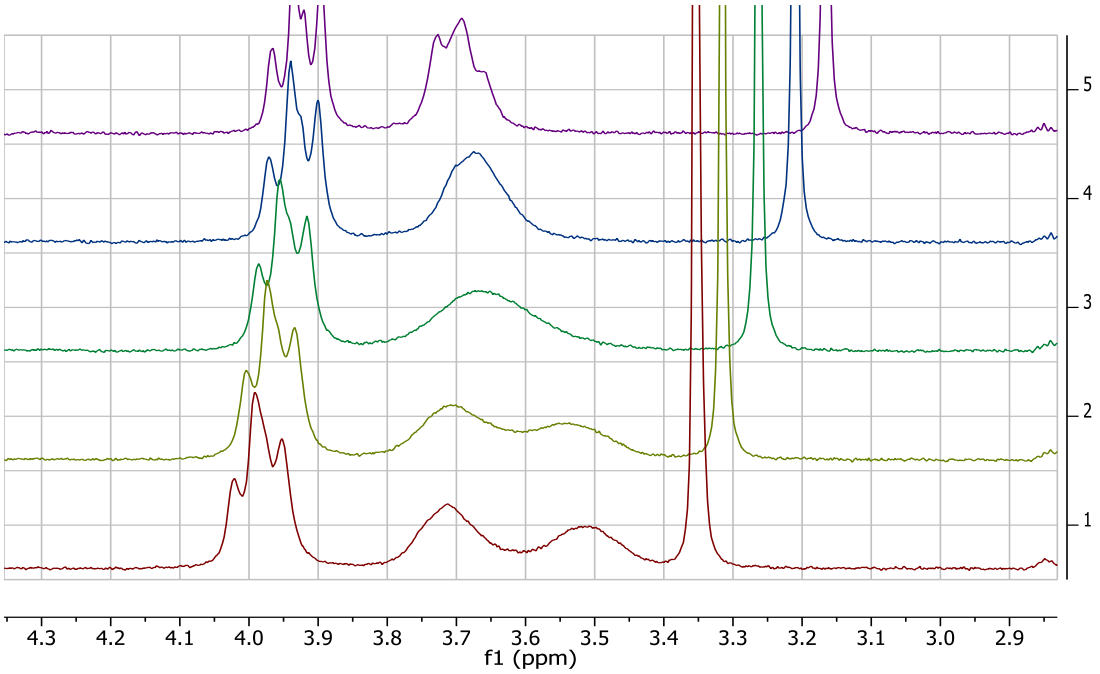

Figure 4.8: The aliphatic region in the ^{1}H NMR-spectra recorded on the DPX200 instrument at 21 °C (bottom red line), 27 °C, 37 °C, 47 °C and 57 °C, for the *N*-benzyl analogue 15, showing coalescence of the signals from the CH_2-groups (around 3.7 ppm) with increasing temperature.

To further confirm that the poor ^{1}H NMR spectra obtained at ambient temperature was not caused by impurities in the synthesis products, analytical HPLC was performed on the *N*-benzyl analogue (**15**), confirming > 98% purity of the product. The chromatogram is shown in the Appendix (Figure 7.28).

In the ^{1}H NMR spectra of the second batch of compound **15,** from the fifth approach, rotamers were also observable, further ensuring the rotamer hypothesis (Figure 4.9).

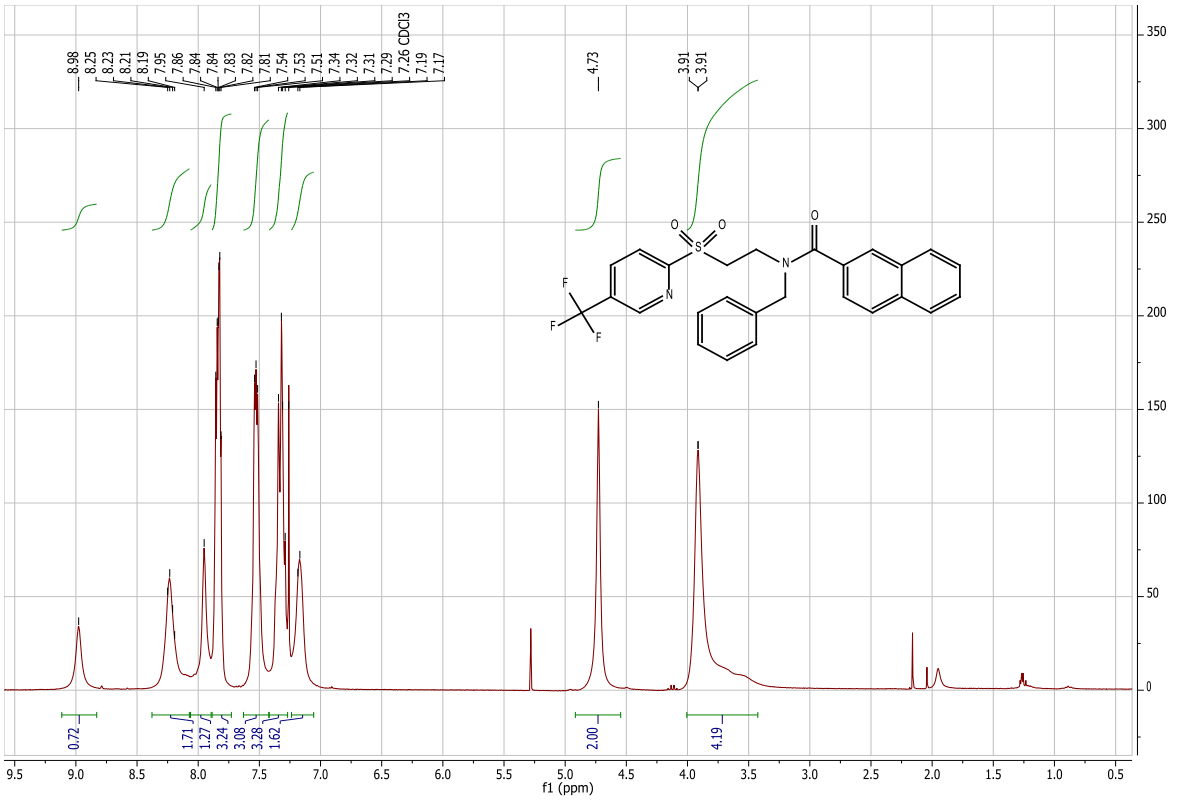

Figure 4.9: ^{1}H NMR of the *N*-benzyl analogue 15 from the fifth approach, showing the same broad signals from the aliphatic protons (around 3.5 - 4.0 ppm) as in the spectra of the same compound (Figure 4.6), prepared by *N*-alkylation on the sulfide 9.

5 Experimental

5.1 Materials and apparata

All reagents and solvents were purchased from Sigma-Aldrich, Fluka or Merck, and used without further purification unless otherwise mentioned. Solutions were prepared prior to use and benzaldehyde was distilled prior to use. TLC silica gel 60 F_{254}-plates from Merck, were used for thin-layer chromatography. Preparative chromatography was performed on silica gel 60 (40-63 µm, Fluka). Inert gas-atmosphere (N_2) and dry solvents were used in experiments with moisture and oxygen sensitive compounds.

NMR spectra were recorded on Bruker Avance DPX-300 or Bruker Avance AVII-400 spectrometers, operating at 300/400 MHz for ^{1}H and 75/101 MHz for ^{13}C, respectively. Spectra were recorded at 25 °C, unless otherwise noted. Coupling constants (*J*) are reported in hertz and chemical shift values (δ) in parts per million relative to the residual peaks for solvents used: ^{1}H /^{13}C, δ7.26/ δ77.16 ($CDCl_3$) and ^{1}H/^{13}C, δ2.50/ δ39.52 (DMSO-d_6). Analytical HPLC was performed on an Agilent 1200 series HPLC apparatus, with UV detection at 254 nm. Melting points were measured with a Stuart™ melting point apparatus (SPM3) and are uncorrected.

5.2 General experimental procedures

5.2.1 General procedure for oxidation with potassium peroxymonosulfate triple salt (Oxone™)

To a stirred solution of the sulfide (1 eq) in water:acetone (1:4, 20 mL), potassium peroxymonosulfate triple salt (Oxone™) (5 eq) was added and the reaction was stirred overnight. The acetone was removed under reduced pressure and the remaining suspension poured into water (40 mL) and extracted with EtOAc (2 x 40 mL). The combined extracts were washed with brine (40 mL) and dried over $MgSO_4$. The solvent was removed under

reduced pressure. The remaining solid was purified with preparative chromatography using the same solvent system as for the reported R_f values, indicated in the specific procedures for each compound.

5.2.2 General procedure for removal of Boc-protection groups

The Boc-protected compound (1 eq) was added to a solution of HCl in dioxane (4 M, 22 mL) and stirred for 3 hours at ambient temperature. The reaction was diluted with Et_2O (22 mL) and the resulting suspension was stirred for 10 minutes, before being filtered on a sintered glass funnel. The filter cake was washed with Et_2O and the solid dried for 2 hours under high vacuum, affording the HCl-salt which was used without further purification.

5.2.3 General procedure for the *N*-alkylation

To a stirred solution of the sulfide (1 eq) in dry THF (7 mL) on ice, was added NaH (60% dispersion in mineral oil) (1.5 eq). After 10 minutes the alkyl halide (10 eq) was added and the reaction was stirred for 4 hours at 40 °C, quenched with a saturated solution of NaH_2CO_3 (2 mL) and extracted with Et_2O (30 mL). The extract was washed with brine (10 mL) and dried over $MgSO_4$. The solvent was removed under reduced pressure and the remaining semisolid was solved in CH_2Cl_2 and filtered through a plug of silica. The solvent was removed under reduced pressure, affording an oil, which was used without further purification.

5.3 Synthesis of intermediates

5.3.1 Synthesis of *tert*-butyl(2-((5-(trifluoromethyl)pyridine-2-yl)thio)ethyl) carbamate (3)

To a stirred solution of 5-(trifluoromethyl)mercaptopyridine (**1**) (1.03 g, 5.73 mmol) in dry DMF (20 mL) at ambient temperature, was added Et_3N (2.00 mL, 14.38 mmol). After 5 minutes a solution of 2-(*N*-Boc-amino)ethyl bromide (**2**) (1.38 g, 6.16 mmol) in dry DMF (10 mL) was added and stirring was continued for 2 hours. The mixture was then poured into water (100 mL) and extracted with EtOAc (3 x 25 mL). The combined extracts were washed

with water (25 mL), brine (25 mL) and dried over $MgSO_4$. The solvent was removed under reduced pressure, yielding a slightly yellow solid (1.69 g, 88%). By ^{1}H NMR analysis the crude product was pure enough to be used without further purification.

Physical data:

^{1}H NMR (400 MHz, $CDCl_3$) δ 8.63 (bs, 1H), 7.70 – 7.62 (m, 1H), 7.32 – 7.26 (m, 1H), 5.09 (bs, 1H), 3.44 (t, *J* = 6.5 Hz, 2H), 3.33 (t, *J* = 6.3 Hz, 2H), 1.41 (s, 9H)

^{13}C NMR (101 MHz, $CDCl_3$) δ 163.56, 155.96, 146.29 (q, *J* = 4.3 Hz), 132.78 (q, *J* = 3.4 Hz), 123.85 (q, *J* = 271.6 Hz), 122.57 (q, *J* = 33.2 Hz), 121.91, 79.51, 40.43, 30.19, 28.47

R_f = 0.42 (1:4/EtOAc:hexane)

Mp: 89 - 92 °C

5.3.2 Synthesis of *tert*-butyl(2-((5-(trifluoromethyl)pyridine-2-yl)sulfonyl) ethyl)carbamate (4)

The title compound was afforded as a colorless solid (1.11 g, 55%) from *tert*-butyl(2-((5-(trifluoromethyl)pyridine-2-yl)thio)ethyl)carbamate (**3**) (1.69 g, 5.0 mmol) according to the general procedure for oxidation (Chapter 5.2.1).

Physical data:

^{1}H NMR (400 MHz, $CDCl_3$) δ 8.99 (s, 1H), 8.29 – 8.19 (m, 2H), 5.13 (s, 1H), 3.85 – 3.47 (m, 4H), 1.38 (s, 9H)

^{13}C NMR (101 MHz, $CDCl_3$) δ 160.67, 155.58, 147.38 (q, *J* = 3.9 Hz), 136.10 (q, *J* = 3.5 Hz), 130.27 (q, *J* = 33.9 Hz), 122.56 (q, *J* = 273.3 Hz), 121.93, 80.12, 52.24, 34.73, 28.39

R_f = 0.38 (40:60/EtOAc:hexane)

Mp: 146 - 148 °C

5.3.3 Synthesis of 2-((5-(trifluoromethyl)pyridine-2-yl)sulfonyl) ethanaminium chloride (5)

The title compound was afforded as a colorless solid (653 mg, 87%) from *tert*-butyl(2-((5-(trifluoromethyl)pyridine-2-yl)sulfonyl)ethyl)carbamate (**4**) (909 mg, 2.57 mmol), according to the general procedure for removal of Boc-protection groups (Chapter 5.2.2).

Physical data:

^{1}H NMR (300 MHz, DMSO-d_6) δ 9.44 – 9.17 (m, 1H), 8.66 (dd, *J* = 8.3, 2.3 Hz, 1H), 8.31 (d, *J* = 8.3 Hz, 1H), 8.22 (bs, 3H), 3.90 (t, 2H), 3.28 – 3.09 (m, 2H)

Mp: 193 - 196 °C

5.3.4 Synthesis of *N*-(2-((5-trifluoromethyl)pyridine-2-yl)sulfonyl)ethyl)2-naphtamide (7)

To a stirred solution of 2-((5-(trifluoromethyl)pyridine-2-yl)sulfonyl)ethanaminium chloride (**5**) (253 mg, 0.87 mmol) in dry THF (10 mL), was added Et_3N (0.60 mL, 4.09 mmol). After 10 minutes the reaction was cooled on ice, and 2-naphthoyl chloride (**6**) (383 mg, 2.00 mmol) was added drop wise. The reaction was stirred for 2 hours allowing the system to reach ambient temperature. The mixture was then poured into water (20 mL) and extracted with EtOAc (3 x 10 mL). The combined extracts were washed with saturated NH_4Cl-solution (3 x 10 mL), water (10 mL), brine (10 mL) and dried over $MgSO_4$. The solvent was removed under reduced pressure and the remaining solid was purified with preparative chromatography (2 % MeOH in CH_2Cl_2) affording a colorless solid (222 mg, 63%).

Physical data:

^{1}H NMR (300 MHz, DMSO-d_6) δ 9.08 – 9.02 (m, 1H), 8.65 (t, *J* = 5.3 Hz, 1H), 8.46 (dd, *J* = 8.2, 1.7 Hz, 1H), 8.26 (d, *J* = 8.2 Hz, 1H), 8.18 (bs, 1H), 7.99 – 7.87 (m, 3H), 7.68 (dd, *J* = 8.6, 1.7 Hz, 1H), 7.65 – 7.53 (m, 2H), 3.94 (t, *J* = 6.2 Hz, 2H), 3.71 (q, *J* = 6.0 Hz, 2H)

^{13}C NMR (101 MHz, DMSO-d_6) δ 165.96, 160.03, 147.17 (q, *J* = 4.0 Hz), 136.83 (q, *J* = 3.4 Hz), 134.15, 131.90, 130.62, 128.74, 128.17 (q, *J* = 33.0 Hz), 127.73, 127.62, 127.51, 127.25, 126.65, 123.59, 122.49 (q, *J* = 274.72 Hz), 122.17, 50.37, 33.86

R_f = 0.41 (2 % MeOH in CH_2Cl_2)

Mp: 175 - 178 °C

5.3.5 Synthesis of 2-((5-(trifluoromethyl)pyridine-2-yl)thio)ethanaminium chloride (8)

The title compound was afforded as a colorless solid (1.13 g, 90%) from *tert*-butyl(2-((5-(trifluoromethyl)pyridine-2-yl)thio)ethyl)carbamate (**3**) (1.65 g, 4.88 mmol) according to the general procedure for removal of Boc-protection groups (Chapter 5.2.2).

Physical data:

^{1}H NMR (300 MHz, DMSO-d_6) δ 8.91 – 8.58 (m, 1H), 8.43 (bs, 3H), 8.01 (dd, *J* = 8.6, 2.4 Hz, 1H), 7.62 (d, *J* = 8.5 Hz, 1H), 3.60 – 3.29 (m, 1H), 3.27 – 2.96 (m, 1H)

^{13}C NMR (101 MHz, DMSO-d_6) δ 162.75, 146.12 (q, *J* = 4.3 Hz), 133.65 (q, *J* = 3.4 Hz), 123.88 (q, *J* = 271.8 Hz), 122.12, 121.51 (q, *J* = 32.7 Hz), 38.24, 26.59

Mp: 215 - 220 °C

5.3.6 Synthesis of 2-((5-(trifluoromethyl)pyridine-2-yl)thio)ethyl)-2-naphtamide (9)

To a stirred solution of 2-((5-(trifluoromethyl)pyridine-2-yl)thio)ethanaminium chloride (**8**) (346 mg, 1.34 mmol) in dry THF (10 mL), was added Et_3N (1.2 mL, 6.29 mmol). After 10 minutes the reaction was cooled on ice and 2-naphthoyl chloride (**6**) (656 mg, 3.44 mmol) was added drop wise. The reaction was stirred for 2 hours, allowing the system to reach ambient temperature. The mixture was then poured into water (20 mL) and extracted with EtOAc (3 x 10 mL). The combined extracts were washed with saturated NH_4Cl-solution (3 x 10 mL), water (10 mL), brine (10 mL) and dried over $MgSO_4$. The solvent was removed under reduced pressure and the remaining solid was purified with preparative chromatography (1.5 % MeOH in CH_2Cl_2) affording a colorless solid (303 mg, 60%).

Physical data:

^{1}H NMR (400 MHz, $CDCl_3$) δ 8.79 – 8.69 (m, 1H), 8.25 (bs, 1H), 7.97 – 7.40 (m, 9H), 3.91 (t, *J* = 6.3 Hz, 1H), 3.72 – 3.57 (m, 1H)

^{13}C NMR (101 MHz, $CDCl_3$) δ 167.93, 164.07, 146.33 (q, *J* = 4.4 Hz), 134.88, 133.11 (q, *J* = 3.1 Hz), 132.72, 131.82, 128.91, 128.51, 127.89, 127.78, 127.43, 126.90, 123.74 (q, *J* = 276.74 Hz) 123.71, 123.04 (q, *J* = 33.5 Hz), 122.36, 41.16, 29.84

R_f = 0.24 (1.5 % MeOH in CH_2Cl_2)

Mp: 115 - 119 °C

5.4 The first approach: direct amide *N*-alkylation of the sulfone 7

5.4.1 Attempted synthesis of *N*-methyl-*N*-(2-((5-(trifluoromethyl)pyridine-2-yl)sulfonyl)ethyl)-2-naphtamide (11)

To a stirred solution of *N*-(2-((5-trifluoromethyl)pyridine-2-yl)sulfonyl)ethyl)-2-naphtamide (**7**) (100 mg, 0.25 mmol) in dry THF (4 mL), was added a solution of *t*-BuOK (92 mg, 0.82 mmol) in dry THF (2 mL). After 10 minutes MeI (0.10 mL, 1.61 mmol) was added and the reaction was stirred overnight at ambient temperature. The reaction was quenched with saturated NH_4Cl-solution (2 mL), poured into water (20 mL), extracted with CH_2Cl_2 (2 x 40 mL) and dried over $MgSO_4$. The solvent was removed under reduced pressure and the remaining brown-yellow semisolid was purified with preparative chromatography. None of the separated products afforded the desired one.

5.5 The second approach: direct amide *N*-alkylation of the sulfide 9

5.5.1 Synthesis of *N*-methyl-*N*-(2-((5-(trifluoromethyl)pyridine-2-yl)thio) ethyl)-2-naphtamide (10)

The title compound was afforded as a colorless oil (324 mg) from 2-((5-(trifluoromethyl)pyridine-2-yl)thio)ethyl)-2-naphtamide (**9**) (308 mg, 0.82 mmol) and MeI (0.50 mL, 8.03 mmol) according to the general procedure for *N*-alkylation (Chapter 5.2.3).

Physical data:

^{1}H NMR (400 MHz, DMSO-d_6) δ 8.84 (s, 1H), 8.16 – 7.06 (m, 9H), 3.98 – 3.44 (m, 4H), 3.06 (s, 3H)

R_f = 0.20 (30:70/EtOAc:hexane)

5.5.2 Synthesis of *N*-methyl-*N*-(2-((5-(trifluoromethyl)pyridine-2-yl) sulfonyl)ethyl)-2-naphtamide (11)

The title compound was afforded as a colorless solid (186 mg, 43% yield over two steps) from *N*-methyl-*N*-(2-((5-(trifluoromethyl)pyridine-2-yl)thio)ethyl)-2-naftamide (**10**) (324 mg) according to the general procedure for oxidation (Chapter 5.2.1).

Physical data:

^{1}H NMR (400 MHz, $CDCl_3$) δ 8.99 (s, 1H), 8.31 – 8.13 (m, 2H), 7.96 – 7.70 (m, 4H), 7.57 – 7.33 (m, 3H), 4.13 – 3.53 (m, 4H), 3.10 (s, 3H)

^{13}C NMR (101 MHz, $CDCl_3$) δ 171.85, 160.35, 147.19 (m), 135.98 (m), 133.72, 132.79, 132.56, 130.07 (q, J = 33.6 Hz), 128.42, 128.33, 127.81, 127.29, 127.01, 126.82, 124.07, 122.88 (q, J = 275.73 Hz), 121.95, 49.38, 42.29, 38.82

R_f = 0.37 (2 % MeOH in CH_2Cl_2)

Mp: 121 - 123 °C

5.5.3 Synthesis of *N*-ethyl-*N*-(2-((5-(trifluoromethyl)pyridine-2-yl)thio) ethyl)-2-naphtamide (12)

The title compound was afforded as a colorless oil (180 mg, 78%) from 2-((5-(trifluoromethyl)pyridine-2-yl)thio)ethyl)-2-naftamide (**9**) (200 mg, 0.53 mmol) and EtI (0.40 mL, 4.97 mmol) according to the general procedure for *N*-alkylation (Chapter 5.2.3).

Physical data:

^{1}H NMR (400 MHz, $CDCl_3$) δ 8.68 (bs, 1H), 7.95 – 6.95 (m, 9H), 3.95 – 3.09 (m, 6H), 1.45 – 1.05 (m, 3H)

R_f = 0.23 (0.5% MeOH in CH_2Cl_2)

5.5.4 Synthesis of *N*-ethyl-*N*-(2-((5-(trifluoromethyl)pyridine-2-yl) sulfonyl) ethyl)-2-naphtamide (13)

The title compound was afforded as a colorless oil (114 mg, 59%) from *N*-ethyl-*N*-(2-((5-(trifluoromethyl)pyridine-2-yl)thio)ethyl)-2-naphtamide (**12**) (180 mg, 0.41 mmol) according to the general procedure for oxidation (Chapter 5.2.1).

Physical data:

^{1}H NMR (400 MHz, $CDCl_3$) δ 9.02 (s, 1H), 8.39 – 7.69 (m, 6H), 7.58 – 7.47 (m, 2H), 7.45 – 7.33 (m, 1H), 4.10 – 3.67 (m, 4H), 3.59 – 3.31 (m, 2H), 1.16 (s, 3H)

^{13}C NMR (101 MHz, $CDCl_3$) δ 172.22, 160.55, 147.26 (m), 135.91 (q, J = 4.0 Hz), 133.69, 133.28, 132.72, 130.18 (q, J = 33.9 Hz), 128.50, 128.44, 127.89, 127.26, 126.91, 126.31, 122.78 (q, J = 274.72 Hz), 121.88, 60.45, 45.26, 39.42, 21.11

R_f = 0.16 (30:70/EtOAc:hexane)

5.5.5 Synthesis of *N*-benzyl-*N*-(2-((5-(trifluoromethyl)pyridine-2-yl)thio) ethyl)-2-naftamide (14)

The title compound was afforded as a colorless oil (151 mg, 61%) from 2-((5-(trifluoromethyl)pyridine-2-yl)thio)ethyl)-2-naftamide (**9**) (200 mg, 0.53 mmol) and BnBr (0.63 mL, 5.31 mmol) according to the general procedure for *N*-alkylation (Chapter 5.2.3), but

by adding TBAI (40 mg, 0.11 mmol) in addition to the other reagents. The temperature was increased to 50 °C instead of 40 °C. The purified product was used in the next step (oxidation) without characterization.

Physical data:

R_f = 0.4 (30:70/EtOAc:hexane)

5.5.6 Synthesis of *N*-benzyl-*N*-(2-((5-(trifluoromethyl)pyridine-2-yl) sulfonyl)ethyl)-2-naphtamide (15)

The title compound was afforded as a colorless crystals (69 mg, 65%) from *N*-benzyl-*N*-(2-((5-(trifluoromethyl)pyridine-2-yl)thio)ethyl)-2-naphtamide (**14**) (150 mg, 0.32 mmol) according to the general procedure for oxidation (Chapter 5.2.1), with additional re-crystallization from acetone:hexane to remove additional impurities.

Physical data:

^{1}H NMR (400 MHz, $CDCl_3$) δ 8.97 (s, 1H), 8.34 – 7.10 (m, 14H), 4.73 (m, 2H), 4.08 – 3.37 (m, 4H)

^{13}C NMR (101 MHz, $CDCl_3$) δ 172.43, 160.39, 147.18 (q, *J* = 3.6 Hz), 136.18 (q, *J* = 3.0 Hz), 135.92, 133.74, 132.69, 132.61, 130.04 (q, *J* = 33.4 Hz), 129.53, 129.03, 128.56, 128.46, 128.03, 127.82, 127.32, 127.17, 126.88, 123.93,122.42 (q, *J* = 272.7), 121.89, 77.32, 54.13, 49.58, 39.67

R_f = 0.31 (30:70/EtOAc:hexane)

Mp: 148 - 150 °C

5.6 The third approach; direct amide *N*-alkylation of the carbamate 3

5.6.1 The first attempt on synthesis of *tert*-butyl isopropyl(2-((5-(trifluoromethyl)pyridin-2-yl)thio)ethyl)carbamate (16)

The title compound was attempted to be afforded from 2-((5-(trifluoromethyl)pyridine-2-yl)thio)ethyl) carbamate (**3**) (338 mg, 1.00 mmol) and *i*-PrBr (0.94 mL, 10.01 mmol) according to the general procedure for *N*-alkylation (Chapter 5.2.3), but by adding TBAI (74 mg, 0.20 mmol) in addition to the other reagents. The reaction was stirred for 2 days at ambient temperature, instead of 4 hours at 40 °C, and was not filtered through a plug of silica. NMR of the crude product showed low yield of the desired product, and was not further purified or used in synthesis.

5.6.2 The second attempt on synthesis of *tert*-butyl isopropyl(2-((5-(trifluoromethyl)pyridin-2-yl)thio)ethyl)carbamate (16)

The title compound was attempted to be afforded from 2-((5-(trifluoromethyl)pyridine-2-yl)thio)ethyl) carbamate (**3**) (338 mg, 1.00 mmol) and *i*-PrBr (0.30 mL, 3.19 mmol) according to the general procedure for *N*-alkylation (Chapter 5.2.3), but by adding TBAI (1.19 g, 3.22 mmol) and Cs_2CO_3 (999 mg, 3.07 mmol) in addition to the other reagents. The reaction was stirred for 1 day at ambient temperature, 1 day at 40 °C and 4 days at 50 °C, instead of 4 hours at 40 °C. Additionally 3 eq. of *i*-PrBr was added to the reaction at day 5. Monitoring the reaction with TLC, showed no or a very low yield of any possible product, and the reaction was abandoned.

5.7 The fourth approach; the reductive amination route

5.7.1 Synthesis of 2-(benzylamino)ethanol (19)

To a stirred solution of benzaldehyde (**17**) (1.58 mL, 23.0 mmol) in methanol (100 mL) on ice, was added ethanolamine (**18**) (1.22 mL, 20.0 mmol) and stirring was continued for 7 hours allowing the reaction to reach ambient temperature. The mixture was re-cooled on ice, and $NaBH_4$ (1.74 g, 46.0 mmol) was added slowly. Stirring was continued overnight at ambient temperature and the reaction was quenched with HCl (6M) to pH 4. The solvent was removed under reduced pressure and the remaining aqueous suspension was poured into water (70 mL) and washed with CH_2Cl_2 (3 x 70 mL). The pH of the aqueous layer was adjusted with Na_2CO_3 (s) to pH 10, extracted with CH_2Cl_2 (2 x 60 mL) and the extracts were dried over $MgSO_4$. The solvent was removed under reduced pressure to afford a colorless oil (2.00 g, 66%), that by ^{1}H NMR analyzes was pure enough to be used without further purification.

Physical data:

^{1}H NMR (400 MHz, $CDCl_3$) δ 7.45 – 7.04 (m, 5H), 3.93 – 3.75 (m, 2H), 3.66 (t, 2H), 2.80 (t, 2H), 2.46 (bs, 2H)

5.7.2 Synthesis of *tert*-butyl benzyl(2-hydroxyethyl)carbamate (20)

To a stirred solution of 2-(benzylamino)ethanol (**19**) (1.98 g, 13.08 mmol) in CH_2Cl_2 (45 mL) and NaOH (1 M, 35 mL), was added a solution of Boc_2O (2.86 g, 13.08 mmol) in CH_2Cl_2 (50 mL) slowly. The reaction was stirred overnight at ambient temperature, and the layers separated. The aqueous layer was extracted with CH_2Cl_2 (2 x 20 mL), the collected extracts washed with water (2 x 20 mL), brine (25 mL) and dried over Na_2SO_4. The solvent was removed under reduced pressure to afford a colorless oil (3.00 g, 93%), that by ^{1}H NMR analyzes was pure enough to be used without further purification.

Physical data:

^{1}H NMR (400 MHz, $CDCl_3$) δ 7.41 – 7.12 (m, 5H), 4.50 (m, 2H), 3.81 – 3.62 (m, 2H), 3.40 (m, 2H), 2.58 (bs, 1H), 1.54 (s, 9H)

R_f = 0.22 (40:60/EtOAc:hexane)

5.7.3 First attempt on synthesis of *tert*-butyl benzyl(2-bromoethyl)carbamate (21)

To a stirred solution of *tert*-butyl benzyl(2-hydroxyethyl)carbamate (**20**) (307 mg, 1.23 mmol) in CH_2Cl_2 (6 mL), was added PPh_3 (402 mg, 1.53 mmol), CBr_4 (601 mg, 1.81 mmol) and pyridine (0.16 mL, 2.04 mmol). The reaction was stirred for 1 hour, the suspension filtered and cold Et_2O was added drop wise to the filtrate until precipitation of a colorless solid was observed. The resulting suspension was filtered, washed with cold Et_2O (2 mL) and the solvent was removed under reduced pressure. This afforded a yellow semisolid that was purified with preparative chromatography, using 1-50% EtOAc in hexane, as the solvent system. The desired product could not be afforded, probably due to its invisibility on TLC plates when analyzing the fractions.

5.7.4 Second attempt on synthesis of *tert*-butyl benzyl(2-bromoethyl)carbamate (21)

To a stirred solution of *tert*-butyl benzyl(2-hydroxyethyl)carbamate (**20**) (157 mg, 0.63 mmol) in CH_2Cl_2 (3 mL), was added PPh_3 (206 mg, 0.78 mmol), CBr_4 (304 mg, 0.92 mmol) and pyridine (0.08 mL, 1.02 mmol). The reaction was stirred for 2 hours, the solvent was removed under reduced pressure and the afforded colorless solid (206 mg) was used without further purification or characterization.

5.7.5 Attempted synthesis of *tert*-butyl benzyl(2-((5-(trifluoromethyl) pyridine-2-yl)thio)ethyl) carbamate (23)

To a stirred solution of the crude product from the synthesis of *tert*-butyl benzyl(2-bromoethyl)carbamate (**21**) (206 mg) in dry DMF (4 mL), was added Et_3N (0.25 mL, 1.8 mmol) and 5-(trifluoromethyl)mercaptopyridine (**1**) (106 mg, 0.6 mmol) and the reaction was stirred overnight at ambient temperature. The mixture was poured into water (50 mL) and extracted with EtOAc (3 x 20 mL). The collected extracts were washed with water (20 mL), brine (20 mL) and dried over $MgSO_4$. The solvent was removed under reduced pressure and

the remaining solid purified with preparative chromatography, affording a yellow oil (102 mg). Due to significant amounts of impurities (probably triphenylphosphineoxide) in the ^{1}H NMR-spectra, the purified product was not used in further synthesis.

5.7.6 Synthesis of 2-(benzyl(*tert*-butoxycarbonyl)amino)ethyl methane sulfonate (22)

To a stirred solution of *tert*-butyl benzyl(2-hydroxyethyl)carbamate (**20**) (308 mg, 1.2 mmol) in dry CH_2Cl_2 (5 mL) on ice, was added Et_3N (0.18 mL, 1.32 mmol). Mesyl chloride (0.10 mL, 1.32 mmol) was then added drop wise to the reaction and stirring was continued for 1 hour at ambient temperature. The mixture was poured into brine (20 mL) and extracted with EtOAc (3 x 5 mL). The collected extracts were washed with a saturated solution of $NaHCO_3$ (2 x 5 mL), brine (2 x 5 mL) and dried over Na_2SO_4. The solvent was removed under reduced pressure and a yellow oil was afforded (345 mg, 88%), that showed one spot by TLC analysis. The crude product was used without further purification or characterization.

Physical data:

R_f= 0.2 (30:70/ EtOAc:hexane)

5.7.7 Synthesis of *tert*-butyl benzyl(2-((5-(trifluoromethyl)pyridin-2-yl) thio)ethyl)carbamate (23)

To a stirred solution of 2-(benzyl(*tert*-butoxycarbonyl)amino)ethyl methanesulfonate (**22**) (345 mg, 1.06 mmol) in dry DMF (6 mL), was added Et_3N (0.42 mL, 3.02 mmol) and 5-(trifluoromethyl)mercaptopyridine (**1**) (166 mg, 0.93 mmol) and the reaction was stirred overnight at ambient temperature. The mixture was poured into water (30 mL) and extracted with EtOAc (3 x 15 mL). The collected extracts were washed with brine (15 mL) and dried over $MgSO_4$. The solvent was removed under reduced pressure and the remaining yellow oil was purified with preparative chromatography, that afforded a yellow oil (15 mg, 4%). ^{1}H NMR data of the product (**23**) is found in Chapter 5.7.8 below, and is from the second synthesis of this compound.

5.7.8 "One-pot" synthesis of *tert*-butyl benzyl(2-((5-(trifluoromethyl) pyridine-2-yl)thio)ethyl) carbamate (23)

To a stirred solution of *tert*-butyl benzyl(2-hydroxyethyl)carbamate (**20**) (302 mg, 1.21 mmol) in dry CH_2Cl_2 (6 mL) on ice, was added Et_3N (0.35 mL, 2.52 mmol). Mesyl chloride (0.12 mL, 1.44 mmol) was then added drop wise to the reaction and stirring was continued for 1 hour at ambient temperature. Monitoring with TLC showed no spot for starting material and a possible spot for product. Another 2 eq. of Et_3N (0.35 mL, 2.52 mmol) and a suspension of 5-(trifluoromethyl) mercaptopyridine (**1**) (214 mg, 1.19 mmol) in dry CH_2Cl_2 (2 mL) was added to the reaction and stirring continued overnight. The mixture was poured into a saturated solution of Na_2CO_3 (40 mL) and extracted with EtOAc (3 x 25 mL). The collected extracts were washed with a saturated solution of Na_2CO_3 (2 x 25 mL), brine (25 mL) and dried over $MgSO_4$. The solvent was removed under reduced pressure and the remaining semisolid (468 mg) purified with preparative chromatography. This afforded a yellow oil (70 mg, 14%).

Physical data:

^{1}H NMR (400 MHz, $CDCl_3$) δ 8.55 (bs, 1H), 7.57 (dd, *J* = 8.5, 2.3 Hz, 1H), 7.33 – 7.08 (m, 6H), 4.61 – 4.32 (m, 2H), 3.50 – 3.33 (m, 2H), 3.33 – 3.13 (m, 2H), 1.40 (s, 9H)

R_f= 0.24 (5:95/EtOAc:hexane)

5.7.9 "One-pot" synthesis of *tert*-butyl benzyl(2-((5-(trifluoromethyl) pyridine-2-yl)thio)ethyl) carbamate (23) in the presence of NaI

The title compound was attempted to be synthesized from *tert*-butyl benzyl(2-hydroxyethyl)carbamate (**20**) (294 mg, 1.18 mmol), mesyl chloride (0.12 mL, 1.44 mmol) and 5-(trifluoromethyl)mercaptopyridine (**1**) (217 mg, 1.20 mmol), according to the procedure for the second attempt on synthesis of the same compound (**23**), chapter 5.7.8, with the exception of addition of NaI (183 mg, 1.20 mmol) to the reaction. TLC showed very low yields of the desired product and the reaction was abandoned.

5.8 The fifth approach; acylation of a *N*-benzyl HCl-salt (29)

5.8.1 *N*-benzyl-*N*-(2-((5-(trifluoromethyl)pyridine-2-yl)sulfonyl)) ethanaminium chloride (29)

Synthesis of **29** was performed by Ph. D. student Åsmund Kaupang according to Scheme 2.11 and experimental details is not reported here.

Physical data:

^{1}H NMR (400 MHz, DMSO-d_6) δ 9.89 (bs, 2H), 9.26 (s, 1H), 8.66 (dd, *J* = 8.3, 2.3 Hz, 1H), 8.31 (d, *J* = 8.2 Hz, 1H), 7.61 – 7.47 (m, 2H), 7.46 – 7.24 (m, 3H), 4.17 (s, 2H), 4.14 – 4.04 (m, 2H), 3.42 – 3.20 (m, 2H)

^{13}C NMR (101 MHz, DMSO-d_6) δ 159.03, 147.57 (q, *J* = 3.9 Hz), 137.44 (q, *J* = 3.6 Hz), 131.76, 129.99, 128.93, 128.87 (q, *J* = 33.1 Hz), 128.62, 122.73 (q, *J* = 273.5 Hz), 122.49, 49.71, 47.83, 39.60

5.8.2 Synthesis of *N*-benzyl-*N*-(2-((5-(trifluoromethyl)pyridine-2-yl) sulfonyl)ethyl)-2-naphtamide (15)

To a stirred solution of *N*-benzyl-*N*-(2-((5-(trifluoromethyl)pyridine-2-yl)sulfonyl)) ethanaminium chloride (**29**) (89 mg, 0.24 mmol) in dry THF (5 mL), was added Et_3N (0.17 mL, 1.13 mmol). After 10 minutes the reaction was cooled on ice and 2-naphthoyl chloride (**6**) (91 mg, 0.47 mmol) was added drop wise. The reaction was stirred for 5 hours, allowing the system to reach ambient temperature. The mixture was then poured into saturated solution of Na_2CO_3 (10 mL) and extracted with EtOAc (3 x 5 mL). The combined extracts were washed with a saturated solution of Na_2CO_3 (3 x 10 mL), brine (10 mL) and dried over $MgSO_4$. The solvent was removed under reduced pressure and the remaining solid was purified with preparative chromatography affording a colorless solid (98 mg, 84%).

Physical data:

^{1}H NMR (300 MHz, $CDCl_3$) δ 8.98 (bs, 1H), 8.40 – 7.07 (m, 14H), 4.94 – 4.53 (m, 2H), 4.03 – 3.42 (m, 4H)

R_f = 0.3 (20:80/EtOAc:hexane)

Mp: 149 - 151 °C

6 References

[1] Kota, B. P.; Huang, T. H. and Roufogalis, B. D. *An overview on biological mechanisms of PPARs*. Pharmacol Res, 2005. **51**(2): p. 85-94.

[2] Berger, J. and Moller, D. E. *The mechanisms of action of PPARs*. Annu Rev Med, 2002. **53**: p. 409-35.

[3] R., Flegal K.M.; Carroll M. D.; Ogden C. L.; Curtin L. *Prevalence and trends in obesity among us adults, 1999-2008*. JAMA, 2010. **303**(3): p. 235-241.

[4] World Health Organization. *Obesity and overweight (Fact sheet N°311)*. 2013. Available from: http://www.who.int/mediacentre/factsheets/fs311/en/ Access date: 14.03.2013

[5] Takahashi, S.; Tanaka, T. and Sakai, J. *New therapeutic target for metabolic syndrome: PPARdelta*. Endocr J, 2007. **54**(3): p. 347-57.

[6] Saltiel, A. R. and Kahn, C. R. *Insulin signalling and the regulation of glucose and lipid metabolism*. Nature, 2001. **414**(6865): p. 799-806.

[7] Nieves, D. J.; Cnop, M.; Retzlaff, B.; Walden, C. E.; Brunzell, J. D.; Knopp, R. H. and Kahn, S. E. *The atherogenic lipoprotein profile associated with obesity and insulin resistance is largely attributable to intra-abdominal fat*. Diabetes, 2003. **52**(1): p. 172-9.

[8] Rang, H. P.; Dale, M. M. and Ritter, J. M. *Rang and Dale's pharmacology*. 6th edition. Churchill Livingstone. England, 2007. (ISBN: 9780443069116)

[9] Smyth, S. and Heron, A. *Diabetes and obesity: the twin epidemics*. Nat Med, 2006. **12**(1): p. 75-80.

[10] Muoio, D. M. and Newgard, C. B. *Obesity-related derangements in metabolic regulation*. Annu Rev Biochem, 2006. **75**: p. 367-401.

[11] Norsk Helse Informatikk. *Metabolsk syndrom*. 2011. Available from: http://nhi.no/livsstil/kosthold/overvekt/metabolsk-syndrom-12407.html?page=all Access date: 14.03.2013

[12] Zhang, F.; Lavan, B. and Gregoire, F. M. *Peroxisome proliferator-activated receptors as attractive antiobesity targets*. Drug News Perspect, 2004. **17**(10): p. 661-9.

[13] Norsk legemiddelhåndbok for helsepersonell. 2010. Available from: http://legemiddelhandboka.no/ Access date: 14.03.2013

[14] Plutzky, J. *PPARs and Their Emerging Role in Vascular Biology, Inflammation, and Atherosclerosis*. 2nd edition. Humana Press. England, 2005. p. 93-105. (ISBN: 978-1-58829-413-5)

[15] Brown, J. D. and Plutzky, J. *Peroxisome proliferator-activated receptors as transcriptional nodal points and therapeutic targets*. Circulation, 2007. **115**(4): p. 518-33.

[16] Aagaard, M. M.; Siersbaek, R. and Mandrup, S. *Molecular basis for gene-specific transactivation by nuclear receptors*. Biochim Biophys Acta, 2011. **1812**(8): p. 824-35.

[17] Zoete, V.; Grosdidier, A. and Michielin, O. *Peroxisome proliferator-activated receptor structures: ligand specificity, molecular switch and interactions with regulators*. Biochim Biophys Acta, 2007. **1771**(8): p. 915-25.

[18] Pirat, C.; Farce, A.; Lebegue, N.; Renault, N.; Furman, C.; Millet, R.; Yous, S.; Speca, S.; Berthelot, P.; Desreumaux, P. and Chavatte, P. *Targeting peroxisome proliferator-activated receptors (PPARs): development of modulators*. J Med Chem, 2012. **55**(9): p. 4027-61.

[19] Schopfer, F. J.; Cole, M. P.; Groeger, A. L.; Chen, C. S.; Khoo, N. K.; Woodcock, S. R.; Golin-Bisello, F.; Motanya, U. N.; Li, Y.; Zhang, J.; Garcia-Barrio, M. T.; Rudolph, T. K.; Rudolph, V.; Bonacci, G.; Baker, P. R.; Xu, H. E.; Batthyany, C. I.; Chen, Y. E.; Hallis, T. M. and Freeman, B. A. *Covalent peroxisome proliferator-activated receptor gamma adduction by nitro-fatty acids: selective ligand activity and anti-diabetic signaling actions*. J Biol Chem, 2010. **285**(16): p. 12321-33.

[20] Ciocoiu, C. C. *Synthesis and biological evaluation of regulators of peroxisome proliferator-activated receptors*. Dissertations for the degree of Ph. D., School of Pharmacy, Faculty of Mathematics and Natural Sciences, University of Oslo, 2010.

[21] Ehrenborg, E. and Krook, A. *Regulation of skeletal muscle physiology and metabolism by peroxisome proliferator-activated receptor delta*. Pharmacol Rev, 2009. **61**(3): p. 373-93.

[22] Poulsen, L. C.; Siersbaek, M. and Mandrup, S. *PPARs: fatty acid sensors controlling metabolism*. Semin Cell Dev Biol, 2012. **23**(6): p. 631-9.

[23] Seedorf, U. and Aberle, J. *Emerging roles of PPARδ in metabolism*. Biochim Biophys Acta, 2007. **1771**(9): p. 1125-1131.

[24] European Medicines Agency. *Questions and answers on the review of medicines containing fibrates*. 2010. Available from: http://www.ema.europa.eu/docs/en_GB/document_library/Referrals_document/Fibrates_31/WC500098373.pdf Access date: 14.03.2013

[25] Cermola, M.; DellaGreca, M.; Iesce, M. R.; Previtera, L.; Rubino, M.; Temussi, F. and Brigante, M. *Phototransformation of fibrate drugs in aqueous media*. Environmental Chemistry Letters, 2005. **3**(1): p. 43-47.

[26] Felleskatalogen. 2013. Available from: http://www.felleskatalogen.no/medisin Access date: 14.03.2013

[27] Sznaidman, M. L.; Haffner, C. D.; Maloney, P. R.; Fivush, A.; Chao, E.; Goreham, D.; Sierra, M. L.; LeGrumelec, C.; Xu, H. E.; Montana, V. G.; Lambert, M. H.; Willson, T. M.; Oliver, W. R., Jr. and Sternbach, D. D. *Novel selective small molecule agonists for peroxisome proliferator-activated receptor delta (PPARdelta)--synthesis and biological activity*. Bioorg Med Chem Lett, 2003. **13**(9): p. 1517-21.

[28] Kang, K.; Hatano, B. and Lee, C. H. *PPAR delta agonists and metabolic diseases*. Curr Atheroscler Rep, 2007. **9**(1): p. 72-7.

[29] Luquet, S.; Lopez-Soriano, J.; Holst, D.; Fredenrich, A.; Melki, J.; Rassoulzadegan, M. and Grimaldi, P. A. *Peroxisome proliferator-activated receptor delta controls muscle development and oxidative capability*. FASEB J, 2003. **17**(15): p. 2299-301.

[30] Holst, D.; Luquet, S.; Nogueira, V.; Kristiansen, K.; Leverve, X. and Grimaldi, P. A. *Nutritional regulation and role of peroxisome proliferator-activated receptor delta in fatty acid catabolism in skeletal muscle*. Biochim Biophys Acta, 2003. **1633**(1): p. 43-50.

[31] Leibowitz, M. D.; Fievet, C.; Hennuyer, N.; Peinado-Onsurbe, J.; Duez, H.; Bergera, J.; Cullinan, C. A.; Sparrow, C. P.; Baffic, J.; Berger, G. D.; Santini, C.; Marquis, R. W.; Tolman, R. L.; Smith, R. G.; Moller, D. E. and Auwerx, J. *Activation of PPARdelta alters lipid metabolism in db/db mice*. FEBS Lett, 2000. **473**(3): p. 333-6.

[32] Akiyama, T. E.; Lambert, G.; Nicol, C. J.; Matsusue, K.; Peters, J. M.; Brewer, H. B., Jr. and Gonzalez, F. J. *Peroxisome proliferator-activated receptor beta/delta regulates very low density lipoprotein production and catabolism in mice on a Western diet*. J Biol Chem, 2004. **279**(20): p. 20874-81.

[33] Adhikary, T.; Brandt, D. T.; Kaddatz, K.; Stockert, J.; Naruhn, S.; Meissner, W.; Finkernagel, F.; Obert, J.; Lieber, S.; Scharfe, M.; Jarek, M.; Toth, P. M.; Scheer, F.; Diederich, W. E.; Reinartz, S.; Grosse, R.; Muller-Brusselbach, S. and Muller, R. *Inverse PPARbeta/delta agonists suppress oncogenic signaling to the ANGPTL4 gene and inhibit cancer cell invasion*. Oncogene online publications, 2012. DOI: 10.1038/onc.2012.549.

[34] Zaveri, N. T.; Sato, B. G.; Jiang, F.; Calaoagan, J.; Laderoute, K. R. and Murphy, B. J. *A novel peroxisome proliferator-activated receptor delta antagonist, SR13904, has anti-proliferative activity in human cancer cells*. Cancer Biol Ther, 2009. **8**(13): p. 1252-61.

[35] Shearer, B. G.; Steger, D. J.; Way, J. M.; Stanley, T. B.; Lobe, D. C.; Grillot, D. A.; Iannone, M. A.; Lazar, M. A.; Willson, T. M. and Billin, A. N. *Identification and characterization of a selective peroxisome proliferator-activated receptor beta/delta (NR1C2) antagonist*. Mol Endocrinol, 2008. **22**(2): p. 523-9.

[36] Shearer, B. G.; Wiethe, R. W.; Ashe, A.; Billin, A. N.; Way, J. M.; Stanley, T. B.; Wagner, C. D.; Xu, R. X.; Leesnitzer, L. M.; Merrihew, R. V.; Shearer, T. W.; Jeune, M. R.; Ulrich, J. C. and Willson, T. M. *Identification and characterization of 4-chloro-N-(2-{[5-trifluoromethyl)-2-pyridyl]sulfonyl}ethyl)benzamide (GSK3787), a selective and irreversible peroxisome*

proliferator-activated receptor delta (PPARdelta) antagonist. J Med Chem, 2010. **53**(4): p. 1857-61.

[37] Naruhn, S.; Toth, P. M.; Adhikary, T.; Kaddatz, K.; Pape, V.; Dorr, S.; Klebe, G.; Muller-Brusselbach, S.; Diederich, W. E. and Muller, R. *High-affinity peroxisome proliferator-activated receptor beta/delta-specific ligands with pure antagonistic or inverse agonistic properties*. Mol Pharmacol, 2011. **80**(5): p. 828-38.

[38] Toth, P. M.; Naruhn, S.; Pape, V. F.; Dorr, S. M.; Klebe, G.; Muller, R. and Diederich, W. E. *Development of improved PPARbeta/delta inhibitors*. ChemMedChem, 2012. **7**(1): p. 159-70.

[39] Lieber, S.; Scheer, F.; Meissner, W.; Naruhn, S.; Adhikary, T.; Muller-Brusselbach, S.; Diederich, W. E. and Muller, R. *(Z)-2-(2-bromophenyl)-3-{[4-(1-methyl-piperazine)amino]phenyl}acrylonitrile (DG172): an orally bioavailable PPARbeta/delta-selective ligand with inverse agonistic properties*. J Med Chem, 2012. **55**(6): p. 2858-68.

[40] Kasuga, J.; Ishida, S.; Yamasaki, D.; Makishima, M.; Doi, T.; Hashimoto, Y. and Miyachi, H. *Novel biphenylcarboxylic acid peroxisome proliferator-activated receptor (PPAR) delta selective antagonists*. Bioorg Med Chem Lett, 2009. **19**(23): p. 6595-9.

[41] Vo, C. X. T. *Synthesis of putative peroxisome proliferator-activated receptor δ antagonists*. Dissertation for the degree of Master of Pharmacy, School of Pharmacy, Faculty of Mathematics and Natural Sciences, University of Oslo, 2012.

[42] Ciocoiu, C. C.; Ravna, A. W.; Sylte, I.; Thoresen, H. G. and Hansen, T. V. *Synthesis, molecular modeling and initial biological evaluation of CC 618: a PPARd antagonist.* (manuscript, 2013).

[43] Salvatore, R. N.; Shin, S. I.; Flanders, V. L. and Jung, K. W. *Efficient and selective N-alkylation of carbamates in the presence of Cs2CO3 and TBAI*. Tetrahedron Letters, 2001. **42**(10): p. 1799-1801.

[44] Clayden, J.; Greeves, N. and Warren, S. *Organic Chemistry*. 1st edition. Oxford University Press. 2000. (ISBN: 9780198503460)

[45] Jiang, X. J.; Lo, P. C.; Tsang, Y. M.; Yeung, S. L.; Fong, W. P. and Ng, D. K. *Phthalocyanine-polyamine conjugates as pH-controlled photosensitizers for photodynamic therapy*. Chemistry, 2010. **16**(16): p. 4777-83.

[46] Baughman, T. W.; Sworen, J. C. and Wagener, K. B. *The facile preparation of alkenyl metathesis synthons*. Tetrahedron, 2004. **60**(48): p. 10943-10948.

7 Appendix

7.1 Intermediates

7.1.1 ^{1}H NMR, ^{13}C NMR, DEPT and HMQC of *tert*-butyl(2-((5-(trifluoromethyl)pyridine-2-yl)thio)ethyl)carbamate (3)

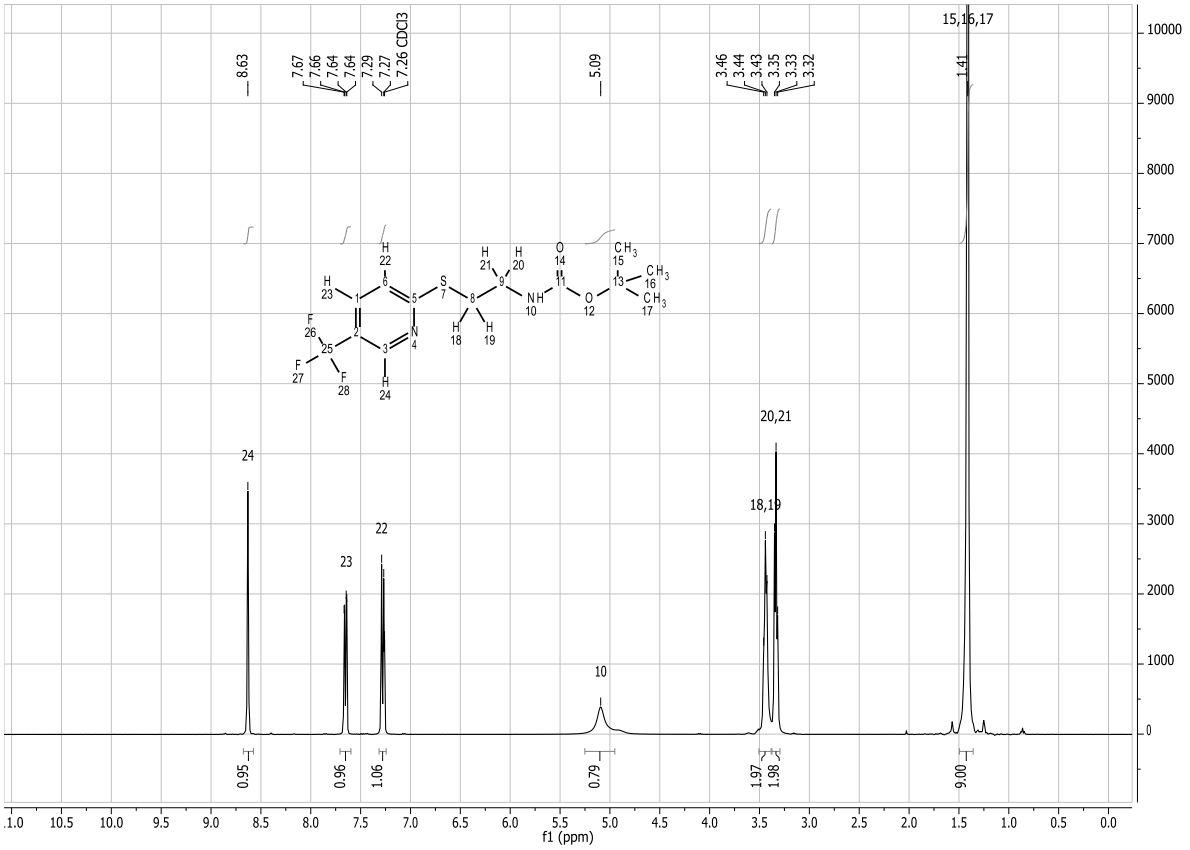

Figure 7.1: ^{1}H NMR spectrum of compound (3).

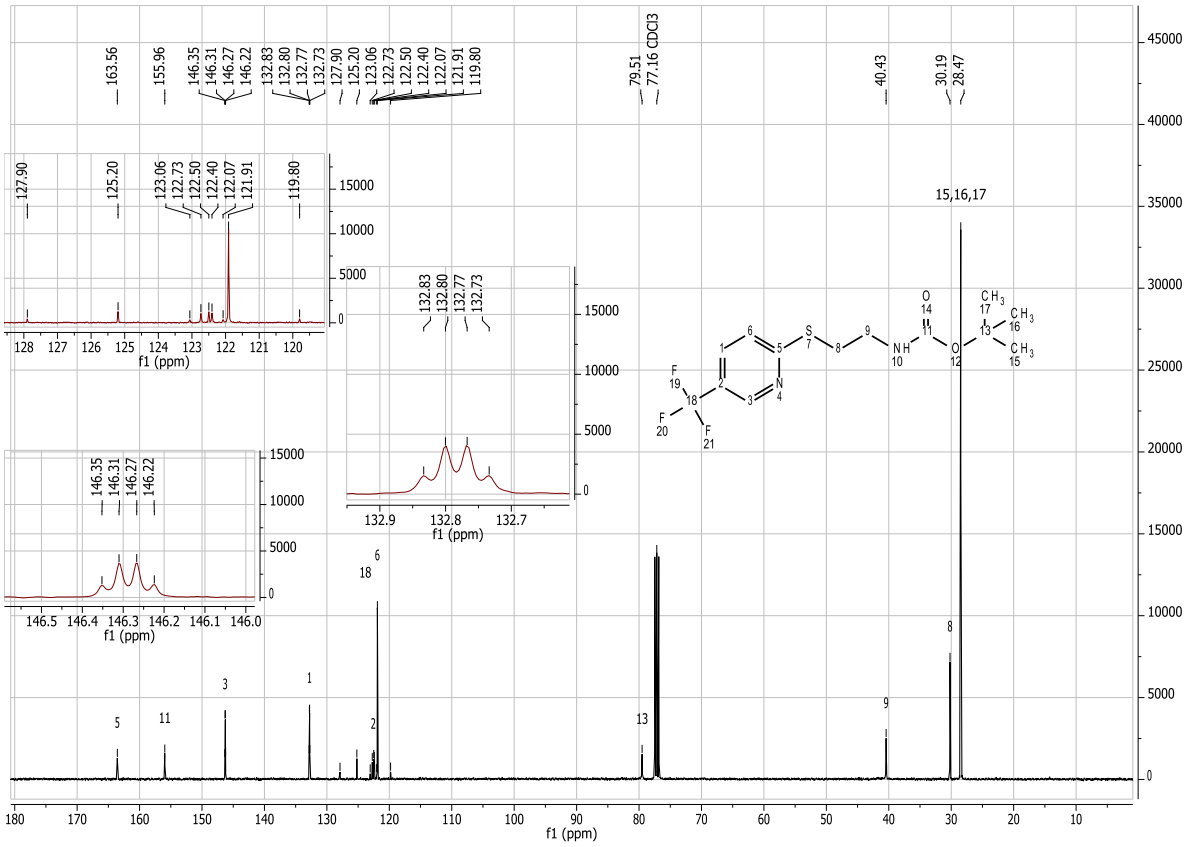

Figure 7.2: ^{13}C NMR spectrum of compound (3).

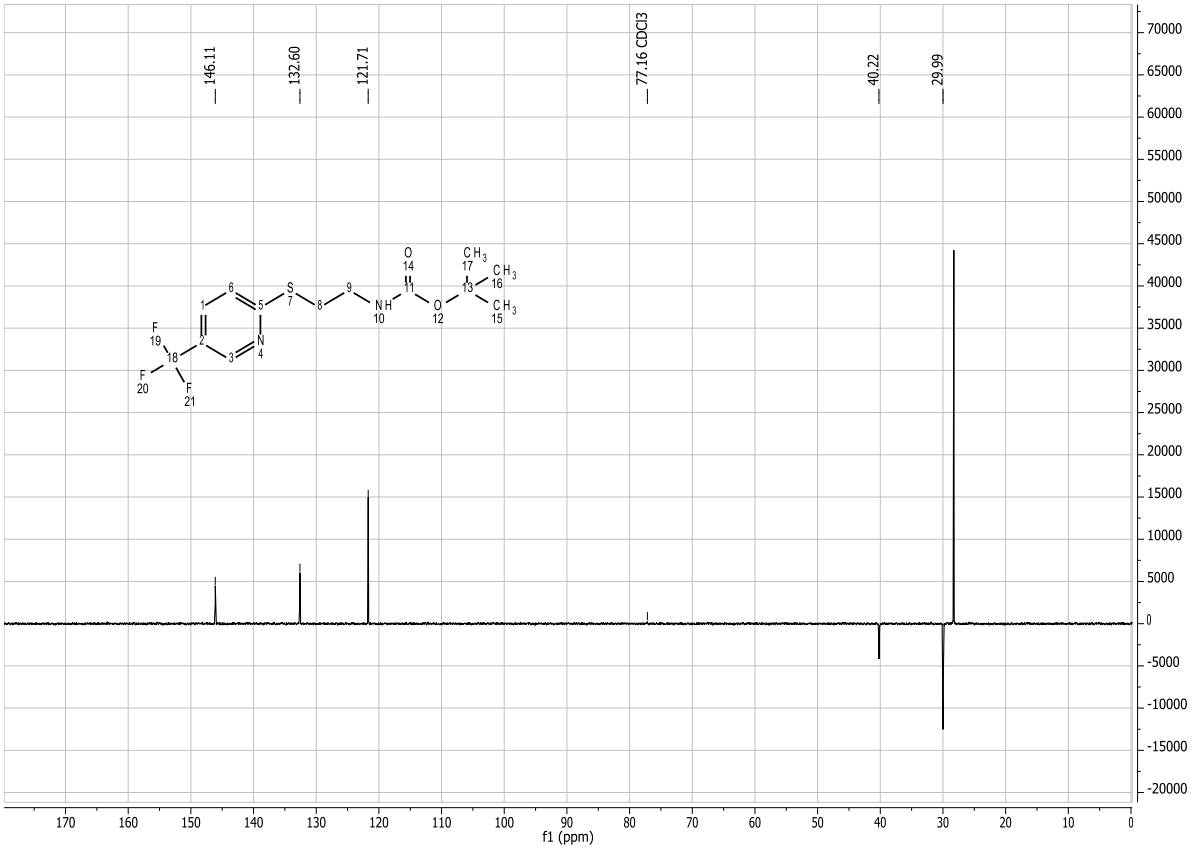

Figure 7.3: DEPT spectrum of compound (3).

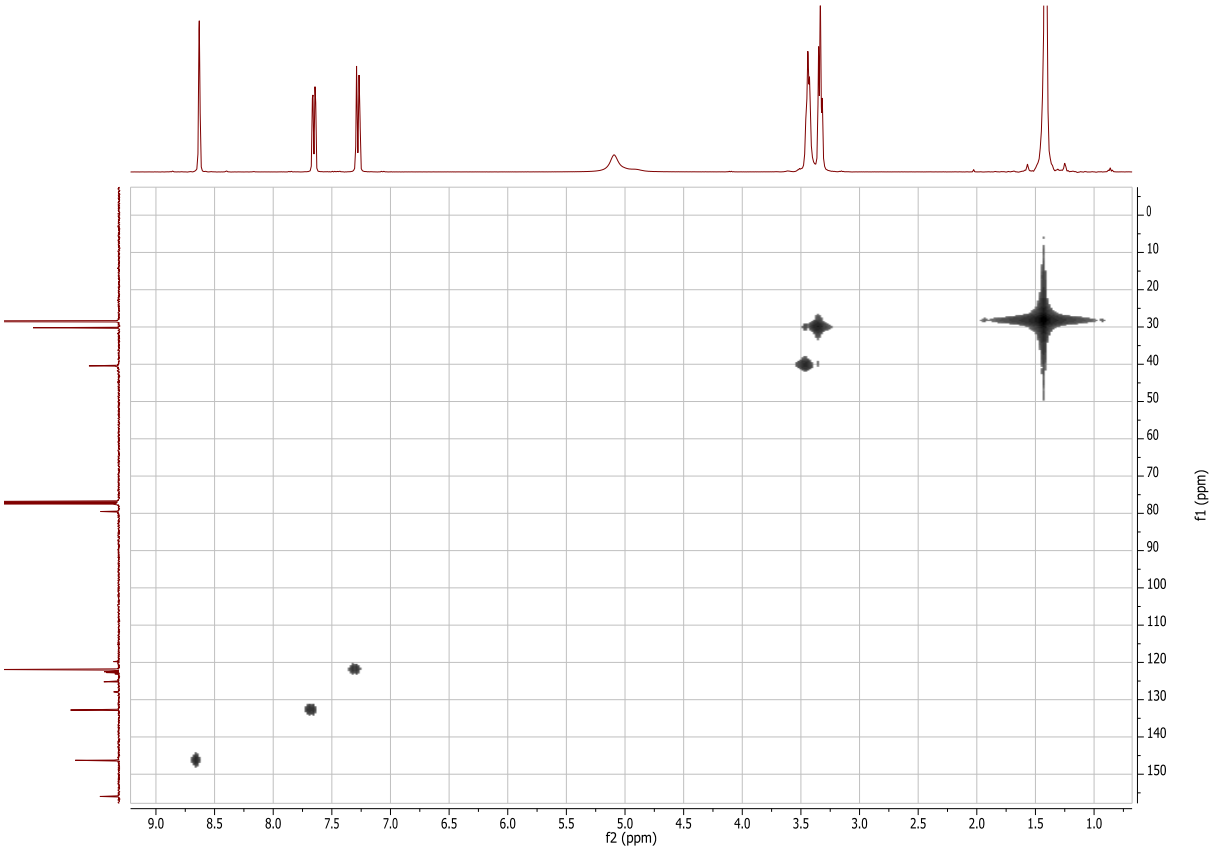

Figure 7.4: HMQC spectrum of compound (3).

7.1.2 ^{1}H NMR, ^{13}C NMR and DEPT of *tert*-butyl(2-((5-(trifluoromethyl) pyridine-2-yl)sulfonyl)ethyl)carbamate (4)

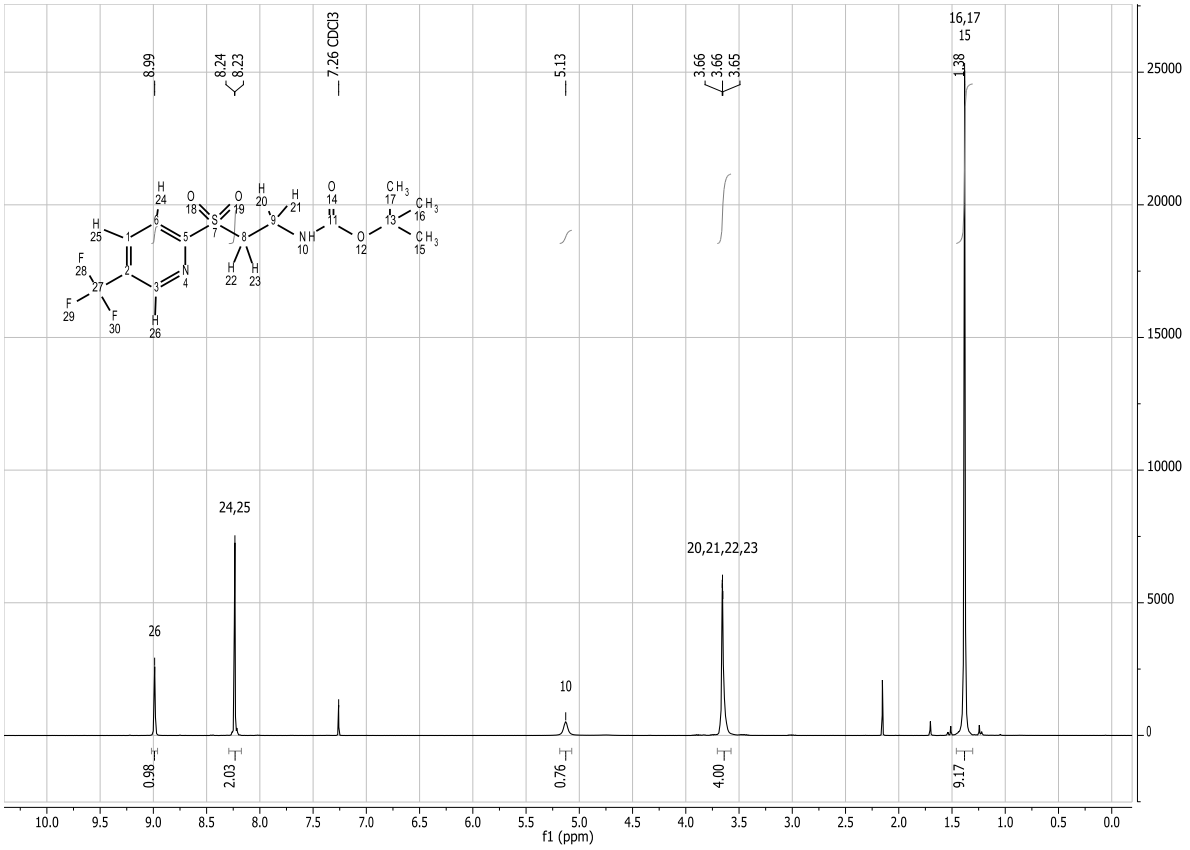

Figure 7.5: ^{1}H NMR spectrum of compound (4).

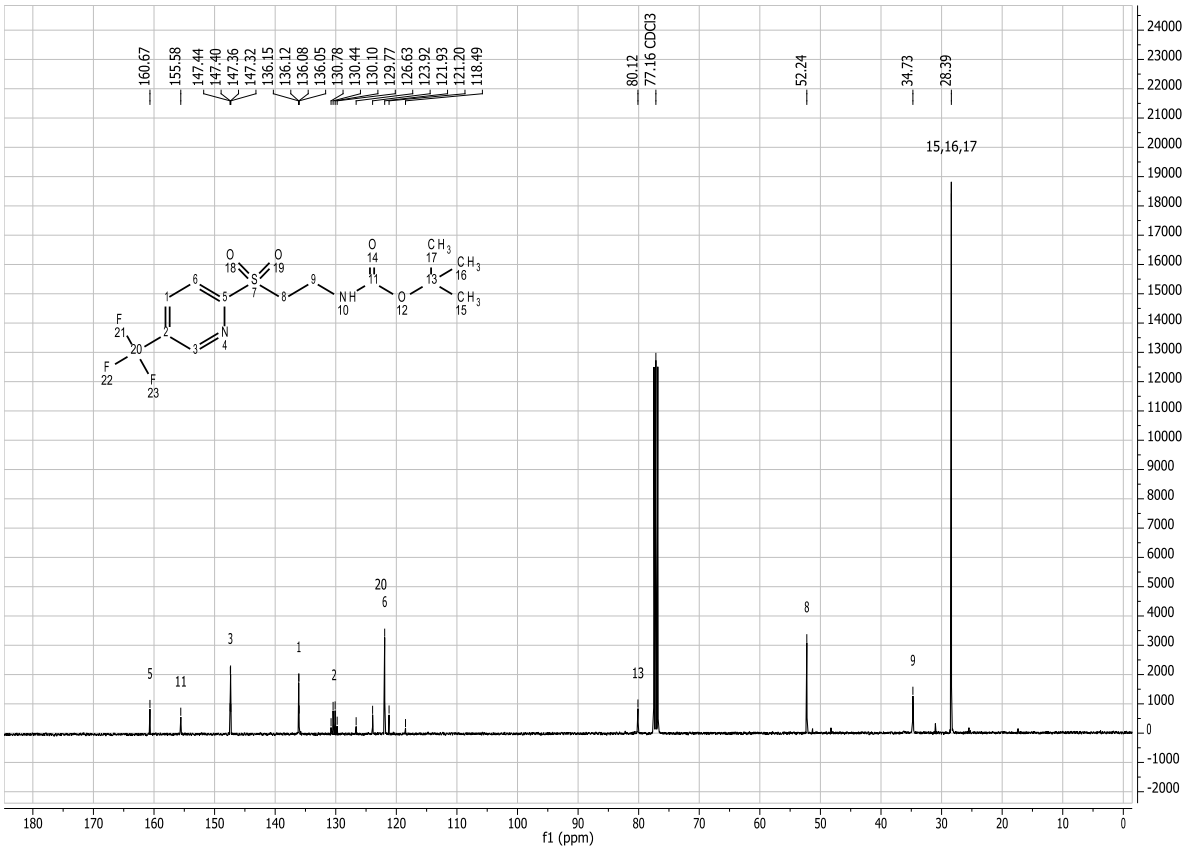

Figure 7.6: ^{13}C NMR spectrum of compound (4).

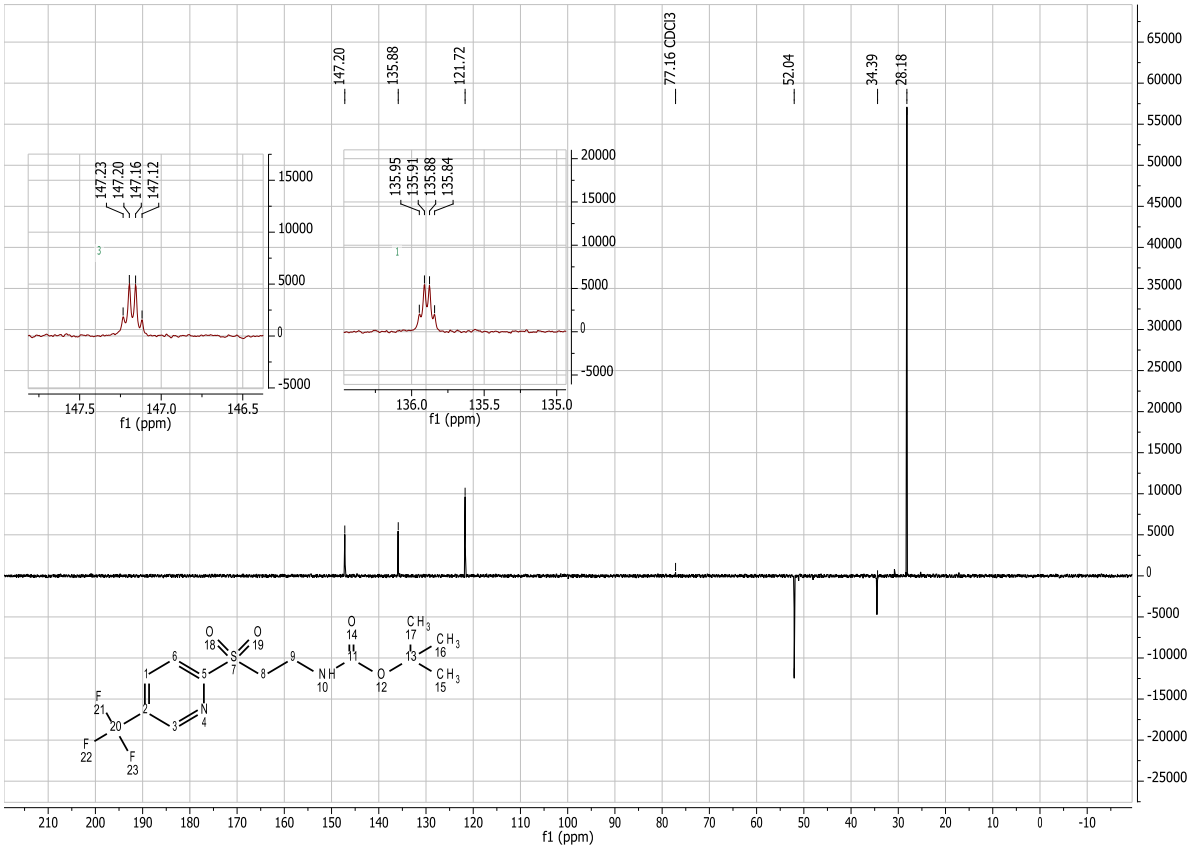

Figure 7.7: DEPT spectrum of compound (4).

7.1.3 ^{1}H NMR of 2-((5-(trifluoromethyl)pyridine-2-yl)sulfonyl) ethanaminium chloride (5)

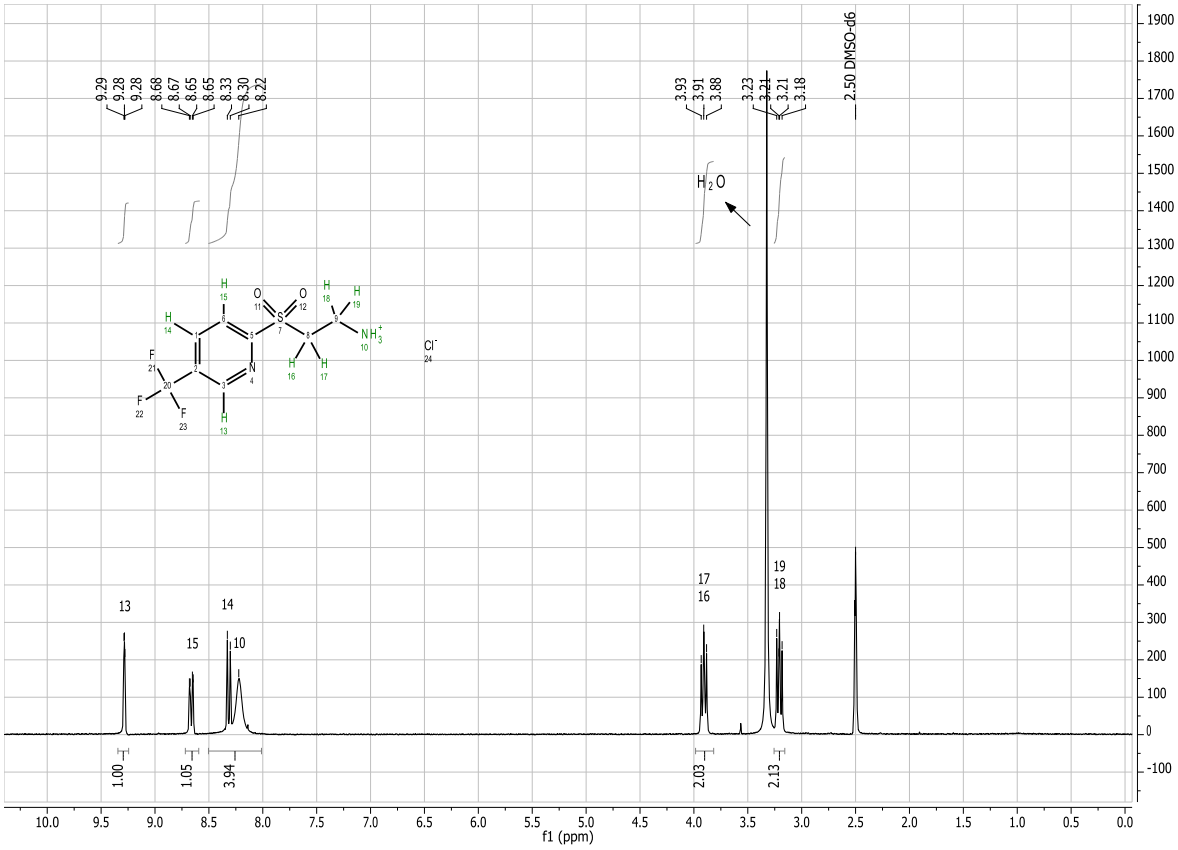

Figure 7.8: ^{1}H NMR spectrum of compound (5).

7.1.4 ^{1}H NMR, ^{13}C NMR and DEPT of *N*-(2-((5-trifluoromethyl)pyridine-2-yl)sulfonyl)ethyl)2-naphtamide (7)

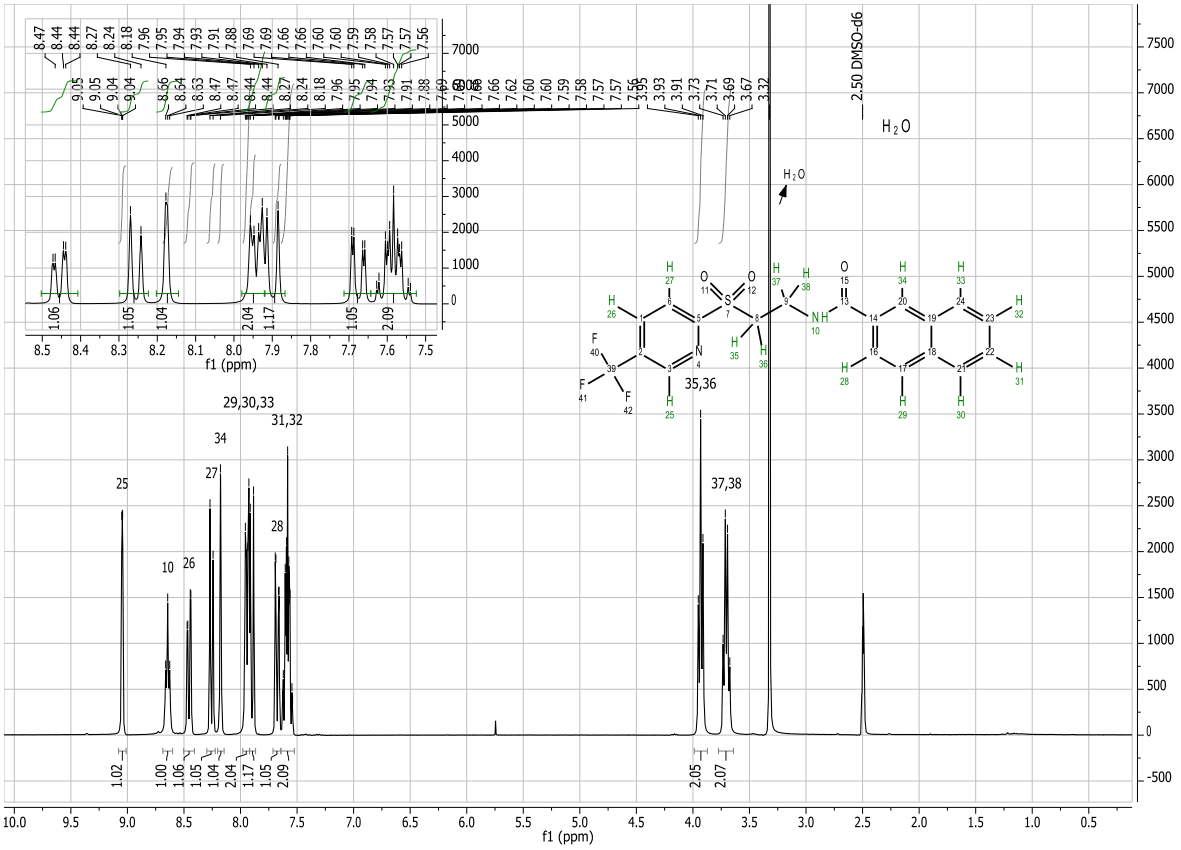

Figure 7.9: ^{1}H NMR spectrum of compound (7).

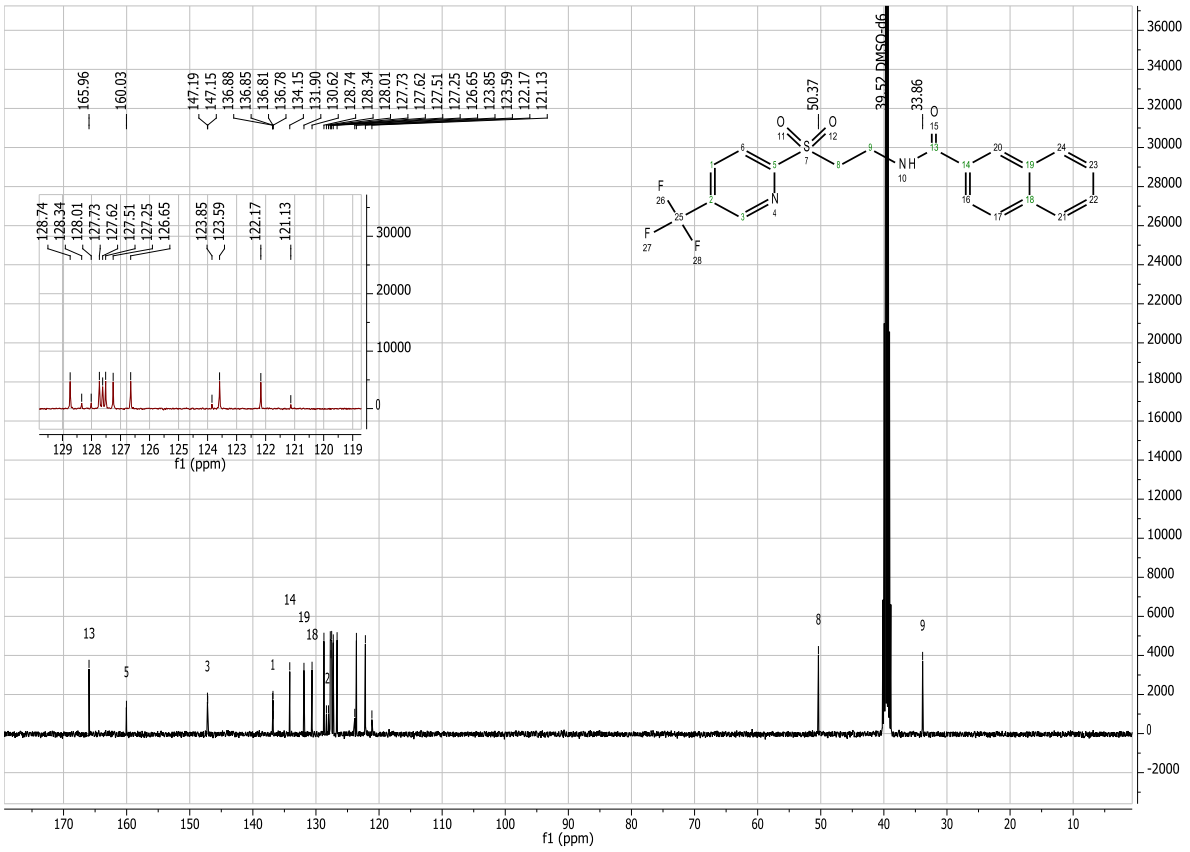

Figure 7.10: ^{13}C NMR spectrum of compound (7).

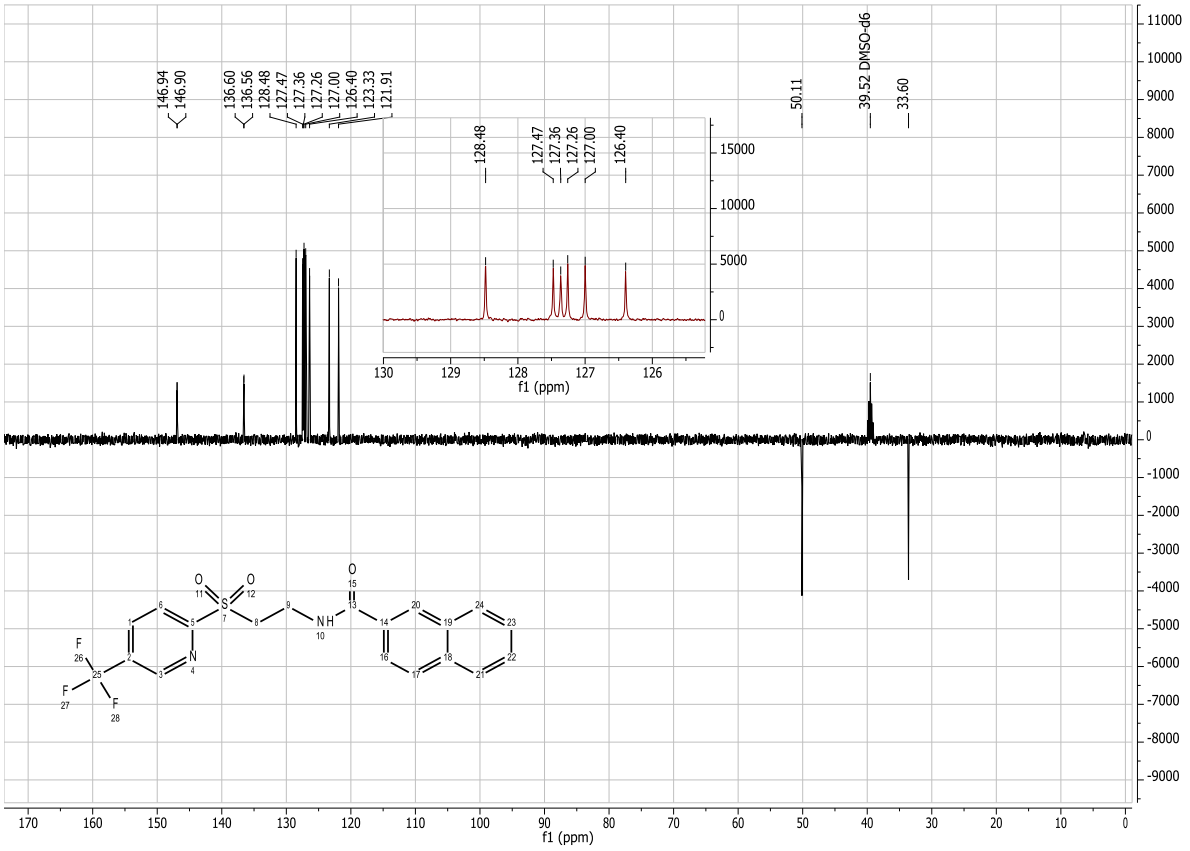

Figure 7.11: DEPT spectrum of compound (7).

7.1.5 ^{1}H NMR, ^{13}C NMR and DEPT of 2-((5-(trifluoromethyl)pyridine-2-yl)thio)ethanaminium chloride (8)

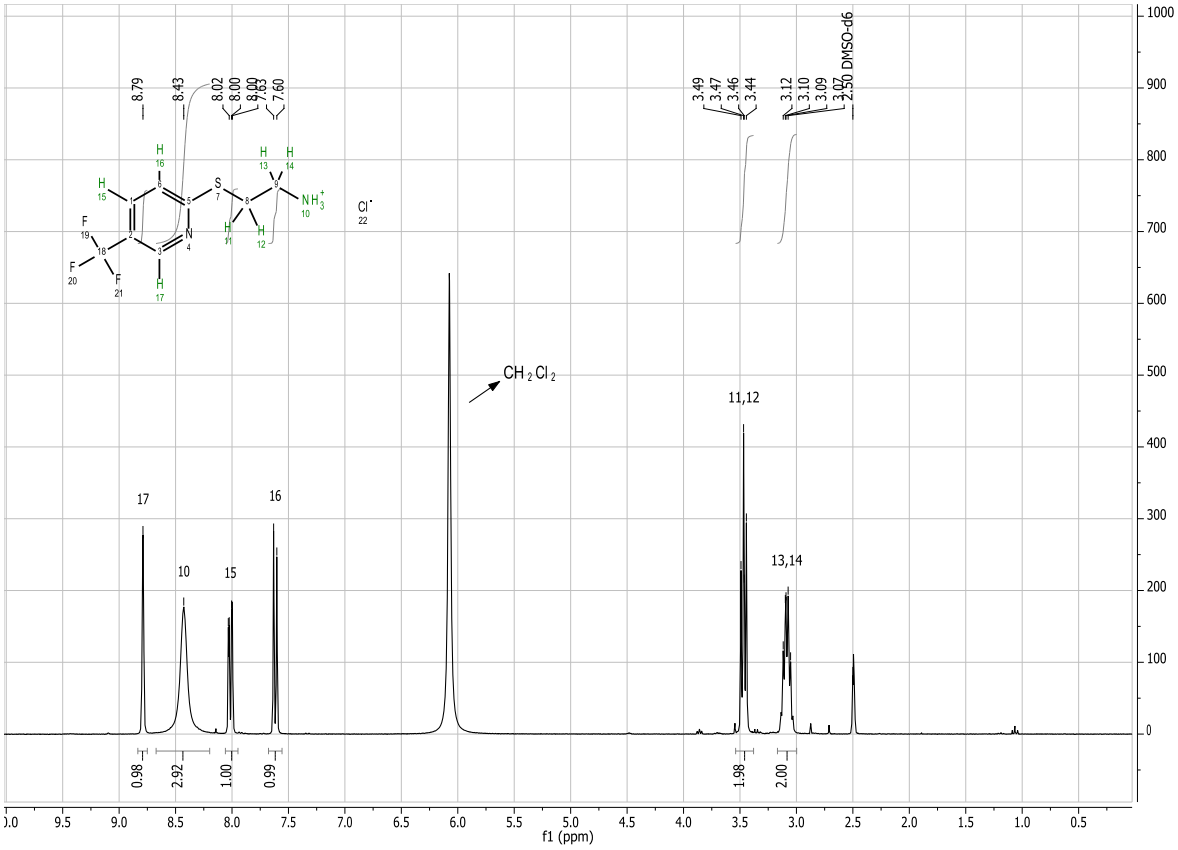

Figure 7.12: ^{1}H NMR spectrum of compound (8).

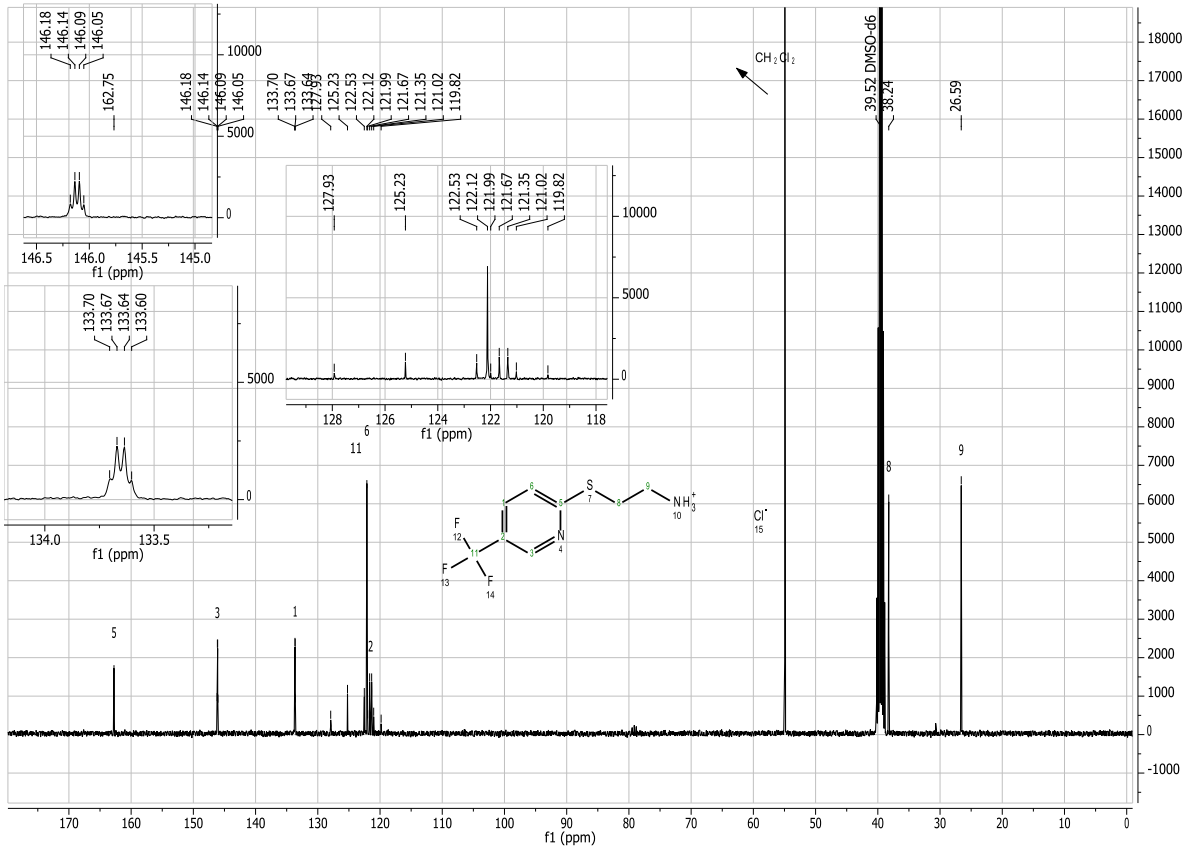

Figure 7.13: ^{13}C NMR spectrum of compound (8).

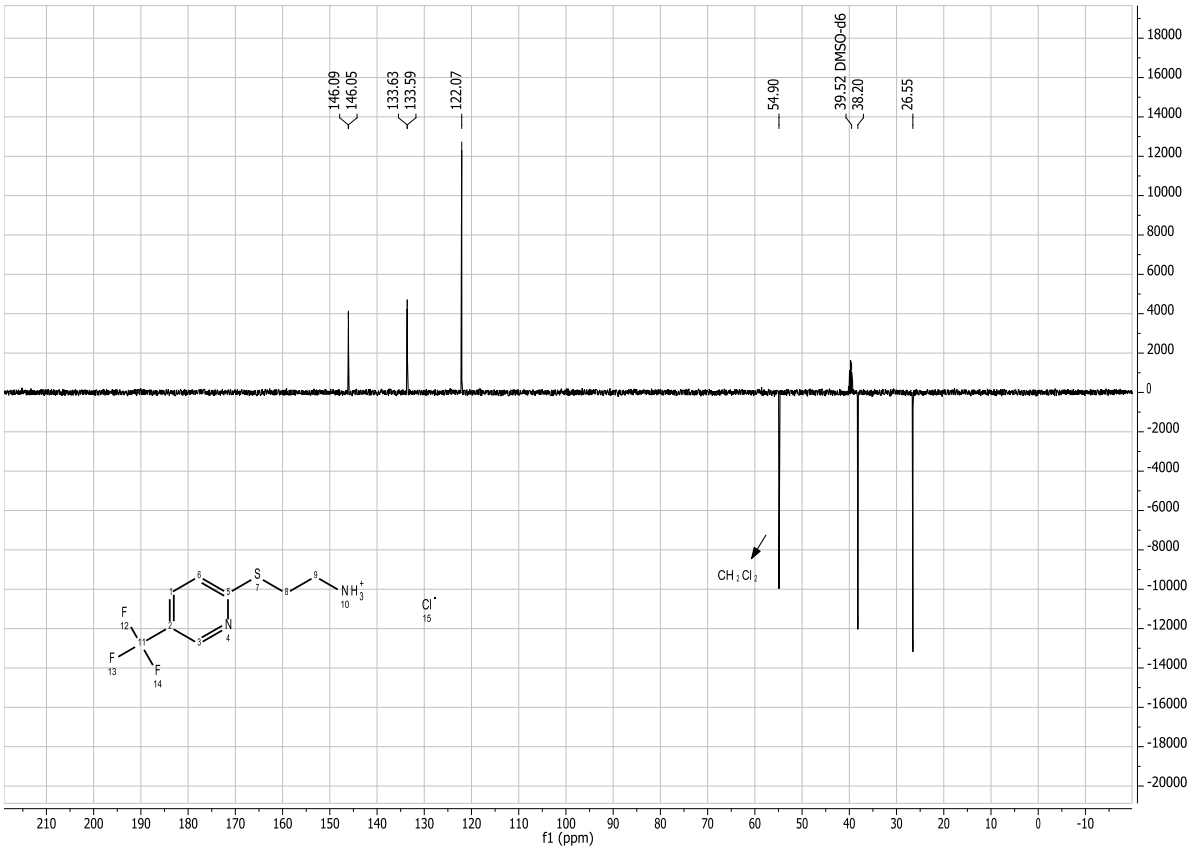

Figure 7.14: DEPT spectrum of compound (8).

7.1.6 ^{1}H NMR and ^{13}C NMR of 2-((5-(trifluoromethyl)pyridine-2-yl)thio)ethyl)-2-naftamide (9)

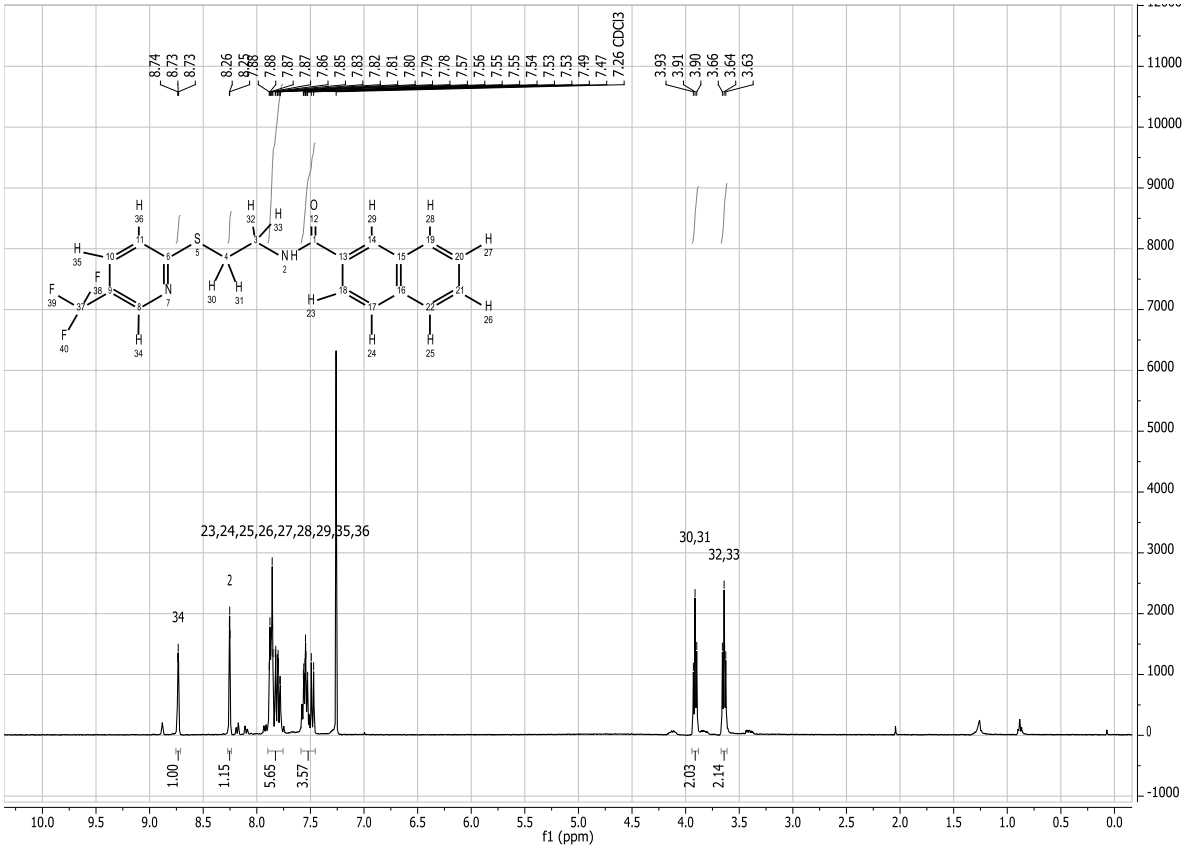

Figure 7.15: ^{1}H NMR spectrum of compound (9).

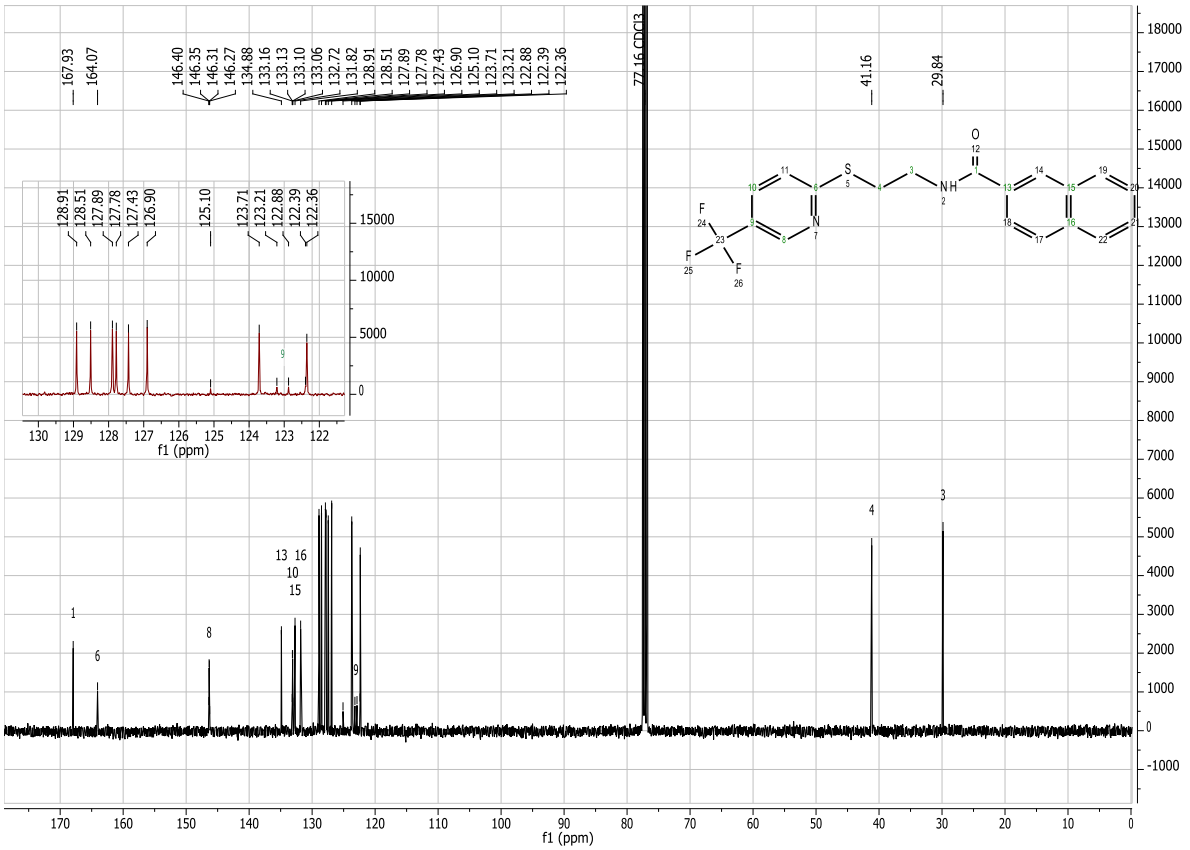

Figure 7.16: ^{13}C NMR spectrum of compound (9).

7.2 *N*-alkylated intermediates and analogues

7.2.1 ^{1}H NMR of *N*-methyl-*N*-(2-((5-(trifluoromethyl)pyridine-2-yl) sulfonyl)ethyl)-2-naftamide (10)

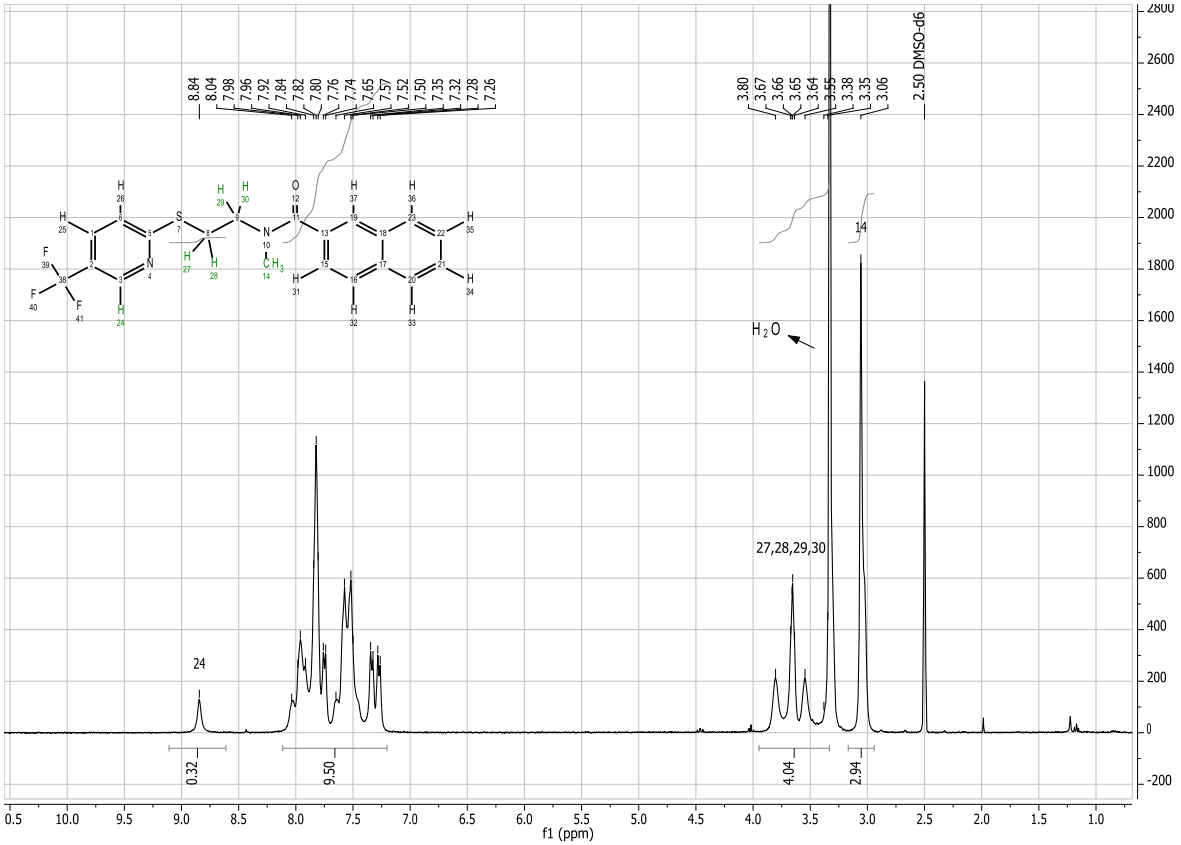

Figure 7.17: ^{1}H NMR spectrum of compound (10).

7.2.2 ^{1}H NMR, ^{13}C NMR and DEPT of *N*-methyl-*N*-(2-((5-(trifluoromethyl)pyridine-2-yl)sulfonyl)ethyl)-2-naftamide (11)

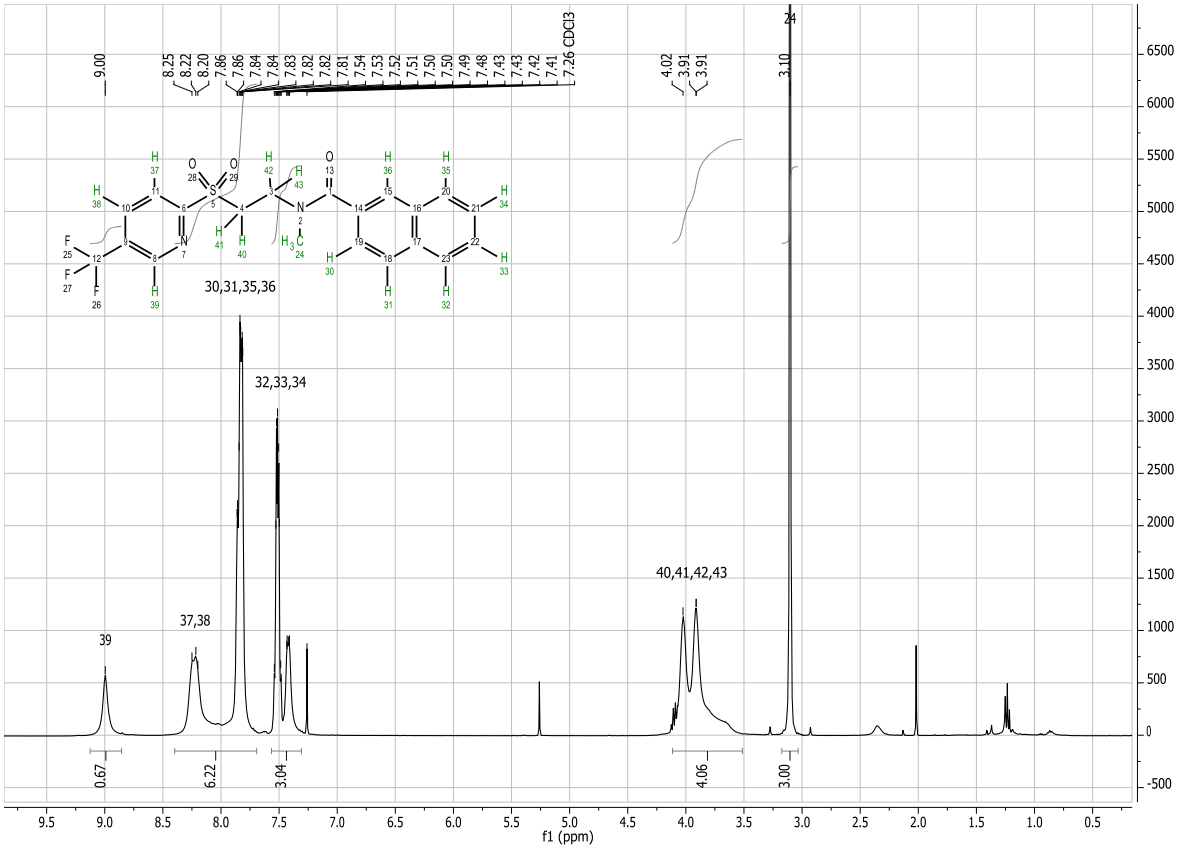

Figure 7.18: ^{1}H NMR spectrum of compound (11).

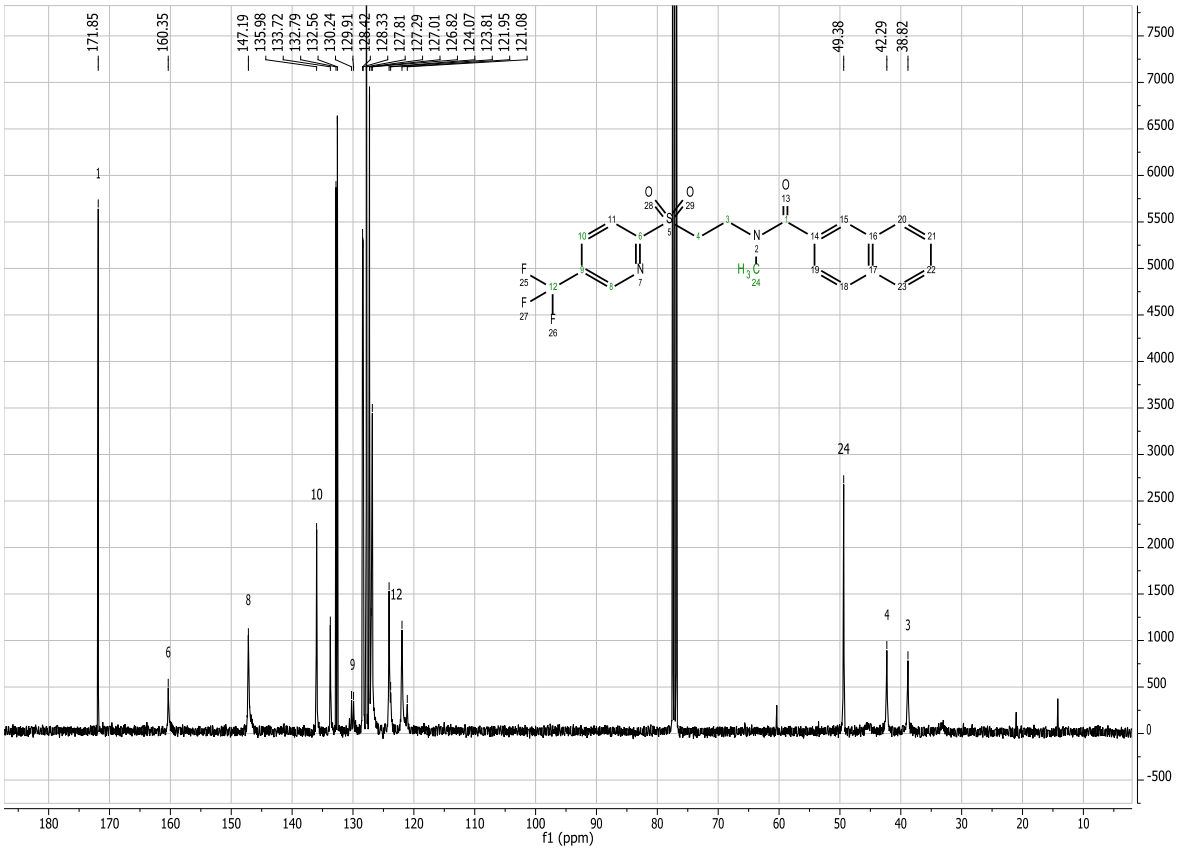

Figure 7.19: ^{13}C NMR spectrum of compound (11).

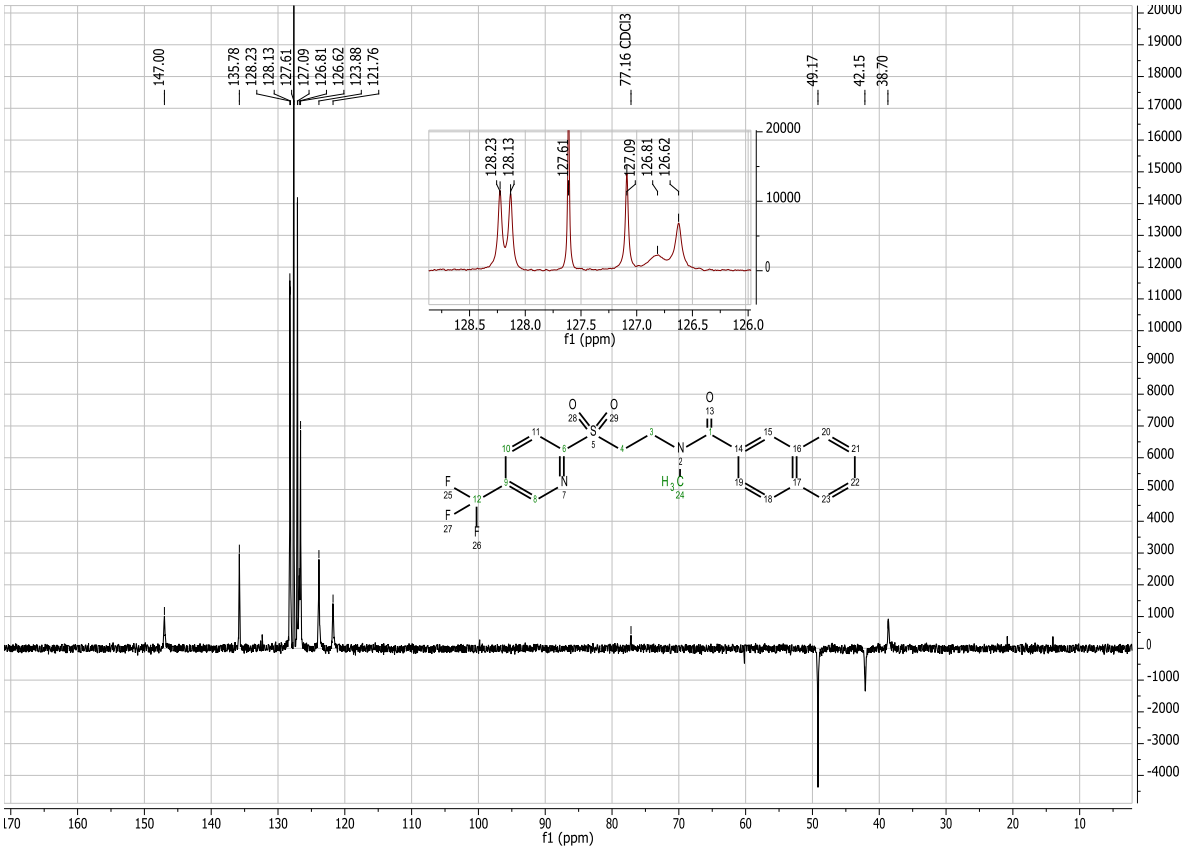

Figure 7.20: DEPT spectrum of compound (11).

7.2.3 ^{1}H NMR of *N*-ethyl-*N*-(2-((5-(trifluoromethyl)pyridine-2-yl)thio) ethyl)-2-naftamide (12)

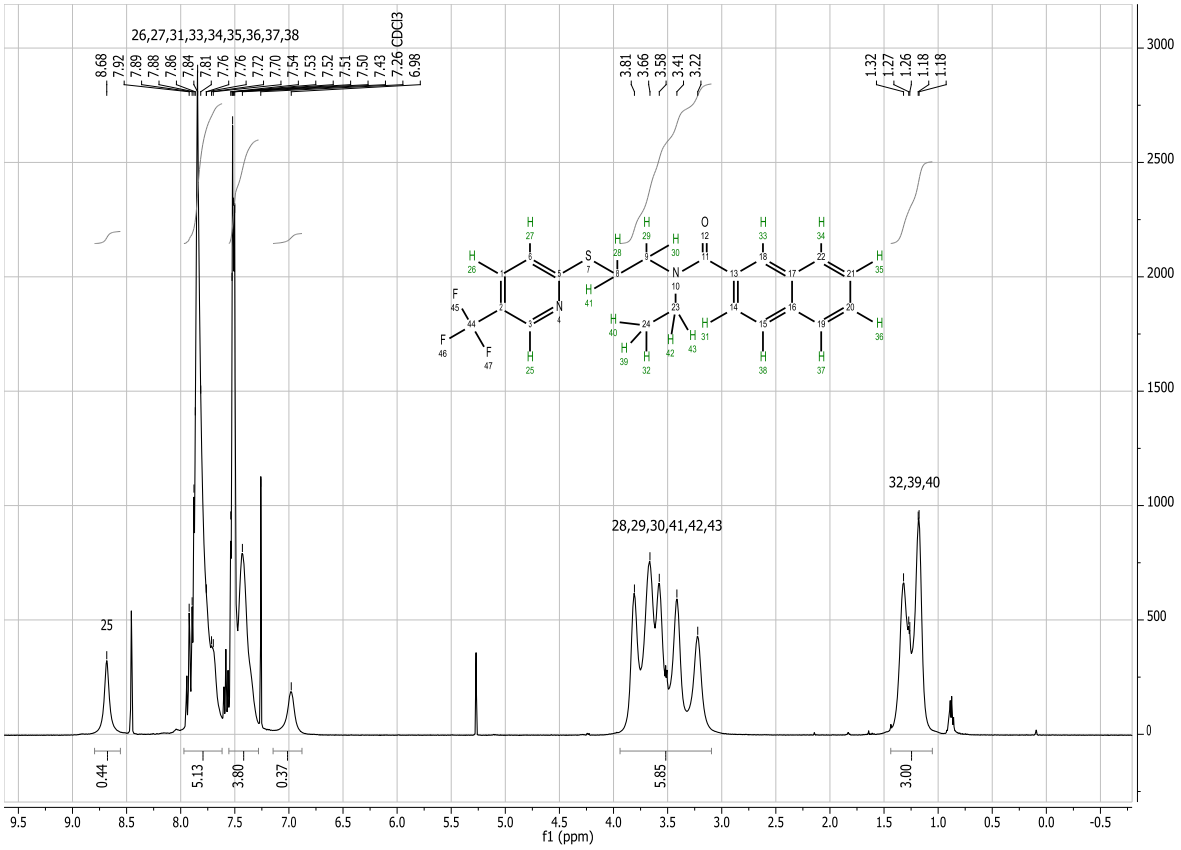

Figure 7.21: ^{1}H NMR spectrum of compound (12).

7.2.4 ^{1}H NMR, ^{13}C NMR and DEPT of *N*-ethyl-*N*-(2-((5-(trifluoromethyl) pyridine-2-yl)sulfonyl)ethyl)-2-naftamide (13)

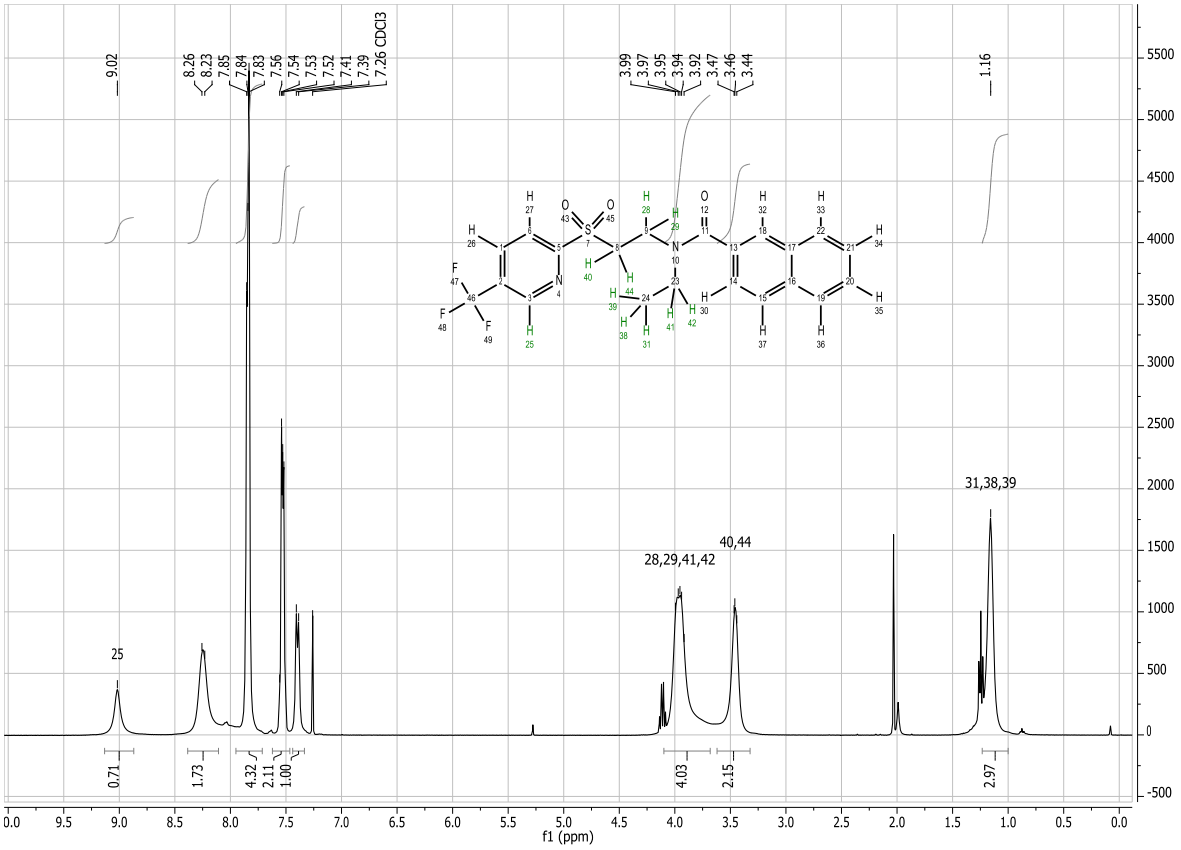

Figure 7.22: ^{1}H NMR spectrum of compound (13).

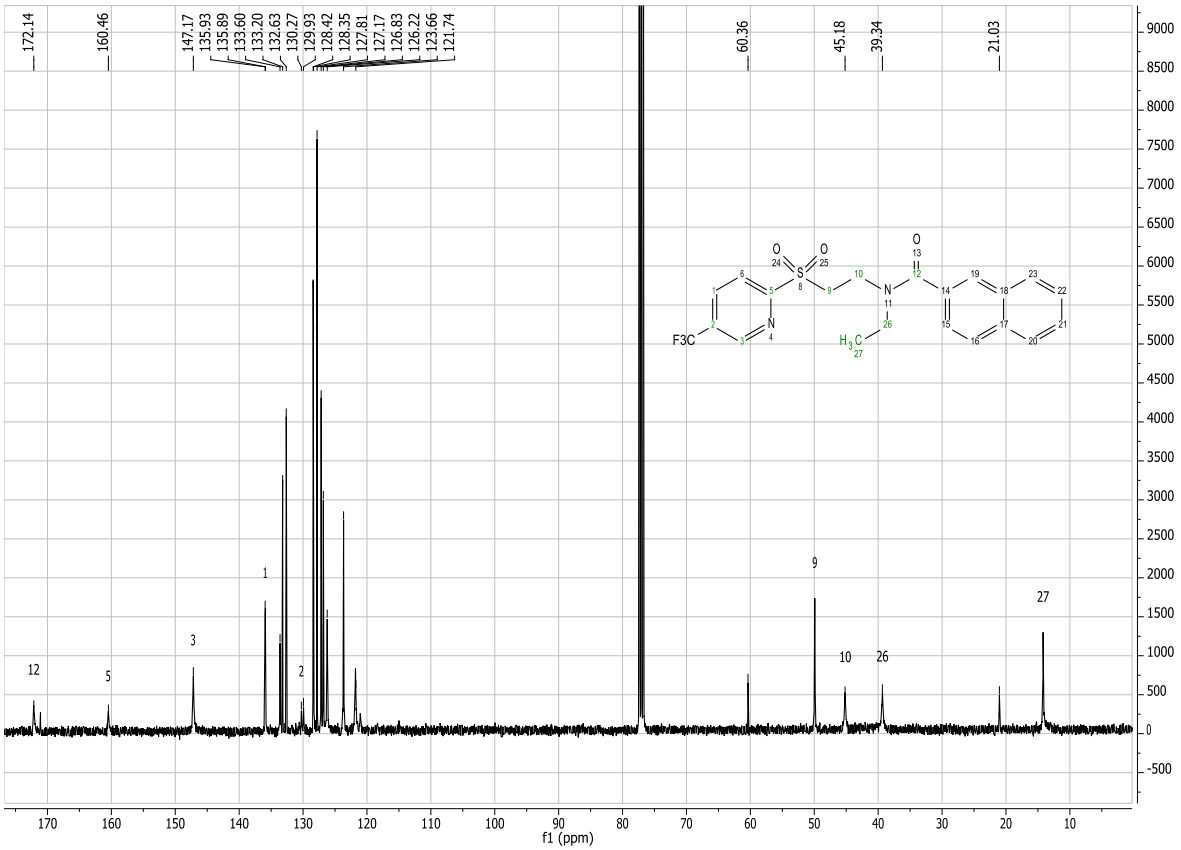

Figure 7.23: ^{13}C NMR spectrum of compound (13).

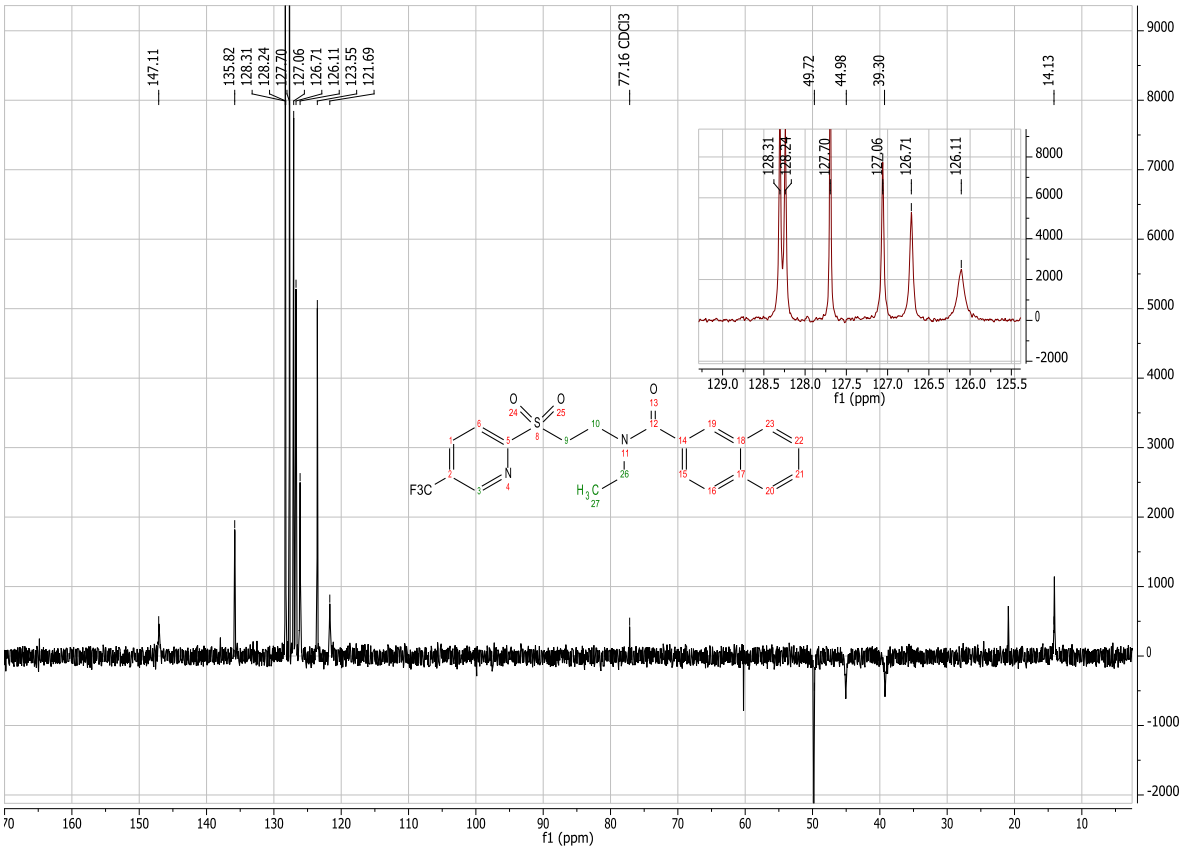

Figure 7.24: DEPT spectrum of compound (13).

7.2.5 ^{1}H NMR, ^{13}C NMR, DEPT and HPLC of *N*-benzyl-*N*-(2-((5-(trifluoromethyl) pyridine-2-yl)sulfonyl)ethyl)-2-naftamide (15)

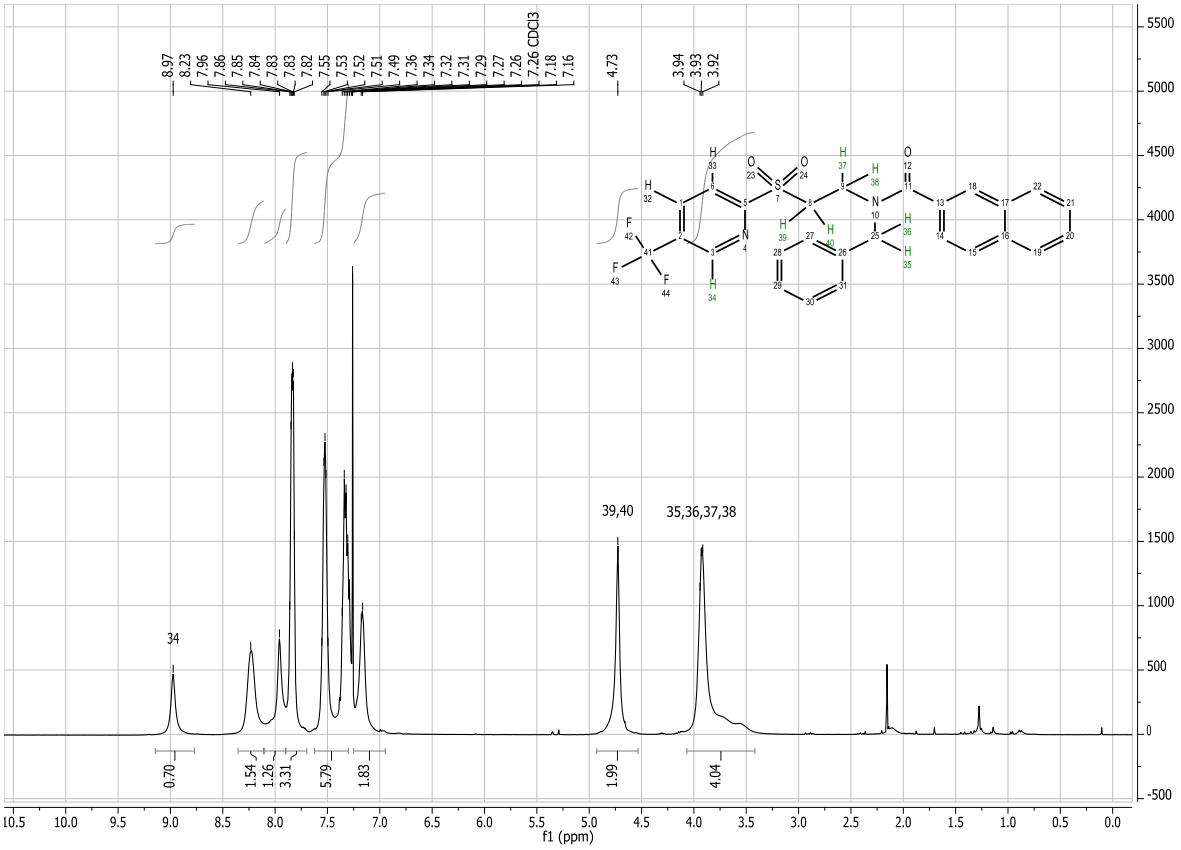

Figure 7.25: ^{1}H NMR spectrum of compound (15).

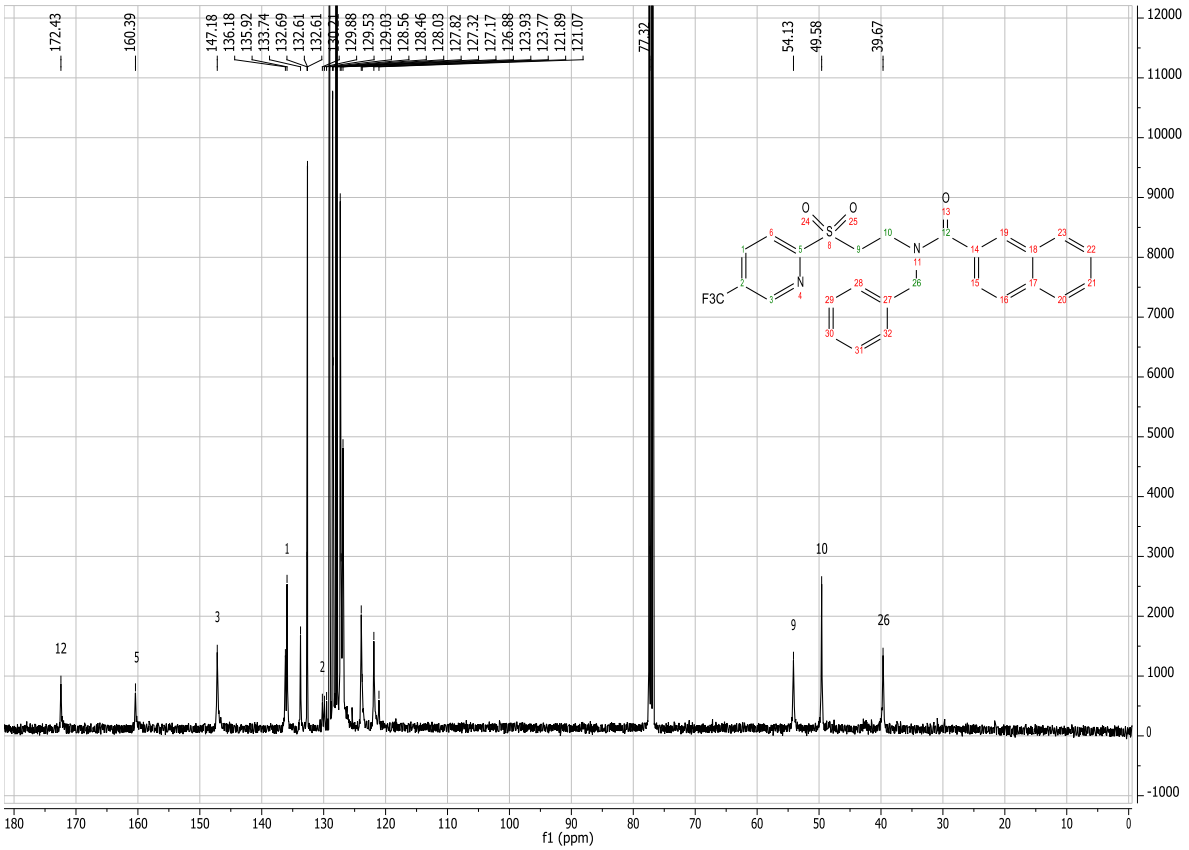

Figure 7.26: ^{13}C NMR spectrum of compound (15).

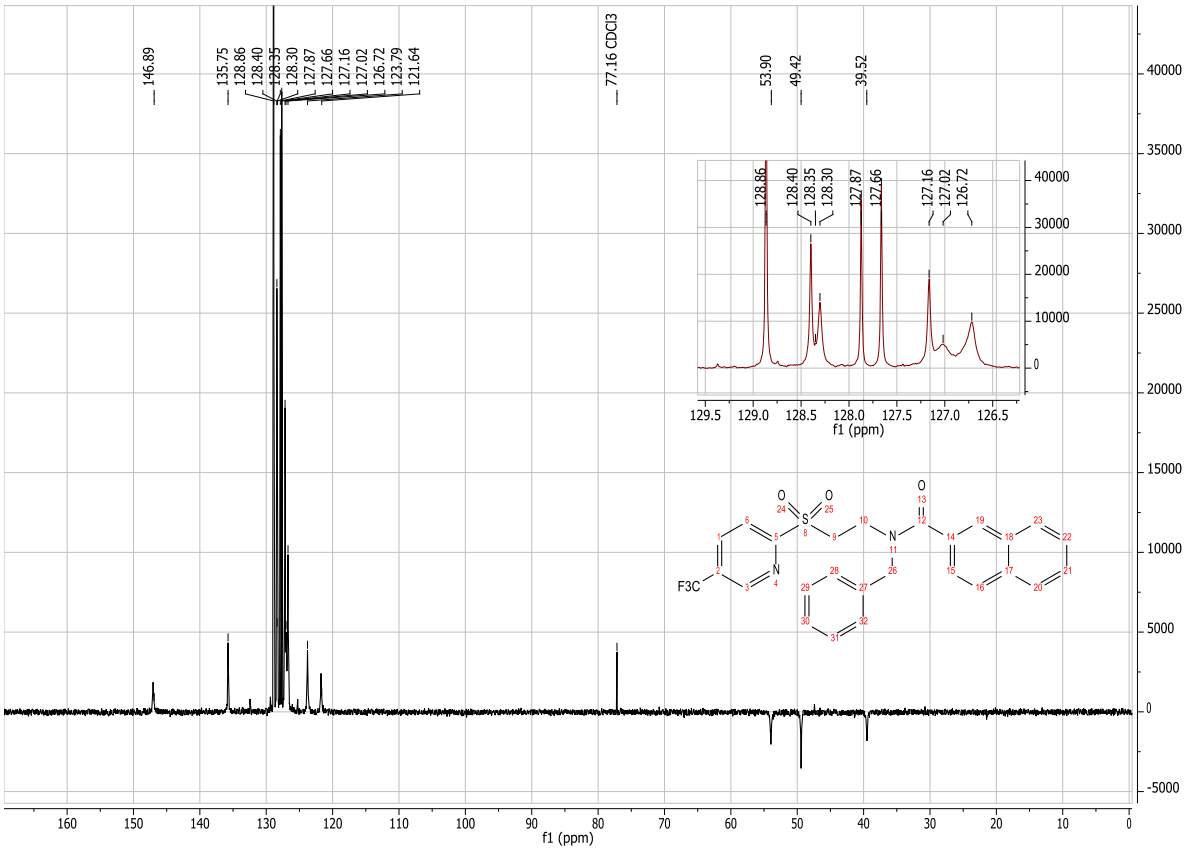

Figure 7.27: DEPT spectrum of compound (15).

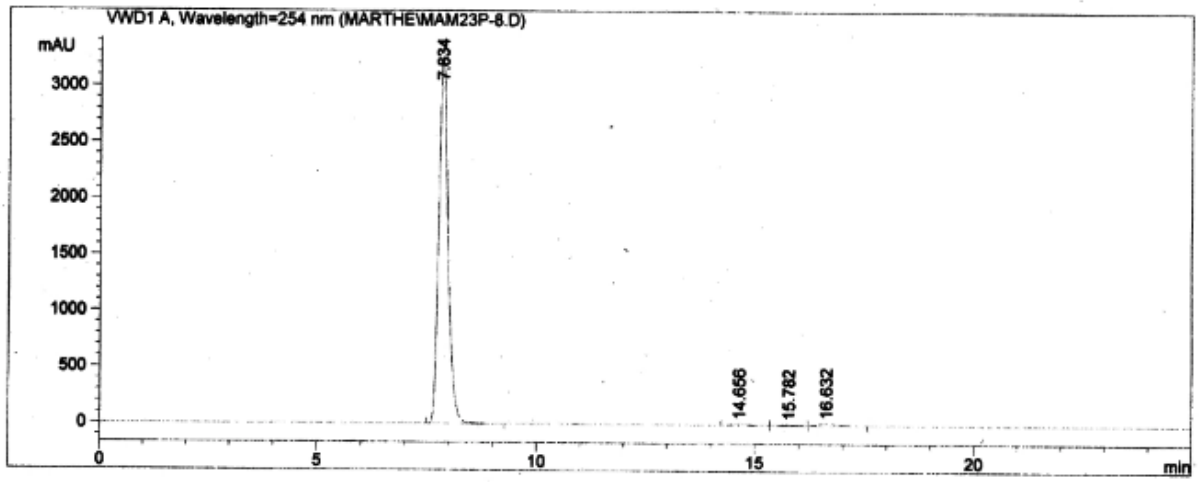

Area Percent Report

Sorted By : Signal
Multiplier : 1.0000
Dilution : 1.0000
Sample Amount : 1.00000 [ng/ul] (not used in calc.)
Use Multiplier & Dilution Factor with ISTDs

Signal 1: VWD1 A, Wavelength=254 nm

Peak #	RetTime [min]	Type	Width [min]	Area mAU *s	Height [mAU]	Area %
1	7.834	BB	0.2246	4.85192e4	3260.66284	98.0730
2	14.656	BV	0.3650	283.48315	11.78883	0.5730
3	15.782	VV	0.3808	152.22795	6.11266	0.3077
4	16.632	VB	0.4152	517.60693	18.75021	1.0463
Totals :				4.94725e4	3297.31454	

Summed Peaks Report

Signal 1: VWD1 A, Wavelength=254 nm

Figure 7.28: HPLC chromatogram of compound (15)

7.2.6 ^{1}H NMR and ^{13}C NMR of *N*-benzyl-*N*-(2-((5-(trifluoromethyl)pyridine-2-yl) sulfonyl))ethanaminium chloride (29)

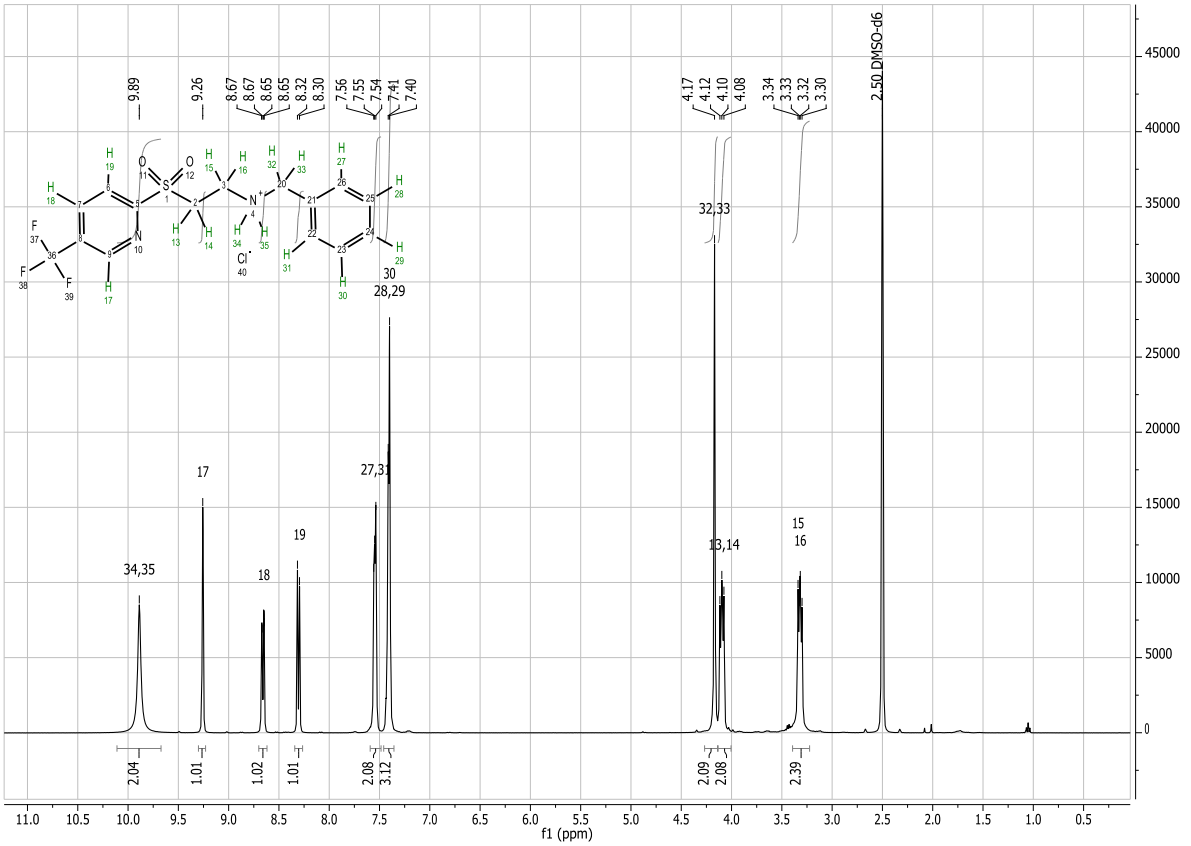

Figure 7.29: ^{1}H NMR spectrum of compound (29).

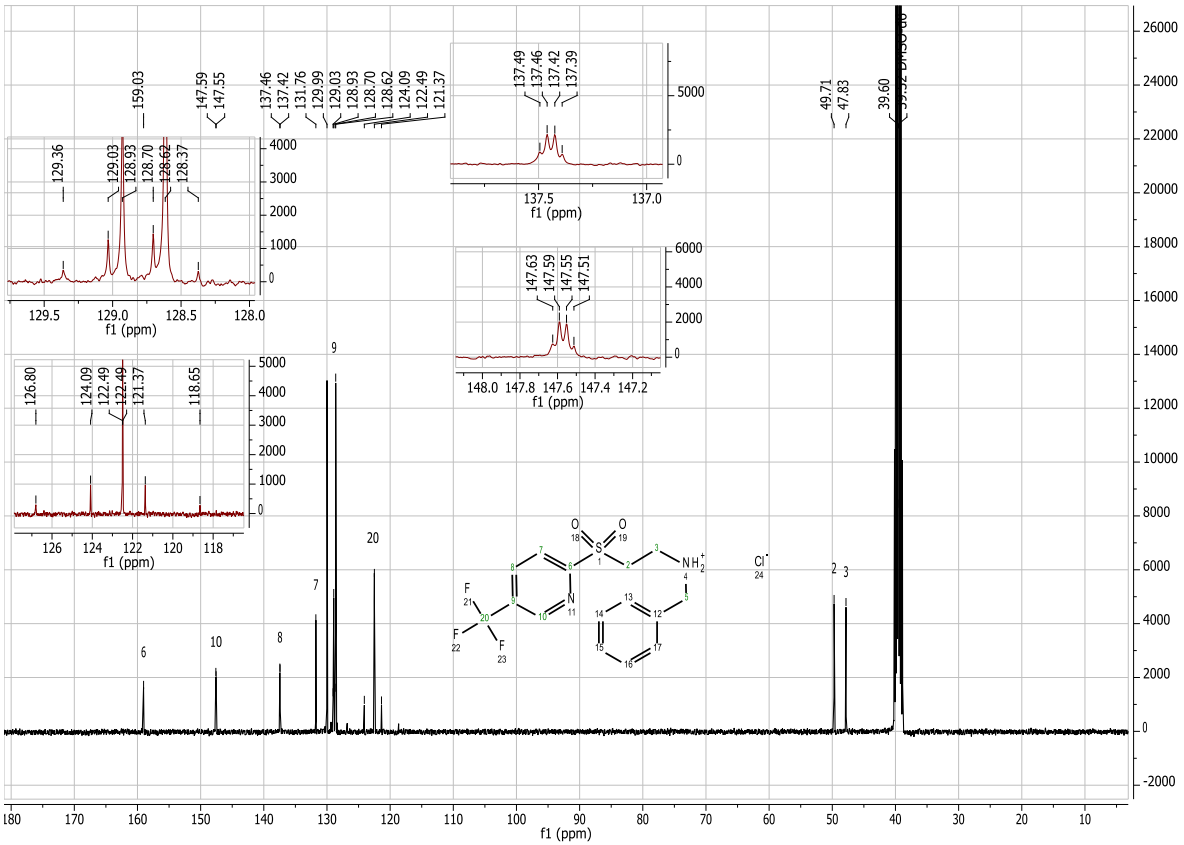

Figure 7.30: ^{13}C NMR spectrum of compound (29).

7.2.7 ^{1}H NMR of *N*-benzyl-*N*-(2-((5-(trifluoromethyl)pyridine-2-yl) sulfonyl)ethyl)-2-naftamide (15) from the fifth approach

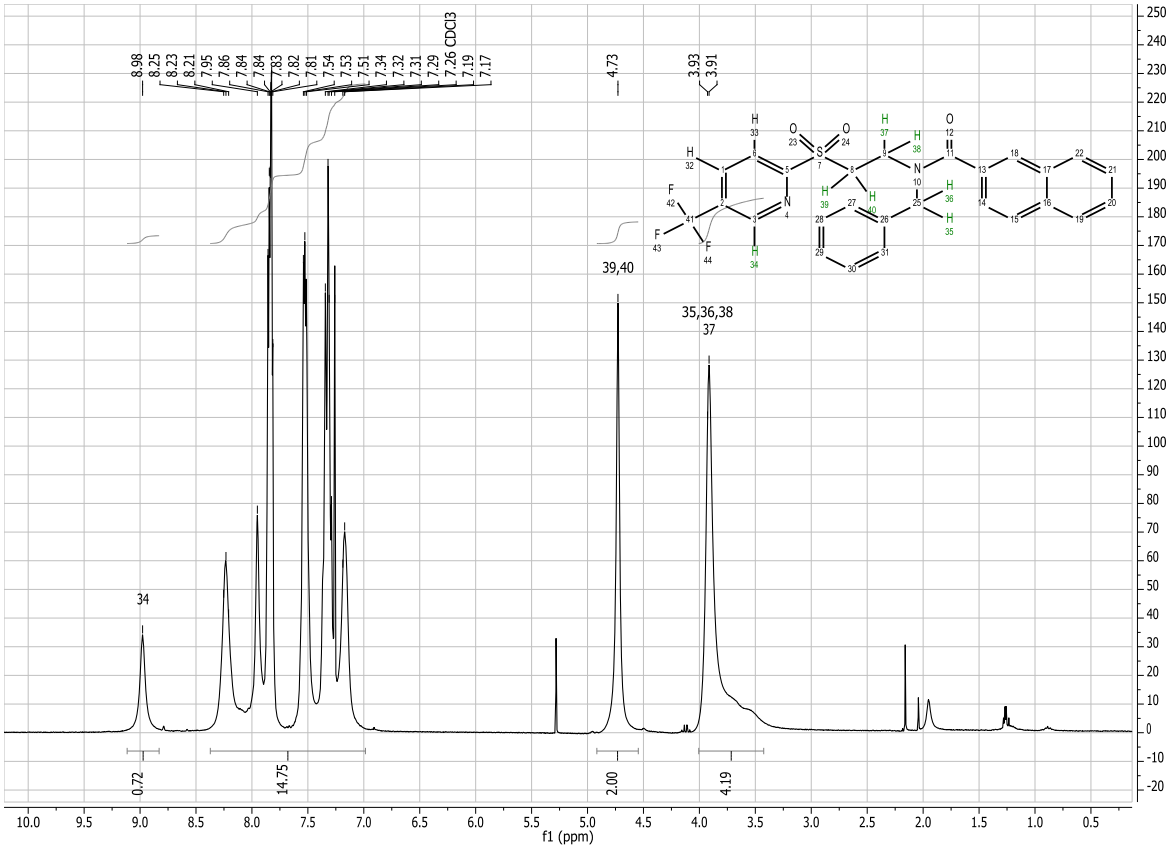

Figure 7.31: ^{1}H NMR spectrum of compound (15).

7.3 Intermediates from the attempted synthesis

7.3.1 ^{1}H NMR of 2-(benzylamino)ethanol (19)

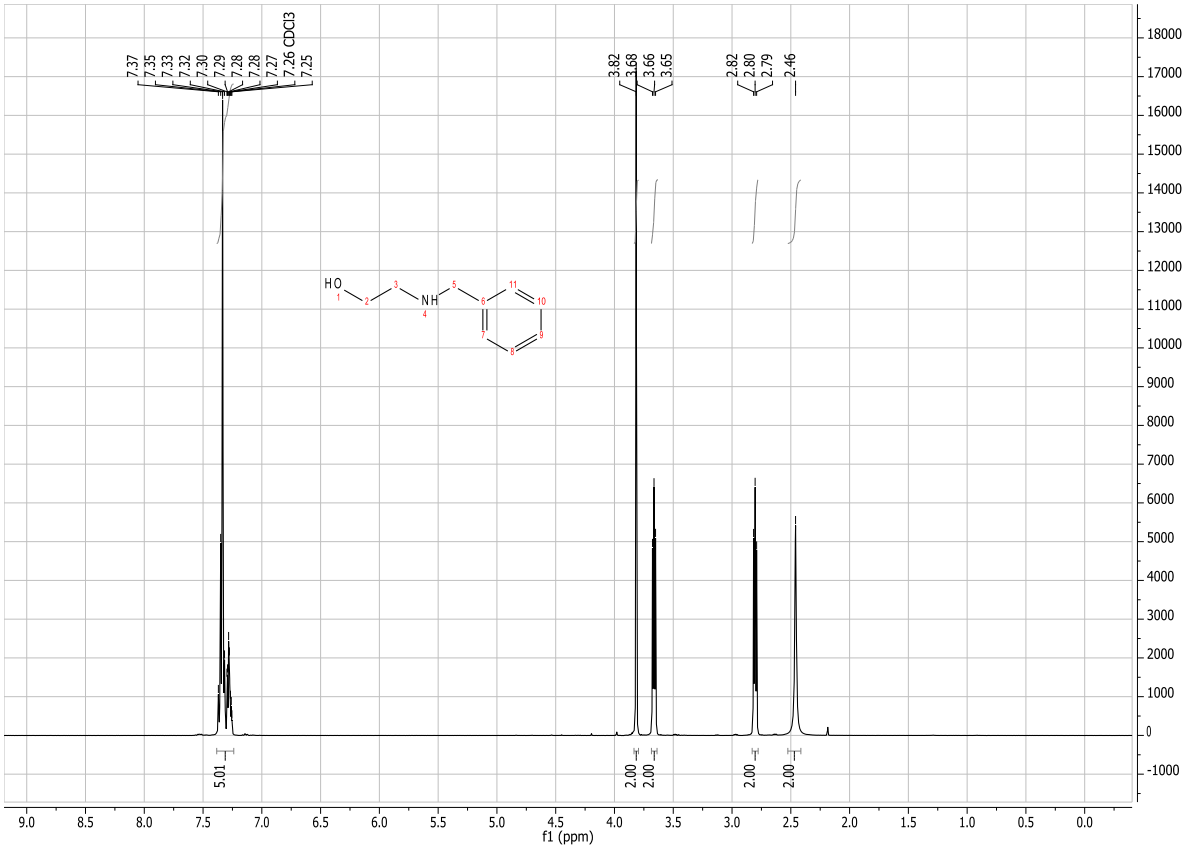

Figure 7.32: ^{1}H NMR spectrum of compound (19).

7.3.2 ^{1}H NMR of *tert*-butyl benzyl(2-hydroxyethyl)carbamate (20)

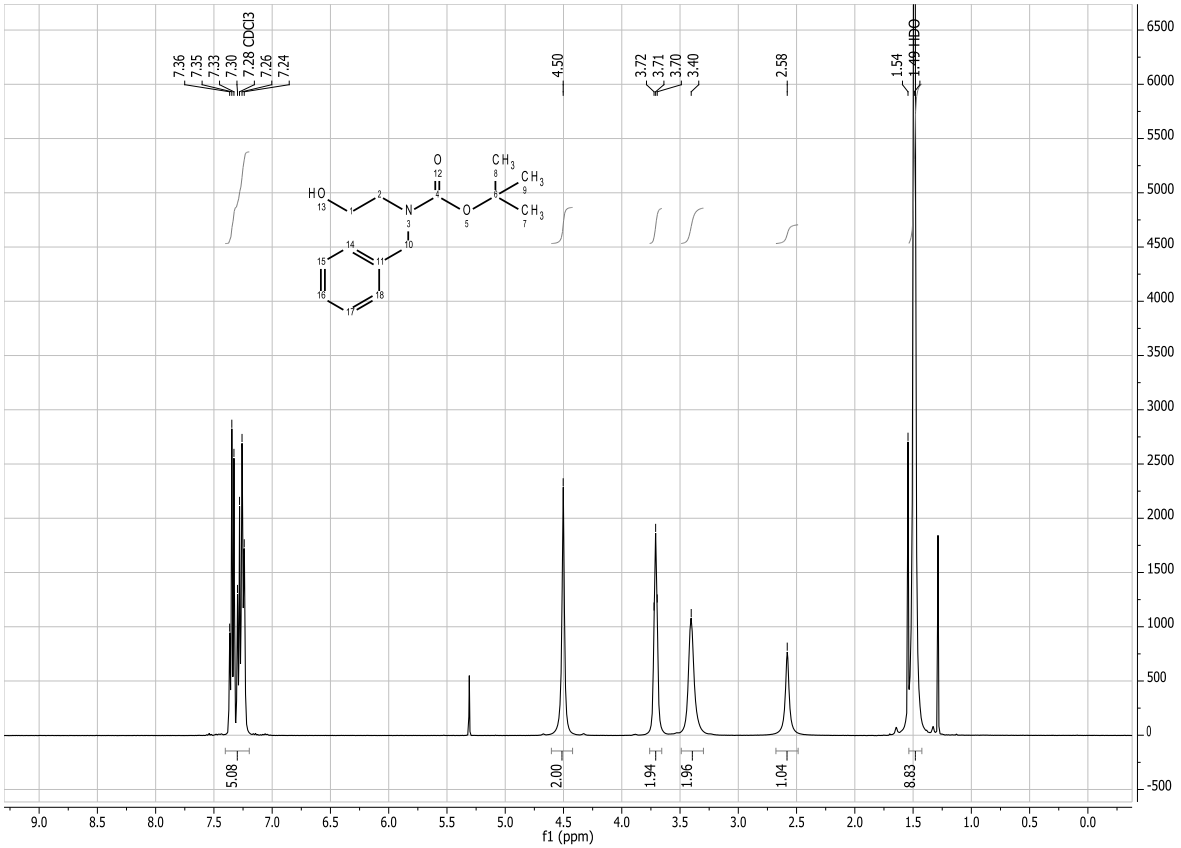

Figure 7.33: ^{1}H NMR spectrum of compound (20).

7.3.3 ^{1}H NMR of *tert*-butyl benzyl(2-((5-(trifluoromethyl)pyridine-2-yl) thio)ethyl)carbamate (23)

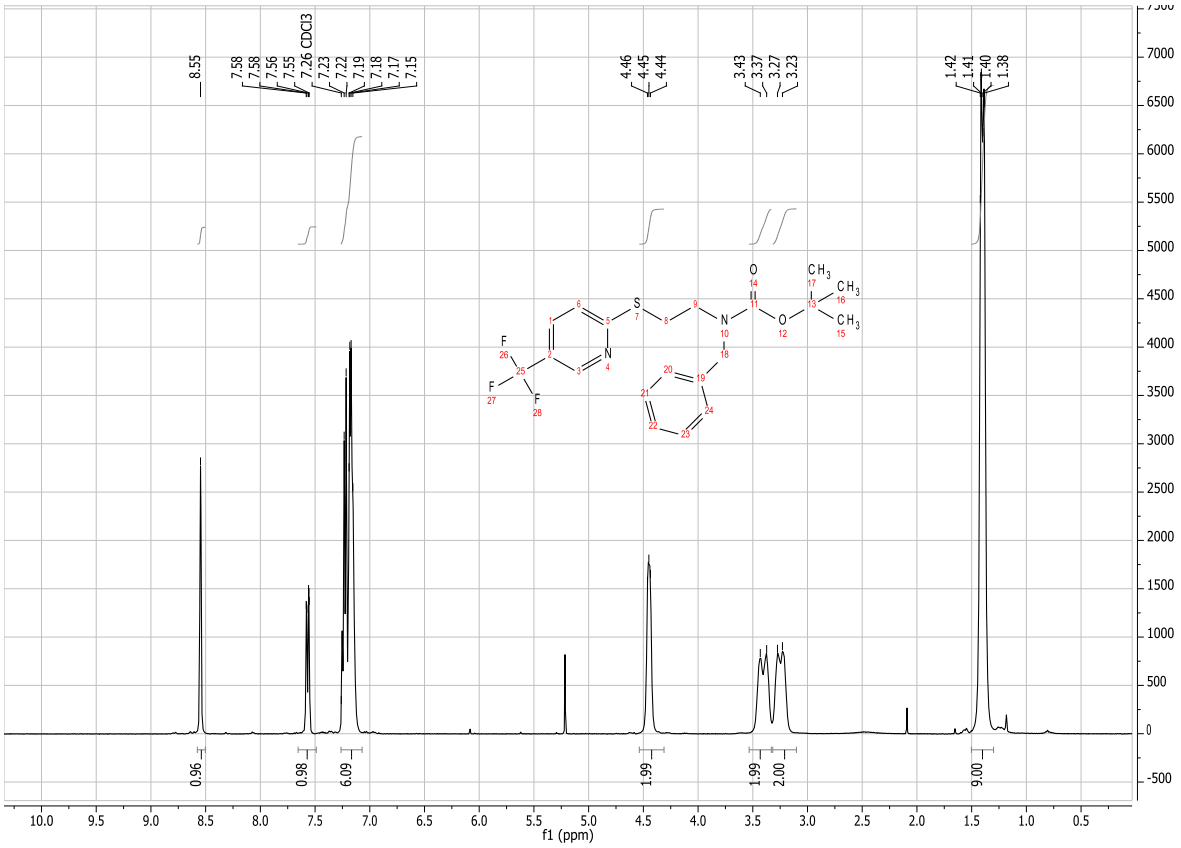

Figure 7.34: ^{1}H NMR spectrum of compound (23).